Novel functions and interactors for Brassinosteroid receptors in Arabidopsis thaliana

Noves funcions i interactors pels receptors de Brassinosteroids d'Arabidopsis thaliana

Norma Fàbregas Vallvé

ADVERTIMENT. La consulta d'aquesta tesi queda condicionada a l'acceptació de les següents condicions d'ús: La difusió d'aquesta tesi per mitjà del servei TDX (**www.tdx.cat**) i a través del Dipòsit Digital de la UB (**diposit.ub.edu**) ha estat autoritzada pels titulars dels drets de propietat intel·lectual únicament per a usos privats emmarcats en activitats d'investigació i docència. No s'autoritza la seva reproducció amb finalitats de lucre ni la seva difusió i posada a disposició des d'un lloc aliè al servei TDX ni al Dipòsit Digital de la UB. No s'autoritza la presentació del seu contingut en una finestra o marc aliè a TDX o al Dipòsit Digital de la UB (framing). Aquesta reserva de drets afecta tant al resum de presentació de la tesi com als seus continguts. En la utilització o cita de parts de la tesi és obligat indicar el nom de la persona autora.

ADVERTENCIA. La consulta de esta tesis queda condicionada a la aceptación de las siguientes condiciones de uso: La difusión de esta tesis por medio del servicio TDR (**www.tdx.cat**) y a través del Repositorio Digital de la UB (**diposit.ub.edu**) ha sido autorizada por los titulares de los derechos de propiedad intelectual únicamente para usos privados enmarcados en actividades de investigación y docencia. No se autoriza su reproducción con finalidades de lucro ni su difusión y puesta a disposición desde un sitio ajeno al servicio TDR o al Repositorio Digital de la UB. No se autoriza la presentación de su contenido en una ventana o marco ajeno a TDR o al Repositorio Digital de la UB (framing). Esta reserva de derechos afecta tanto al resumen de presentación de la tesis como a sus contenidos. En la utilización o cita de partes de la tesis es obligado indicar el nombre de la persona autora.

WARNING. On having consulted this thesis you're accepting the following use conditions: Spreading this thesis by the TDX (**www.tdx.cat**) service and by the UB Digital Repository (**diposit.ub.edu**) has been authorized by the titular of the intellectual property rights only for private uses placed in investigation and teaching activities. Reproduction with lucrative aims is not authorized nor its spreading and availability from a site foreign to the TDX service or to the UB Digital Repository. Introducing its content in a window or frame foreign to the TDX service or to the UB Digital Repository is not authorized (framing). Those rights affect to the presentation summary of the thesis as well as to its contents. In the using or citation of parts of the thesis it's obliged to indicate the name of the author.

Universitat de Barcelona
Departament de Genètica

Centre de Recerca en Agrigenòmica (CRAG)
Departament de Genètica Molecular

Novel functions and interactors for Brassinosteroid receptors in Arabidopsis thaliana

Noves funcions i interactors pels receptors de Brassinosteroids d'Arabidopsis thaliana

Dissertation submitted in partial fulfillment of the requirements for obtaining the degree of Doctor (PhD) by Universitat de Barcelona (Barcelona, Spain)

By
Norma Fàbregas Vallvé

Supervisor
Ana I. Caño Delgado

Tesis Doctoral:

Novel functions and interactors for Brassinosteroid receptors in Arabidopsis thaliana

Noves funcions i interactors pels receptors de Brassinosteroids d'Arabidopsis thaliana

Universitat de Barcelona
Departament de Genètica
Programa de doctorat Genètica 2012-2013

Centre de Recerca en Agrigenòmica (CRAG)
Departament de Genètica Molecular

Aquesta tesi doctoral ha estat realitzada per l'estudiant Norma Fàbregas Vallvé sota la supervisió de la Dra. Ana Caño Delgado al Departament de Genètica Molecular del Centre de Recerca en Agrigenòmica CSIC-IRTA-UAB-UB i tutelada pel Dr. Marc Valls i Matheu, per accedir al títol de Doctorat Europeu per la Universitat de Barcelona.

La directora de tesis	**La doctoranda**	**El tutor**
Dra. Ana I. Caño Delgado	Norma Fàbregas Vallvé	Dr. Marc Valls i Matheu

Barcelona, Juny del 2013

TABLE OF CONTENTS

CHAPTER 1. GENERAL INTRODUCTION **11**

INTRODUCTION 15
BRASSINOSTEROID PERCEPTION AND SIGNALING PATHWAY: STATE OF THE ART 15
BRASSINOSTEROID SIGNALING IS CLOSELY CONNECTED TO VASCULAR DEVELOPMENT 20
THE POWER OF ROOT STUDIES FOR UNDERSTANDING BR ACTION IN PLANT DEVELOPMENT 23
BRS FUNCTION IN ORGAN BOUNDARY DEVELOPMENT IN THE SHOOT APEX. 28
CONCLUSIONS AND PERSPECTIVES 31

OBJECTIVES **33**

CHAPTER 2. RESULTS **35**

A MATHEMATICAL MODEL FOR VASCULAR PATTERNING IN THE SHOOT OF ARABIDOPSIS 42
AUXIN LEVELS APPEAR NOT TO MODIFY THE NUMBER OF VASCULAR BUNDLES 47
BRS CONTROL THE NUMBER OF VASCULAR BUNDLE THROUGH PROVASCULAR CELL PROLIFERATION. 48

ADDENDUM TO CHAPTER 2 **58**

AUXIN POLAR TRANSPORT, AUXIN MAXIMA AND SHOOT VASCULAR PATTERNING 61
BRASSINOSTEROIDS, VASCULAR BUNDLE NUMBER AND CELL DIVISIONS 63
SHOOT APICAL MERISTEM AND VASCULAR PATTERNING INITIATION 64

CHAPTER 3. RESULTS **66**

AUXIN INFLUX CARRIERS MODULATE THE PATTERN PERIODICITY 70
LOSS-OF-FUNCTION MUTATIONS IN AUX/LAX RESULST IN REDUCED NUMBER OF VASCULAR BUNDLES 72
AUXIN INFLUX CARRIERS PROMOTE XYLEM DIFFERENTIATION WITHIN THE VASCULAR BUNDLE 75

CHAPTER 4. RESULTS **78**

PROTEIN EXPRESSION OF BRI1-LIKE FAMILY MEMBERS 82
IDENTIFICATION OF BRI1-INTERACTING PROTEINS 86
IDENTIFICATION OF BRL3-INTERACTING PROTEINS 89
COMPARISON OF BRI1 AND BRL3 RECEPTORS COMPLEXES 93
BRL3 ASSEMBLE HETERO-OLIGOMERS COMPLEXES WITH BAK1 IN VIVO 96
THE BRL1/BRL3/BAK1 RECEPTOR COMPLEX ACCOUNTS FOR ROOT GROWTH AND QC ORGANIZATION 101

CHAPTER 5. GENERAL DISCUSSION **108**

A BREAKTHROUGH IN THE BRL RECEPTOR FIELD 111
BR CONTROL VASCULAR PATTERNING BY MODULATING PROCAMBIAL CELL NUMBER 112
A NEW ROLE FOR INFLUX AND EFFLUX AUXIN CARRIERS IN VASCULAR DIFFERENTIATION OF ARABIDOPSIS SHOOTS 114
GENETIC REDUNDANCY MAY FACILITATE SIGNAL TRANSDUCTION WITHIN DISTINCT CELL-TYPES 115
SPECIFIC BR PERCEPTION COMPLEXES FOR SPECIFIC CELL TYPES 117
CONCLUSIONS AND FUTURE PERSPECTIVES 120
FUTURE PERSPECTIVES 121

CONCLUSIONS **122**

1. BRASSINOSTEROID SIGNALING AND AUXIN TRANSPORT CO-OPERATE TO ESTABLISH THE PERIODIC PATTERN OF VASCULAR BUNDLES IN ARABIDOPSIS. 124

2. AUXIN INFLUX CARRIERS MODULATE THE VASCULAR DIFFERENTIATION AND PERIODICITY IN ARABIDOPSIS SHOOTS. 124
3. BRASSINOSTEROID RECEPTORS FROM THE BRI1-LIKE FAMILY SHOW COMPLEMENTARY SPATIAL LOCALIZATION IN VASCULAR AND STEM CELLS IN THE PLANT. 124
4. BRI1 AND BRL3 RECEPTORS BELONG TO COMMON AND DISTINCT COMPLEXES AT THE PLASMA MEMBRANE. 125
5. THE BRL1/BRL3/BAK1 RECEPTOR COMPLEX IS FUNCTIONALLY REQUIRED TO CONTROL BR-MEDIATED ROOT GROWTH, VASCULAR DEVELOPMENT AND STEM CELL HOMEOSTASIS. 125
6. MULTIDISCIPLINARY APPROACHES COMBINING GENETICS AND PROTEOMICS ARE A POWERFUL TOOL TO STUDY UNCHARACTERIZED SIGNALING PATHWAYS IN PLANTS. 126
7. MATHEMATICAL MODELING SUPPORT EXPERIMENTAL ANALYSIS TO UNRAVEL THE MECHANISMS THAT CONTRIBUTE TO PLANT VASCULAR DEVELOPMENT. 126

MATERIAL AND METHODS 128

1. METHODS IN PLANT BIOLOGY 130
1.1. PLANT MATERIAL AND GROWTH CONDITIONS 130
1.2. QUANTITATIVE VASCULAR ANALYSIS: MEASUREMENT SETTINGS 131
1.3. ROOT LENGTH AND BL SENSITIVITY ASSAYS 132
2. METHODS IN MOLECULAR BIOLOGY 132
2.1. MOLECULAR CLONING 132
2.2 GENERATION OF TRANSGENIC LINES 133
3. METHODS IN BIOCHEMISTRY 134
3.1. PROTEIN EXTRACTION AND WESTERN BLOT 134
3.2. IMMUNOPRECIPITATION 135
3.3. PROTEIN TRYPTIC DIGESTION AND SAMPLE PREPARATION FOR LC-MS/MS ANALYSIS 135
3.4. MAXQUANT ANALYSIS 136
3.5. MS DATA STATISTICS 136
4. METHODS IN CELL BIOLOGY 137
4.1. PARAFFIN EMBEDDING 137
4.2. GUS ACTIVITY STAINING 137
4.3. HISTORESIN EMBEDDING 137
5. IMAGING 138
5.1. CONFOCAL MICROSCOPY 138
5.2. ARABIDOPSIS PROTOPLAST FRET-FLIM ANALYSIS 139
6. THEORETICAL METHODS 139
6.1. MATHEMATICAL MODELING (CHAPTER 2) 139
6.2. MATHEMATICAL MODELING (CHAPTER 3) 140
6.3. SIMULATION DETAILS (CHAPTER 3) 141

CATALAN SUMMARY 142

RUTA DE SENYALITZACIÓ DELS BRASSINOSTEROIDES 144
ELS BRASSINOSTEROIDS JUNTAMENT AMB LES AUXINES, JUGUEN UN PAPER ESSENCIAL EN LA FORMACIÓ DEL PATRÓ DE FEIXOS VASCULARS PERIÒDICS DE LA TIJA D'ARABIDOPSIS 154
ELS TRANSPORTADORS D'IMPORTACIÓ D'AUXINA CONTROLEN EL DESENVOLUPAMENT DEL TEIXIT VASCULAR D'ARABIDOPSIS. 156
FUNCIONS NOVES I ESPECÍFIQUES PER A LA SENYALITZACIÓ DE BRS A TRAVÉS DELS RECEPTOR BRL3 157

BIBLIOGRAPHY 162

APENDIX 1: ANNEXED SUPPLEMENTARY TABLES FROM CHAPTER 4 186

APENDIX 2: CV AND PUBLICATIONS 192

ABBREVIATIONS

ARF: AUXIN RESPONSE FACTOR

ATP: ADENOSINE TRIPHOSPHATE

AUX: AUXIN INFLUX CARRIER

BAHD: BENZYL-ALCOHOL O-ACETYLTRANSFERASE, ANTHOCYANIN O-HYDROXYCINNAMOYLTRANSFERASE, ANTHRANILATE N-HYDROXYCINNAMOYL/BENZOYLTRANSFERASE, AND DEACETYLVINDOLINE 4-O-ACETYLTRANSFERASE

BAK1: BRI1 ASSOCIATED KINASE 1

BAS1: PHYB ACTIVATION-TAGGED SUPPRESSOR 1

BES1: BRI1 EMS SUPPRESSOR 1

BIN2: BR INSENSITIVE 2

BKI1: BRI1 KINASE INHIBITOR 1

BL: BRASSINOLIDE

BR: BRASSINOSTEROID

BRI1: BRASSINOSTEROID INSENSITIVE-1

BRL1: BRI1-LIKE 1

BRL3: BRI1-LIKE 3

BRX: BREVIS RADIX

BRZ: BRASSINAZOLE

BSK1: BR SIGNALING KINASE 1

BSK3: BR SIGNALING KINASE 3

BSU: BRI1 SUPPRESSOR 1

BZR1: BRASSINAZOLE RESISTANT 1

CDG: CONSTITUTIVE DIFFERENTIAL GROWTH

CDP: CONSTITUTIVE PHOTOMORPHOGENIC DWARF

CSC: COLLUMELA STEM CELLS

CUC: CUP SHAPED COTYLEDON

DET2 (DWARF6)/DET 3: DE-ETIOLATED 2 / DE-ETIOLATED 3

DIM1: DIMINUTO 1

DWF4: DWARF 4

FLIM: FLUORESCENCE LIFETIME IMAGING

FRET: FLUORESCENCE RESONANCE ENERGY TRANSFER

GFP/YFP: GREEN/YELLOW FLUORESCENT PROTEIN

GL2: GLABRA 2

GSK3: GLYCOGEN SYNTHASE KINASE 3

GUS: β-GLUCURONIDASE

ID: ISLAND DOMAIN

IF: INTERFASCICULAR FIBERS

KIP: KINASE INTERACTING PROTEIN

KRP2: KIP RELATED PROTEIN 2

LAX1, LAX2, LAX3: LIKE AUX 1, LIKE AUX 2, LIKE AUX 3

LC-MS/MS: LIQUID CHROMATOGRAPHY-TANDEM MASS SPECTROMETRY

LOB: LATERAL ORGAN BOUNDARIES

LRR-RLK: LEUCINE-RICH REPEAT – RECEPTOR-LIKE KINASE

MAPK: MITOGEN ACTIVATED PROTEIN KINASE

NPA: NAPHTHYLPHTHALAMIC ACID1

PCD: PROGAMMED CELL DEATH

PGP: P-GLYCOPROTEIN

PP2A/RCN1: PROTEIN PHOSPHATASE 2A / ROOT CURLS IN NPA

PPP: PHLOEM POLE PERICYCLE

QC: QUIESCENT CENTRE

SAM: SHOOT APICAL MERISTEM

SBI1: SUPRESSOR OF BRI1

SERK: SOMATIC EMBRIOGENESIS RECEPTOR KINASE

SPCH: SPEECHLESS

TF: TRANSCRIPTION FACTOR

VB: VASCULAR BUNDLE

VHA: VACUOLAR H+ ATPase

WER: WEREWOLF

WT: WILD TYPE

YDA: YODA

CHAPTER 1

GENERAL INTRODUCTION

Turning on the microscope turret: a new view for the study of Brassinosteroid signaling in plant development

Norma Fàbregas and Ana I. Caño-Delgado

Published as:
Turning on the microscope turret: a new view for the study of Brassinosteroid signaling in plant development.
Norma Fàbregas and Ana I. Caño-Delgado*
(2013*) Physiologia Plantarum* (Review submitted)

SUMMARY

Brassinosteroid (BR) hormones control multiple developmental responses that are essential for plant growth and development. In Arabidopsis, the general understanding of BR signaling has been greatly attained by genetic and biochemical approaches that led to the identification of the main BR signaling components, from the BRI1 receptor at the plasma membrane to downstream acting BES1/BZR1 transcription factors in the nuclei. Recently, an emerging trend is being established to further advance our understanding of the BR signaling pathway in plant development. Scientists have turned on the microscopy lens turret to revisit the pleiotropic phenotypes of BR mutants at a higher magnification, uncovering the specific cellular defects in the plant. In-depth phenotypic analysis in combination with the search for cell-specific signaling components that are responsible for those particular defects in the BR mutants are leading to: (i) definition of novel roles for BRs in vascular development (Yamamoto et al., 2001; Ohashi-Ito et al., 2005; Ibañes et al., 2009; Fàbregas et al., 2010; Hossain et al., 2012), (ii) unraveling BR function in cell division trough quantitative analysis of Arabidopsis root growth (González-García et al., 2011; Hacham et al., 2011), (iii) establishment of a molecular connection between known patterning and BR-signaling components in organ boundary and stomata development (Bell et al., 2012; Gendron et al., 2012; Gudesblat et al., 2012; Kim et al., 2012), and (iv) development of novel strategies towards the identification of BR signaling components with spatiotemporal resolution (Caño-Delgado and Blazquez, 2013); Fàbregas et al. 2013, submitted). In this review, we summarize the potential of these emerging studies to investigate the spatiotemporal control of BR pathways in plant development.

OUTLINE

1. **State of the art of BR pathway**
2. **BR contribution to plant meristem development**

   2.1. Vascular development

   2.2. Root apical meristem

   2.3. Shoot meristem
3. **Conclusions and perspectives**

KEYWORDS: Brassinosteroid, hormone, receptor, BRI1, vascular, cell division, cell elongation.

HIGHLIGHTS:

- **Quantitative phenotypic analyses in combination with mathematical modeling provide a means to identify novel roles for BRs in vascular development.**
- **BR signaling controls the normal progression of cell cycle and cell elongation of the primary root of Arabidopsis.**
- **BR responses are tissue specific and modulate a myriad of plant developmental processes.**

INTRODUCTION

Brassinosteroid perception and signaling pathway: State of the art

Brassinosteroid (BR) hormones are essential regulators of plant growth and development. BRs have been intensively studied at the physiological and molecular levels mainly in the plant model species Arabidopsis (*Arabidopsis thaliana*) and rice (*Oryza sativa*) (Vert et al., 2005; Kim and Wang, 2010; Clouse, 2011; Wang et al., 2012b). Nowadays, the main BR signaling components have been characterized (Figure 1; for a recent review see (Wang et al., 2012b). Despite the resemblance of BRs to animal steroids (Li and Chory, 1997; Thummel and Chory, 2002), it is characteristic of the plant kingdom that BR perception occurs via direct binding of BR to the extracellular domain of the Leucine-Rich-Repeat-Receptor-Like-Kinase (LRR-RLK) proteins at the cell membrane (Wang et al., 2001; Kinoshita et al., 2005). Binding of BRs to BRI1 (BRASSINOSTEROID INSENSITIVE-1) LRR-RLK receptor initiates a signal cascade that is rapidly transmitted to the nucleus where transcriptional responses of BR-regulated genes control plant growth and development. Biochemical and structural studies have demonstrated that Brassinolide (BL), the most active BR compound, binds directly the island domain (ID) of BRI1, an extracellular pocket made by the 21st and 22nd LRR domains (Li and Chory, 1997; Wang et al., 2001; Kinoshita et al., 2005; Hothorn et al., 2011; She et al., 2011). Upon ligand binding BRI1 activates and heterodimerizes with the co-receptor BAK1 (BRI1 ASSOCIATED KINASE 1) (Li et al., 2002; Nam and Li, 2002; Russinova et al., 2004), a process accompanied by the dissociation of the BKI1 (BRI1 KINASE INHIBITOR 1) repressor (Wang and Chory, 2006; Jaillais et al., 2011).

Early BR events are mediated by the BRI1 receptor in concert with BKI1, BAK1 and BSKs (BR SIGNALING KINASES) partners (Wang et al., 2012b). BKI1 binds to BRI1 cytoplasmic kinase domain inhibiting its activity, although BKI1 does not interact with the kinase domains of BRI1 homologue receptors BRL1 or BRL3 (BRI1-LIKE 1 and BRI1-LIKE 3; (Caño-Delgado et al., 2004) in yeast two hybrid assays (Wang and Chory, 2006). Once BKI1 is released, BRI1 can activate BSK and CDG (CONSTITUTIVE DIFFERENTIAL GROWTH) cytoplasmic kinases by trans-phosphorylation events started between BRI1 and BAK1 LRR-RLKs kinase domains (Tang et al., 2008; Wang et al., 2008; Kim et al.,

2011). Upon BSK1 phosphorylation the phosphatase BSU1 (BRI1 SUPPRESSOR 1) (Mora-García et al., 2004; Kim et al., 2011) is activated, which in turn inactivates cytoplasmic GSK3-like (GLYCOGEN SYNTHASE KINASE 3) kinase BIN2 (BR INSENSITIVE 2) (Li et al., 2001). At low BR levels, BIN2 kinase keeps BR signaling repressed by phosphorylation of homologous transcription factors BZR1 (BRASSINAZOLE RESISTANT 1) and BES1/BZR2 (BRI1 EMS SUPPRESSOR 1), which retains them inactive in the cytoplasm (Figure 1A; He et al., 2002; Yin et al., 2002). The phosphorylated forms of BZR1 and BES1 interact with 14-3-3 phosphoproteins promoting proteasome-mediated degradation (Ryu et al., 2007). Conversely, high BR levels activate the pathway, which involves downstream BSU-mediated dephosphorylation of BIN2 kinase and its subsequent degradation (Figure 1B; Mora-García et al., 2004; Peng et al., 2008). In the cytoplasm, BR-regulated BZR1 and BES1 transcription factors are dephosphorylated by PP2A (PROTEIN PHOSPHATASE 2A; Tang et al., 2011), leading to the active forms of BZR1 and BES1 active entering the nucleus and activating the transcription of approx. 2000 BR-responsive genes, which represent approximately the 6% of the Arabidopsis genome (Figure 1B; Sun et al., 2010; Gudesblat and Russinova, 2011; Yu et al., 2011).

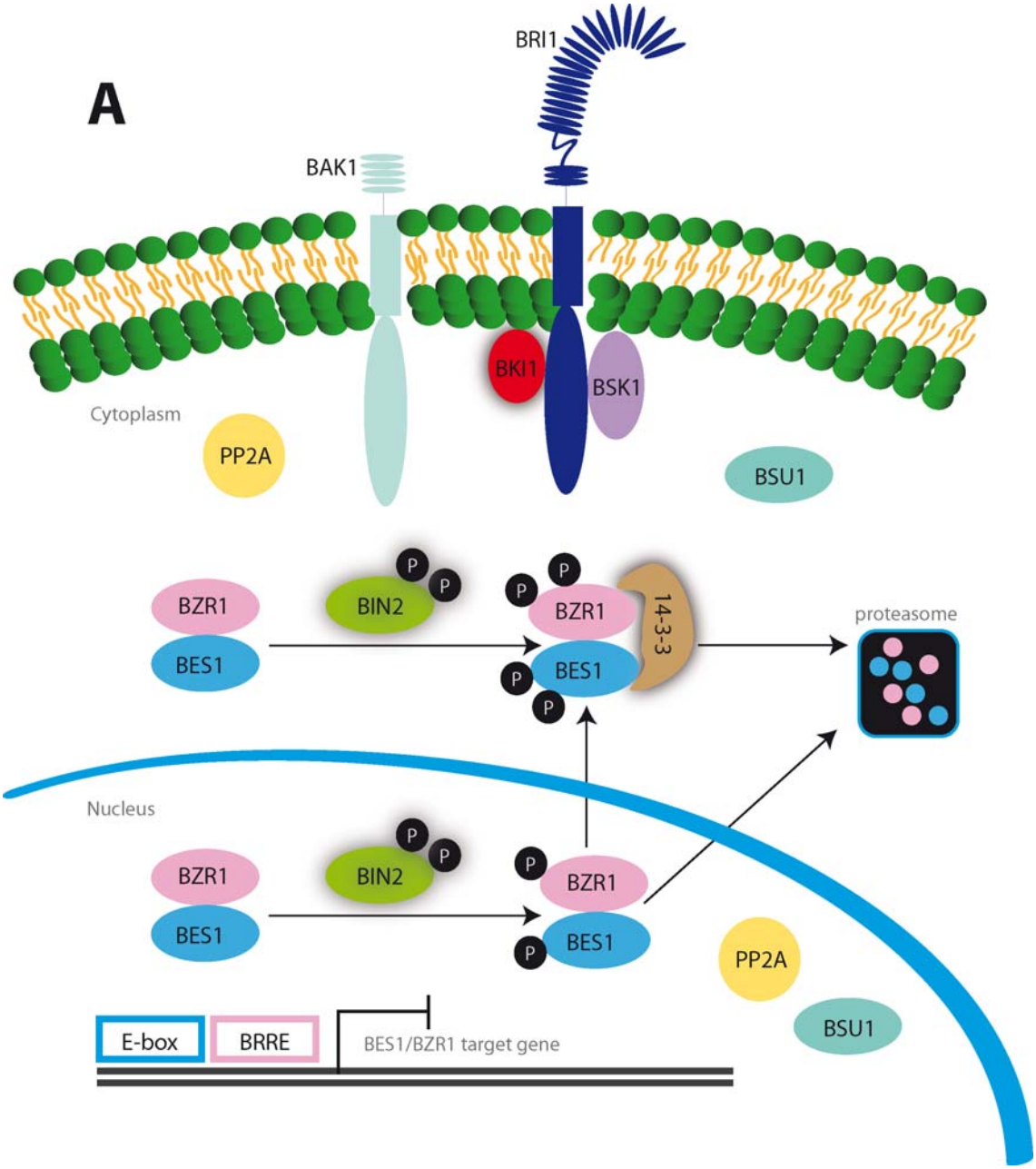

Figure 1. BR signaling pathway in Arabidopsis
(A) Schematic representation of BR signaling pathway when is inactive. In the absence of the ligand BL, BKI1 is repressing BRI1 and BSK1 kinase activities in the membrane. In both, the cytoplasm and the nucleus, BIN2 kinase is repressing the BR signaling by phosphorylating the BR transcription factors BZR1 and BES1 (BRASSINAZOLE RESISTANT 1 and BRI1 EMS SUPPRESSOR 1), which retains them inactive in the cytoplasm. The phosphorylated forms of BES1 and BZR1 interact with 14-3-3 phospho-proteins promoting proteasome-mediated degradation.

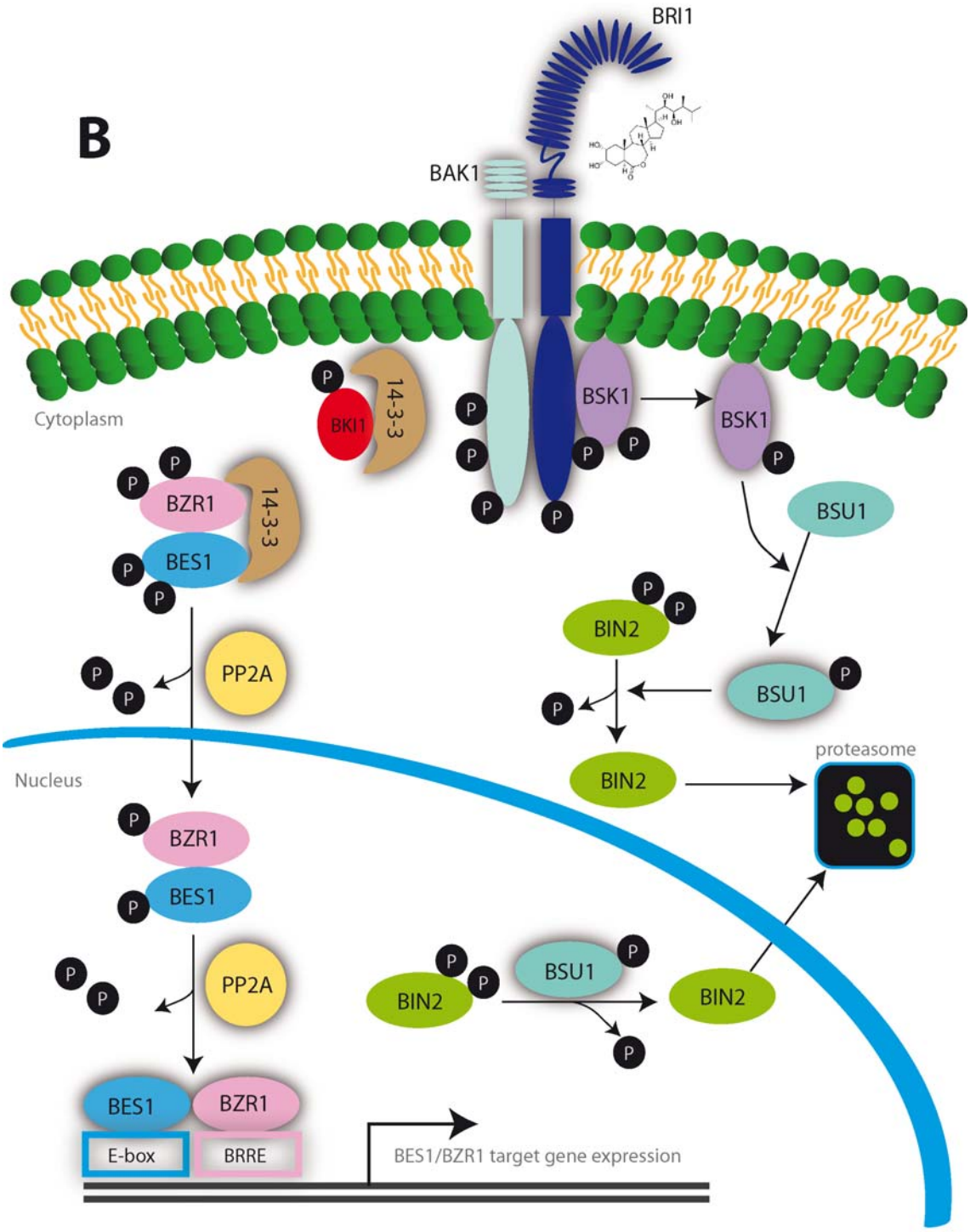

Figure 1. BR signaling pathway in Arabidopsis

(B) Schematic representation of BR signaling pathway when is active. Upon BL binding to the extracellular domain of BRI1 receptor, BRI1 kinase phosphorylates BKI1 and its release allows the heterodimerization with the BAK1 co-receptor. Transphosphorylation events between BRI1 and BAK1 activate and phosphorylate BSK1. BSK1 phosphorylates BSU1 phosphatase activating it. BSU1, inactivates BIN2 kinase and targets it to degradation. Thus, BZR1 and BES1 are dephosphorylated by PP2A (PROTEIN PHOSPHATASE 2A), leading BZR1 and BES1 active forms enter the nucleus and activate transcription of approx. 2000 BR-response genes.

In addition to BR signaling, BR synthesis and homeostasis are also critical for optimal plant growth and development (Szekeres et al., 1996). BR degradation is mainly carried by the hydroxylation of BR biosynthetic products through BAS1 (PHYB ACTIVATION-TAGGED SUPPRESSOR 1; Neff et al., 1999) and by esterification of BRs through BAHD acetyltransferase (Roh et al., 2012; Wang et al., 2012a). While no proof for long distance transport of BRs has been provided (Symons and Reid, 2004; Symons et al., 2008), the precise auto-regulation of BR biosynthetic genes such as DET2, CPD and DWF4 (DE-ETIOLATED 2, CONSTITUTIVE PHOTOMORPHOGENIC DWARF and DWARF4) through a feedback loop represents as the main regulatory mechanism to maintain BR levels across the different plant tissues (Li et al., 1996; Szekeres et al., 1996; Choe et al., 1998; Mussig et al., 2002; He et al., 2005), which is further supported by positive feedback regulation of DWF4 transcription and TCP1 levels (Guo et al., 2010).

At the receptor level, BRI1-mediated endocytosis is required for signal attenuation. BRI1 receptor can be internalized in different cell compartments, yet the active BRI1 receptor is mostly located in the plasma membrane (Geldner et al., 2007; Irani et al., 2012). Another mechanism of feedback regulation is provided through BR induction of SBI1 expression (SUPRESSOR OF BRI1), which methylates PP2A retaining it in the membrane, where it dephosphorylates and inactivates the BRI1 receptor (Wu et al., 2011).

In general, mutations in BR synthesis and signaling components are deleterious for plant growth and compromise development of seed germination, roots, hypocotyls, shoots, leaves and flowers (Vilarrasa-Blasi et al., 2012; Wang et al., 2012b). It has been proposed that BRI1, BES1 and BZR1 proteins display a ubiquitous expression pattern in Arabidopsis seedlings (Friedrichsen et al., 2000; Wang et al., 2002; Yin et al., 2002), although recent quantification of BRI1 receptors (van Esse et al., 2011; van Esse et al., 2012) and microscopic analysis of BZR1 protein localization in the shoot apex (Gendron et al., 2012) together with our root data (Fàbregas et al., submitted and chapter 4 of this thesis) unveiled a cell-specific localization patterns for these proteins. In this review, we summarize the most recent advances of tissue-specific regulation of plant growth and development.

Brassinosteroid signaling is closely connected to vascular development

The plant vascular system transports water and nutrients, which are essential for proper plant growth and development (Lucas et al., 2013). Vascular tissues are organized in a complex manner that accommodates distinct and specialized cell types, which are the subject of multiple signaling and gene regulation events (Caño-Delgado et al., 2010). Since most of the plant biomass on earth comes from the xylem tissues (Caño-Delgado et al., 2010), understanding mechanisms underlying vascular development becomes essential. While effects of BRs in overall plant and cell growth control have been widely studied (Vilarrasa-Blasi et al., 2012; Wang et al., 2012b), recent lines of evidence linking BR signaling to vascular development suggest a more specific roles for BRs in specific cell types within the vascular tissue.

Initial studies using *Zinnia elegans* (Zinnia) as a model system for *in vitro* analysis to study tracheary elements (TE) differentiation, demonstrated that BRs are required to initiate the mesophyll cells differentiation process (Fukuda, 1997; Yamamoto et al., 1997; Yamamoto et al., 2001). Conductive tissues in vascular plants are composed of aligned TEs that have entered the programmed cell death (PCD). BRs are a key factors in the initiation of both PCD and secondary wall formation in plants (Fukuda, 2000) as BRs biosynthetic pathway is activated before PCD, and the synthesized BR induces PCD and formation of secondary walls (Yamamoto et al., 2001).

The potent BR-synthesis inhibitor Brassinazole (BRZ_{220}) was found to modify the ratio of phloem versus xylem differentiation in cress plants (Asami et al., 2000), while reducing xylem differentiation in cress and Arabidopsis (Choe et al., 1999b; Nagata et al., 2001; Caño-Delgado et al., 2004). In agreement, secondary cell wall formation is impaired in DWARF4 and DIM1 (DIMINUTO 1) BR-biosynthetic mutants (Takahashi et al., 1995; Choe et al., 1998; Hossain et al., 2012). Furthermore, BR biosynthetic genes *DWARF* and *CPD* accumulate in procambium and immature xylem cells of Zinnia and Arabidopsis (Kim et al., 2006; Yamamoto et al., 2007). These results collectively suggest that BRs promote xylem differentiation, while BR levels are essential for proper phloem development. BRs regulate cell wall components at the transcriptional level by controlling the expression of *CESA* genes (CELLULOSE SYNTHASE A), which are direct targets of BES1 (Xie et al., 2011). *CESA-3* also display cellulose defects and

increased lignification of secondary cell walls (Caño-Delgado et al., 2003) while BR signaling regulates cell wall pectinases (Wolf et al., 2012), further linking BRs signaling and xylem differentiation.

In Arabidopsis, the shoot vascular tissue is organized by forming a radial arrangement of vascular bundles and its periodical alternation with interfascicular fibers, which together form the vascular ring. This pattern arises from a ring of procambial cells which divide and differentiate into xylem centripetally and phloem centrifugally, giving rise to collateral vascular bundles around the procambium (Esau, 1965). BR-deficient mutants exhibit reduced xylem and fewer vascular bundles in Arabidopsis shoot inflorescence stems (Choe et al., 1999b; Caño-Delgado et al., 2004; Savaldi-Goldstein et al., 2007). Besides BRI1, two additional BR receptors BRL1 and BRL3 (BRI1-LIKE 1 AND BRI1-LIKE 3) were identified that share high homology with the BRI1 receptor in Arabidopsis (Caño-Delgado et al., 2004) and rice (Nakamura et al., 2006). While BRL1 and BRL3 showed a similar capacity to bind the BL to that of BRI1, the expression pattern of these receptors differed from that of BRI1 and appeared enriched at the vascular tissues (Caño-Delgado et al., 2004). Genetic analysis revealed that are BRL receptors function redundantly with BRI1 in the collateral patterning of vascular bundle in the shoot (Caño-Delgado et al., 2004; Zhou et al., 2004). Such functional specialization of BRI1 homologues may have occurred during evolution before the separation of monocots/dicots since rice homologues OsBRI1 and OsBRL3 also mediate vascular cell-type specific BR responses (Nakamura et al., 2006; Santner and Estelle, 2009). In addition to BRL1 and BRL3, BRL2 (BRI1-LIKE 2) a non-active BR receptor among the BRI1 family genes (Caño-Delgado, 2004), was function in leaf venation patterning formation in Arabidopsis (Ceserani et al., 2009).

A quantitative characterization of several loss-of-function and gain-of-function BR signaling and synthesis mutants was done to further understand BR contribution to vascular development (Ibañes et al., 2009). Different parameters were first established for Col-0 wild type (WT) shoot inflorescence stems of adult plants and next measured in BR mutants. Quantitative data together with computational modeling that integrated experimental data to theoretical predictions indicated a role for BRs in promoting procambial cells divisions in the shoot stem of Arabidopsis (Ibañes et al.,

2009). Moreover, the BR induced changes in the number of procambial cells is crucial for determining the number of vascular bundles, which are previously positioned by auxin concentration levels (maxima), within the shoot stem (Figure3, (Ibañes et al., 2009). These results provide new evidence for the role of BRs in cell division within the procambial cells where BR components are preferentially expressed. Despite these findings, how the procambial stem cells are connected to the apical meristem in the shoot is still unclear (Fàbregas et al., 2010). In summary, auxin transport and BR signaling are required for a correct establishment of the periodic vascular pattern in the shoot inflorescence stem of Arabidopsis.

Several evidences point to a concerted role of auxin and BRs in several developmental responses. First, BRs and auxin act synergistically to promote cell elongation in the hypocotyl (Clouse and Sasse, 1998; Nemhauser et al., 2004; Walcher and Nemhauser, 2012) and in lateral root initiation (Bao et al., 2004). Second, promoters of auxin-regulated and BR-induced genes are rich in binding sites for both hormones and they are likely involved in cell elongation promoting processes (Goda et al., 2002; Yin et al., 2002; Nemhauser et al., 2004). Thus, BIN2 inhibits ARF2 binding to DNA and its repressor activity, while ARF2 is required for normal BR response (Vert et al., 2008). Third, exogenous BR and BRZ application selectively regulate PIN4 and PIN7 auxin efflux carriers (PIN FORMED 4 and 7) reducing or increasing their transcriptional activities, respectively (Nakamura et al., 2004; Hacham et al., 2012) while mutations in BRI1 and exogenous BRZ application reduce PIN4 and PIN7 protein levels, revealing a complex mechanism of regulation (Hacham et al., 2012). In addition, BRs promote root gravitropism by increasing polar accumulation of the PIN2 protein (Li et al., 2005). Systems biology studies elucidated a coordinated role for PIN1 (PIN FORMED 1) auxin efflux transporter and BRs in the formation of the shoot vascular patterning (Ibañes et al., 2009) while showing that auxin influx carriers modulate the periodicity of shoot vascular bundles and promote vascular xylem differentiation in the shoot inflorescence stem (Fàbregas and Formosa et al. in preparation, and chapter 3 of this thesis). Additionally, BRX (BREVIS RADIX) gene is expressed in the root vascular tissue where it is induced by auxin while repressed by BL (Mouchel et al., 2006). BRX promotes PIN3 expression within the root meristem (Scacchi et al., 2010), further indicating that auxin

transport and BR signaling have coordinated roles in the vasculature.

Overall, these observations suggest that BRs and auxin crosstalk events occur at different levels, but a global and directional mechanism remains unclear. Since no proof for long distance transport of BRs has been provided (Symons and Reid, 2004; Symons et al., 2008), while auxin is actively transported across the plant tissues (Friml, 2003), it might be that BRs profit from auxin signal mobility to specify function in different plant tissues.

Further studies in this direction will help to delineate the specific and coordinated roles of BRs and auxin within the vascular tissues. Thus, BRs specific functions and signaling within vascular cells may be further investigated through: (i) purification of BRL receptor complexes from the vascular tissues, (ii) characterization of both transcriptomic and metabolomic profiles from the vascular cells in response to BRs (Moussaieff et al., 2013) and (iii) quantitative analysis of BR mutants using super-resolution microscopy to visualize vascular tissues in detail.

The power of root studies for understanding BR action in plant development

The primary root of Arabidopsis offers a superior system to study BR signaling in plant development (Mussig et al., 2003). Primary roots display a simple and stereotyped pattern of cell layers with a spatial separation of cellular activities along the longitudinal axis, which has been extensively used for the study of plant development (Dolan et al., 1993; Scheres, 2013).

Previous studies of BR responses using the hypocotyl and leaf petiole elongation have demonstrated that BRs are important modulators of plant cell elongation (Gudesblat and Russinova, 2011). In addition, the severity of growth defects observed in BR deficient mutants are indicative of the important role of BR in cellular growth, while the role of BRs in cell divisions has remained elusive for years (Hu et al., 2000; Miyazawa et al., 2003). The quantitative analysis of vascular patterning defects (Ibañes et al., 2009) together with the characterization of BR mutants in the roots (González-García et al., 2011; Hacham et al., 2011), have established that BR-control of plant growth is in turn carried by important control of cell division.

Root analysis of BR mutants unveiling a novel role for BRs in cell cycle progression has

been established (González-García et al., 2011; Hacham et al., 2011). Both BRs loss-of-function and gain-of-function mutations result in shorter roots due to an impaired root meristem length. Such reduction is caused by alterations in the cell-cycle progression, as reported by misexpression of cell division markers *Cyclin B1;1* , KNOLLE and plant-specific cell cycle inhibitor KRP2/ICK1, which appeared misexpressed in the roots of BR mutants and plants treated with BL (Figure 2; González-García et al., 2011).

In addition, BRs control epidermal cell fate by modulating regulators of the hair/non hair cell patterning WER and GL2 (WEREWOLF and GLABRA 2)(Kuppusamy et al., 2009). Decreased levels of BRs cause a reduction of WER and GL2 levels while misexpressed GL2 in non hair cells where it is not expressed in WT normal conditions (Figure 2). Indeed, BRs perception from the root epidermal cells is sufficient to control overall shoot (Savaldi-Goldstein et al., 2007) and root growth (Hacham et al., 2011) supporting distinct roles for BRs within specific cell types.

The stem cell niche is composed of the quiescent centre (QC) surrounded by stem cells that give rise to the different cell files of the root. At the distal side of the QC are the columella stem cells (CSCs) whose daughter cells differentiate to starch-containing cells that can sense gravity. In WT plants, QC cells divide rarely and CSCs show mostly one layer of undifferentiated cells. BR exogenous application and *bri1* mutant genetic analysis revealed a primary role for BRs in the differentiation of CSC, indicating a new role for BR in the control of root stem cell dynamics (González-García et al., 2011). A specific role for BR in QC activity has been recently reported (González-García et al., 2011; Fàbregas et al. 2013, submitted). While BRI1 is localized along all the root meristem, BRL1 and BRL3 proteins are expressed predominantly in stem cell niche cells where BRI1 density is diminished (Caño-Delgado et al., 2010; Fàbregas et al. 2013, submitted; van Esse et al., 2011). These results together with *in vivo* immunoprecipitation and mass spectrometric data for the BRI1 and BRL3 receptor complexes, suggested the existence of different BR receptor complexes in different cell-types. A model showing specific and non-redundant roles for the BRL3 signalosome in the control of QC activity at the Arabidopsis root apex has been proposed (Fàbregas et al. 2013, submitted, Figure 2 and chapter 4 of this thesis).

This role for BR in cell division primarily discovered in roots is further supported by the

reduced cell number and cell size of the *cpd* BR synthesis mutant in leaves, which is caused by a slower progression of the cell cycle (Zhiponova et al., 2013). The analysis of cell cycle marker genes such as *Cyclin B1;1*, KNOLLE and CDK demonstrated that not only *cpd* but also *bri1* signaling mutants are impaired in cell division. In addition, BRs promote cell expansion and vascular differentiation (Zhiponova et al., 2013) while regulating stomatal development in Arabidopsis leaves (Kim et al., 2012). Stomata are small pores present in leaves and on the stem epidermis surface that function in gas exchange (Bergmann and Sack, 2007). In dicots, most of them are on the lower epidermis of leaves. Both, BR gain-of-function mutations and BL exogenous application both reduced the number of stomata per leaf area. In contrast, leaves of BR loss-of-function mutants showed stomatal clustering and an increased number of stomata per leaf area (Kim et al., 2012). Yeast-two hybrid, pull-down and kinase assays and *in vivo* co-immunoprecipitation demonstrated that BIN2 interacts with stomatal MAPK kinase YODA (YDA) inhibiting YDA activity by phosphorylation (Kim et al., 2012). In summary, BR controls stomatal development by inhibiting both YDA activity and the stomata formation in Arabidopsis leaves. Additionally, transcription factors involved in stomatal development SPCH, MUTE and FAMA, are regulated by a repressive signaling pathway consisting of EPFs factors, ERECTA family LRR-RLK and TOO MANY MOUTHS (TMM) LRR-RLK. Downstream of these receptors are the MAPK signaling kinases, YODA, MKK4/MKK5 and MPK3/MPK6, whose activation consequently inactivates SPCH by phosphorylation. A recent study revealed that loss-of-function BR mutants *cpd* and *bri1* displayed fewer stomata in hypocotyls whereas gain-of-function BR mutants DWARF4 and BRI1-GFP showed more stomata in hypocotyls (Figure 2; Gudesblat et al., 2012). Several differences between BR positive role in hypocotyl stomata and BR inhibiting role in cotyledon stomata exist, although recent work supporting the BR promoting role in stomata formation in the hypocotyl confirmed previous data on hypocotyl (Fuentes et al., 2012). Moreover, cotyledons and hypocotyls may respond differently to BRs due to a different spatial regulation of the BIN2 regulated proteins. Thus, high abundance of MAPK signaling module components in cotyledon cells, would allow BIN2 kinase to repress both YDA and MKK4, promoting stomata formation within cotyledon cells. In contrast, low MAPK levels in hypocotyl would allow BIN2 regulation

of SPCH, repressing stomata formation in hypocotyl cells (Serna, 2013).

BRs control male fertility by regulating key genes for anther and pollen development in Arabidopsis. To date, defects in pollen tube elongation have been understood as the major cause of the male sterility in BR mutants (Clouse et al., 1996). A more detailed analysis of BR mutants have revealed that defects in male fertility are caused by defects within the pollen grains development, rather than by a failed elongation of the pollen tube as originally proposed (Szekeres et al., 1996). The reduced microspore mother cells resulting in a lower number of pollen grains in *cpd* and *bri1-116* mutants support the role of BR in controlling cell division is a general trend in the BR-regulated plant development (Ye et al., 2010).

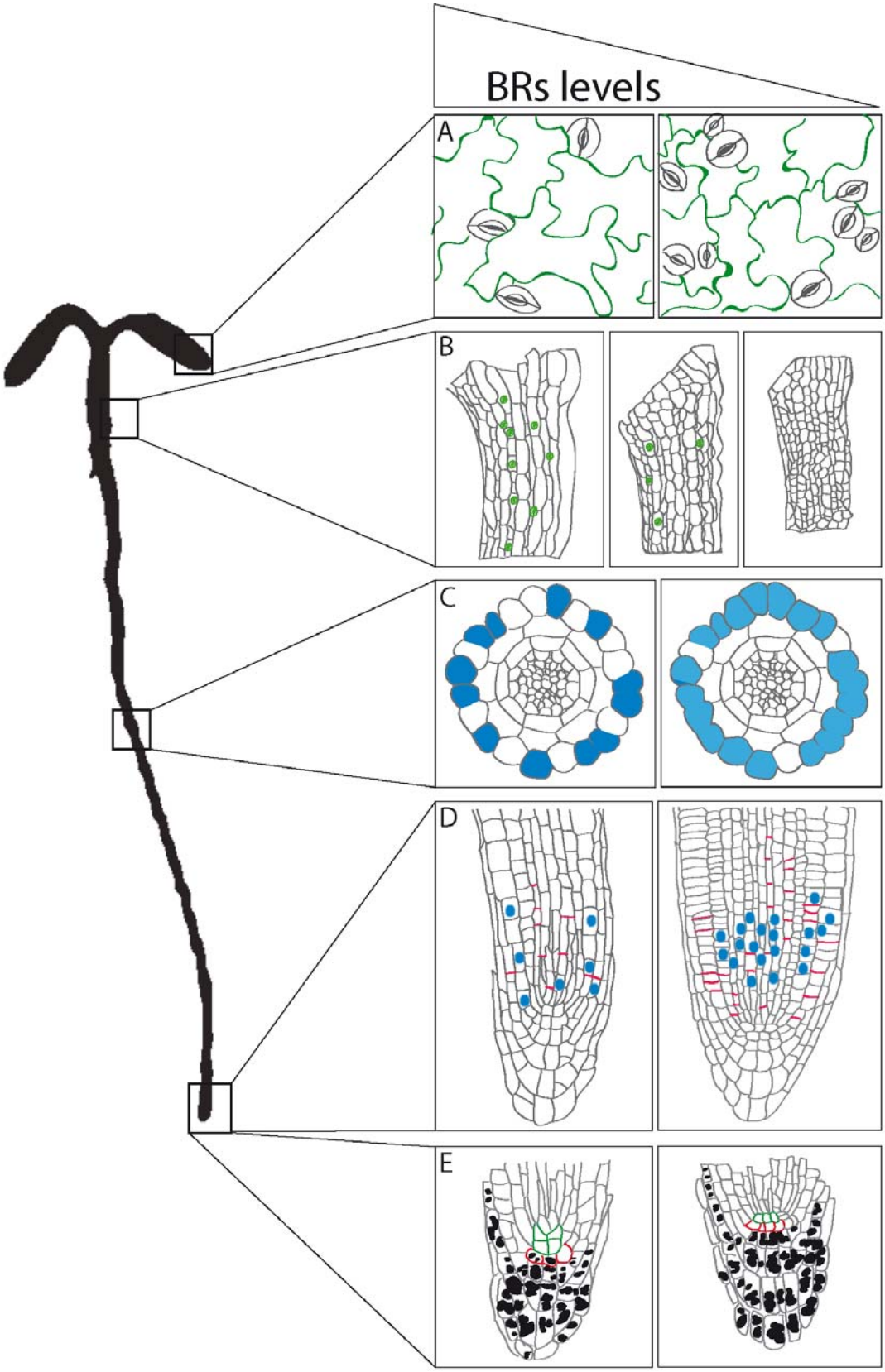

Figure 2. Schematic representation of described tissue-specific effects of BRs in Arabidopsis seedlings

(A) WT cotyledons epidermis shows, in average, one single and independent stoma per mesophyll cell (left panel). BR loss-of-function mutants mesophyll cells display more stomata

frequently grouped in clusters of stomata (right panel). Mesophyll cells are depicted in green and stomata are grey.
(B) Hypocotyl of BR gain-of-function mutants (left panel) shows increased number of stomata when compared to WT (central panel). BR loss-of-function mutants hypocotyl (right panel) rarely shows any stomata. Stomata structures are depicted in green.
(C) Arabidopsis WT roots show a periodic alternation pattern of hair/non hair cells (left panel). Hair cells identity is traced by GL2 marker fused to GUS reporter, denoted in blue (left panel). BR loss-of-function mutants (right panel) show reduced and misexpressed GL2 hair cell marker in non hair cells, where it is not expressed in WT conditions.
(D) BRs control cell cycle progression of Arabidopsis root meristem. Both exogenous BL application and BR gain-of-function mutants showed decreased number of mitosis marker CYCLINB1;1 and cell division planes monitored by KNOLLE (left panel). BR loss-of-function mutants display increased CYCLINB1;1:GUS and KNOLLE promoting cell cycle (right panel). CYCLINB1;1 promoter fused to GUS reporter is represented by blue dots and KNOLLE immunolocalization depicted in pink lines.
(E) BRs control root stem cell dynamics. BR gain-of-function mutants and exogenous BL application both promote the division of QC cells and accelerate differentiation of CSCs, which accumulate starch granules (left panel). QC cells are not divided and CSC are not differentiated in WT plants (right panel). QC cells are depicted in green, CSCs are depicted in red, and starch granules are represented by black dots.

BRs function in organ boundary development in the shoot apex.

To date, the most significant understanding for the action of BRs in specific tissues have been achieved through the analysis of BR- defects at the shoot apical meristem (SAM). The local analysis of BRI1 receptor at the epidermal cells revealed that BRI1 signaling from epidermis is sufficient to control plant shoot growth (Savaldi-Goldstein et al., 2007). By expressing the BRI1 receptor driven by the ML1 epidermal promoter in the *bri1* mutant background, the *bri1* dwarf plants are restored to the wild type phenotype (Savaldi-Goldstein et al., 2007). More recently, a role for BRs in boundaries of the SAM was shown that further demonstrates the importance of BRs roles in different cell-types (Bell et al., 2012; Gendron et al., 2012; Caño-Delgado and Blazquez, 2013). It is known that the SAM is delimited by boundary regions, which are formed by small quiescent cells that divide rarely, compared to the other cell types (Fletcher, 2002). In Arabidopsis, a transcription factor called Lateral Organ Boundaries (LOB) is specifically expressed in the boundaries cells. Thus, loss-of-function mutations in LOB1 exhibits fused organs (Bell et al., 2012), whereas gain-of-function mutations for the LOB1 gene impacts in organ size reduction and loss of sensitivity to BR (Shuai et al., 2002), suggesting an interplay between the two pathways. On the other hand, BR gain-

of-function mutants *Bzr1-D* partially complemented the LOB over-expression phenotype, suggesting that LOB acts upstream of BZR1 (Figure 3; Bell et al., 2012). In addition, both microarray and chromatin immunoprecipitation (ChIP) analysis revealed that there is regulation and interaction between LOB1 and BAS1 while *pBAS1:GUS* plants expression pattern show overlapping domains with *pLOB1:GUS*. In conclusion, organ boundary growth limitation occurs in order to produce junctions and give rise to new organ primordial, and BR specifically regulates this growth limitation in those cells (Bell et al., 2012).

In agreement, gain-of-function mutations in BR signaling components resulted in fused organs, whereas loss-of-function mutations showed enhanced boundaries (Gendron et al., 2012). A direct repression of organ-boundary identity genes by BZR1 revealed a specific mechanism for BR regulation on the boundary developmental program. BZR1 transcription factor fused to fluorescent reporter proteins revealed an accumulation of BZR1 in the SAM which was depleted in the boundaries, consistent with its inhibitory role in boundary formation and its positive role in promoting cell growth (Figure 3). BRs repress the expression of CUC genes, which have been described to play important roles in organ primordia and boundary formation together with LOF genes and auxin (Lee et al., 2009). Moreover, a spatial regulation of the BR signaling pathway contributes to proper organ boundary development in the SAM specifically by repressing organ boundary identity genes.

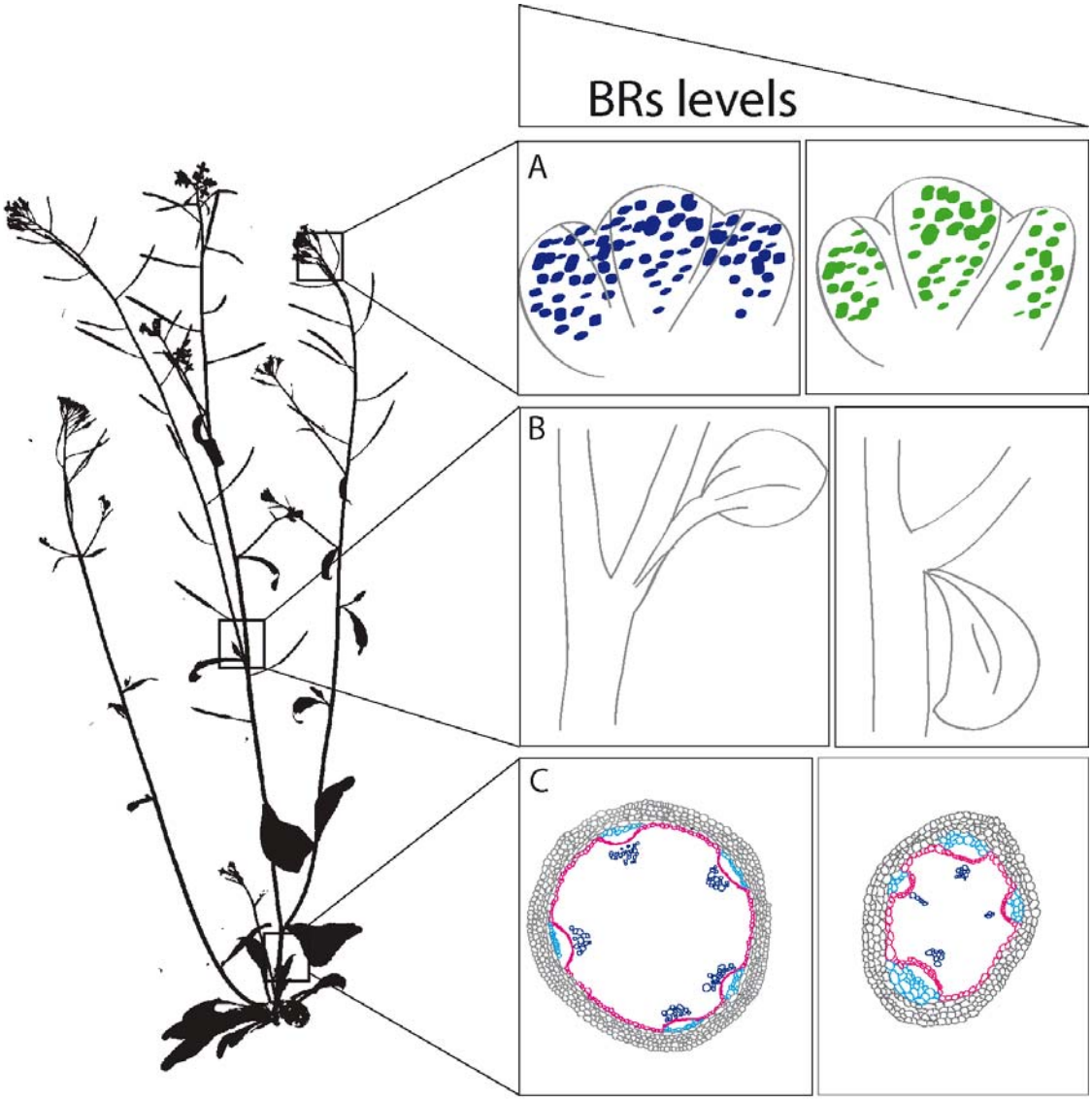

Figure 3. Schematic representation of characterized BR effects in specific cell types in Arabidopsis adult plants

(A) BZR1 dominant form (*bzr1-D*; depicted in blue) accumulates in SAM boundary regions, causing organ fusions (left panel). In WT plants, BZR1 WT protein (depicted in green) is absent in the SAM boundary regions (right panel).

(B) Cauline leaves are frequently fused to axillary stems in *lob-3* mutant (left panel). Low BR levels scenario, by expressing BAS1 enzyme in the LOB junction domains can revert *lob-3* mutant fusions by locally removing BR (*pLOB:BAS1* ; right panel).

(C) BR gain-of-function mutants show more vascular bundles and increased procambial cells number compared to WT in shoot inflorescence stem sections (left panel). BR loss-of-function mutants show les vascular bundles and reduced procambial cells number compared to WT in the shoot inflorescence stem of Arabidopsis thaliana (right panel).

Conclusions and perspectives

This review summarizes the current information of BR signaling in specific tissues, highlighting the recent advances in the study of spatiotemporal control of BRs pathways in plant development. First, new specific roles for BRs in cell-cycle progression of meristematic cells and elongation of epidermal cells to control the primary root growth of Arabidopsis have been established (González-García et al., 2011; Hacham et al., 2011). How different cellular activities are coordinated during root growth and whether BR signal specificity is conferred at the receptor level and/or at downstream of the perception modules will be interesting areas of study in the coming years. Second, it has been proposed that specific but opposed roles for BRs in stomatal development of cotyledons and hypocotyls (Gudesblat et al., 2012; Kim et al., 2012) likely occurred due to a spatial regulation of the BIN2 protein (Serna, 2013). Third, a role for BRs in boundary cells of the SAM unveils novel cell-type specific roles for BRs (Bell et al., 2012; Gendron et al., 2012). In agreement, cell-type and quantitative analyses of BRs signaling mutants revealed: (i) a specific role for BRs in procambial cells divisions in the vascular tissue of the shoot inflorescence stem (Ibañes et al., 2009), (ii) a promoting role for BRs in the pollen microspore mother cells (Ye et al., 2010) and (iii) a key role for BRs perception in epidermal cells of the SAM (Savaldi-Goldstein et al., 2007).

The development of novel microscopy techniques with high-throughput molecular analyses of specific spatiotemporal domains will be key to continue to decipher how plants uses BRs to decode environmental signals into developmental responses.

OBJECTIVES

The general objective of this PhD Thesis is to investigate the mechanistic bases for Brassinosteroid action in plant vascular development.

To this end, the following specific objectives have been accomplished:

1. Investigate the contribution of BRs to the vascular development in the shoot of Arabidopsis plants by comprehensive phenotypic analysis of vascular-patterning defects in BR-signaling and synthesis mutants.

2. Biochemical characterization of BRI1 and BRL3 signalosome complexes by Mass Spectroscopy analysis *in planta*.

3. Functional characterization of BRL3 signalosome in plant growth and development by genetic analysis of candidate interactors identified by biochemical analysis.

CHAPTER 2

Brassinosteroid signaling and auxin transport are required to establish the periodic pattern of Arabidopsis shoot vascular bundles

Marta Ibañes, Norma Fàbregas, Jonne Chory and Ana I. Caño-Delgado

Published as:
Brassinosteroid signaling and auxin transport are required to establish the periodic pattern of *Arabidopsis* shoot vascular bundles.
Ibañes M[a] , Fàbregas N[b], Chory J[c] and Caño-Delgado AI[b].
Proc Natl Acad Sci USA (PNAS) 2009 August 11; 106(32): 13630–13635.

SUMMARY

The plant vascular system provides transport and support capabilities that are essential for plant growth and development, yet the mechanisms directing the arrangement of vascular bundles within the shoot inflorescence stem remain unknown. We used computational and experimental biology to evaluate the role of auxin and Brassinosteroid hormones in vascular patterning in Arabidopsis. We show that periodic auxin maxima controlled by polar transport and not overall auxin levels underlie vascular bundle spacing, whereas Brassinosteroids modulate bundle number by promoting early procambial divisions. Overall, this study demonstrates that auxin polar transport coupled to Brassinosteroid signaling is required to determine the radial pattern of vascular bundles in shoots.

INTRODUCTION

The variety and complexity of vascular patterns among plant species have attracted the attention of both biologists and mathematicians for many years (Essau, 1965; Sachs, 1981; Rolland-Lagan and Prusinkiewicz, 2005; Scarpella et al., 2006; Fisher and Turner, 2007). In the Arabidopsis shoot, the vascular pattern is set up in embryogenesis by asymmetric divisions of the procambium cells (Jurgens, 2001). After germination, subsequent procambial cell division and differentiation gives rise to the xylem, the water conducting tissues, and the phloem, through which photosynthetic compounds and signaling molecules are transported (Berleth and Mattsson, 2000; Sieburth and Deyholos, 2006). This primary provascular growth derives from the activity of primary plant growth and serves as a vascular template along plant development (Esau, 1965). The vasculature forms a continuous apico-basally connected structure along the plant shoot. At the base of the main inflorescence stem of wild-type (WT) plants, the completion of primary provascular growth is observed. Procambial cells have produced functional xylem and phloem forming a vascular bundle (VB) and differentiated interfascicular fibers (IF) in between bundles (Figure 2A). IFs are composed of three to four layers of fiber cells and are mostly responsible for the mechanical strength of the mature stem (Zhong et al., 1997). The procambium places xylem centripetally and phloem centrifugally, contributing to the formation of collateral VBs (Essau, 1965). Across a cross section, the stem vasculature exhibits a radial organization made by the periodic alternation of VBs with the IF in between, together forming the vascular ring (Figure 2A).

Genetic studies have identified a number of vascular patterning mutants (Carland et al., 1999; Mahonen et al., 2000; Clay and Nelson, 2002; Fisher and Turner, 2007), but the mechanisms underlying VB pattern formation are still unknown. Two plant hormones, auxin and Brassinosteroids (BRs), have been implicated in vascular differentiation. Auxin is essential for vascular tissue formation and differentiation (Fukuda, 1997; Berleth and Sachs, 2001). In leaves it has been shown that auxin accumulates in the procambial cells (Uggla et al., 1996; Mattsson et al., 2003), leading to the gradual canalization of auxin into the leaf vascular strands through polarization of auxin efflux carriers (Sachs, 1981; Scarpella et al., 2006; Wenzel et al., 2007). In the

shoot, it has been shown that the auxin efflux carrier PIN1 is expressed in the procambium and xylem cells, at the basal side and in a fraction of the lateral cell membranes (Galweiler et al., 1998). Mutations in *pin1* or chemical inhibition of auxin transport with naphthalene acetic acid (NPA) induces a dramatic increase of differentiated xylem cells, which expand the VBs along the ring adjacent to cauline leaves (Galweiler et al., 1998; Mattsson et al., 1999). Altogether these results raise the intriguing question of how auxin is participating in shoot VB patterning.

Brassinosteroids, the steroid hormones of plants, play a major role in promoting cell expansion, and a signaling pathway that controls cell expansion has been elucidated (Vert et al., 2008). BRs are also involved in vascular cell differentiation of vegetative organs. In *Zinnia* mesophyll cell cultures, BRs have been shown to regulate xylem differentiation (Fukuda et al., 1994; Nagata et al., 2001; Yamamoto et al., 2001). Moreover, a number of BR mutants of rice (Nakamura et al., 2006) and Arabidopsis (Szekeres et al., 1996; Choe et al., 1999a; Caño-Delgado et al., 2004) show various vascular differentiation defects; however, a full characterization of the alterations induced by BRs on the periodic VB pattern in Arabidopsis shoots is lacking and the mechanism by which BRs contribute to this patterning is not yet understood.

The goal of this study is to examine the roles of auxin and BRs in vascular patterning in the shoot inflorescence stem. Because the Arabidopsis shoot is not as amenable to studies of auxin polar transport as leaves and the shoot apical meristem, we used a systems biology approach. By means of a mathematical and computational model and quantitative experimental data, we show that BR signaling and auxin polar transport, not auxin levels, are required to set the number and arrangement of plant shoot vasculature.

RESULTS

Schematically, the shoot vascular pattern can be decomposed into circularly and periodically distributed vascular units, each of which consists of a VB and the clockwise adjacent IF (Figure 2C). While incipient xylem differentiating cells appear spaced across a ring-like geometry at the shoot apex (at ≈100 μm below the shoot apex; see Figure

1 A-D), the periodic pattern of differentiated VBs is set up at ≈2 cm below the apex being maintained along the inflorescence stem (Figure 1 E-G).

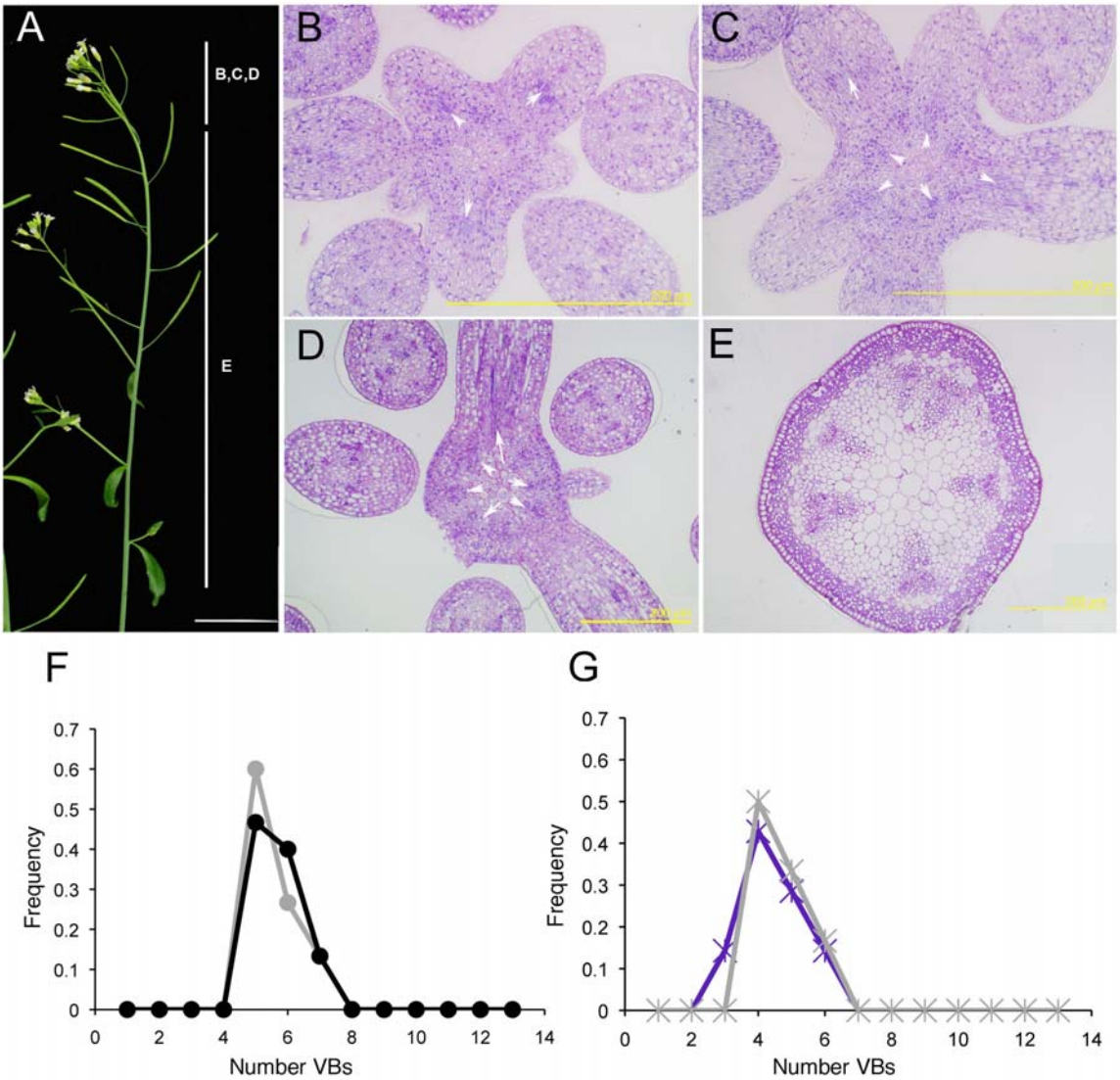

Figure 1. Spatiotemporal analysis of vascular pattern in the Col-0 WT.
(**A-D**) Shoot apical part of Arabidopsis Col-0 WT inflorescence stem**.** Radial sections at 50 µm (**B**), 120 µm (**C**), 200 µm (**D**) and 2 cm (**E**) below the shoot apical meristem. Xylem differentiation present (white arrowheads) at the nascent vascular bundles reveals that periodical pattern is established close to the shoot apex following a 2D ring-like geometry (n=3)**.** (**F-G**) Frequency of the total number of vascular bundles at the base of the inflorescence stem (Z1) and at apical regions (Z3, ~3cm below the shoot apical meristem) for Col-0 WT (**F**) and BR loss-of-function *bri1-116* (**G**). Statistical analysis of the number of vascular bundles and of the total number of cells at the base of the vascular ring revealed no statistical significant differences between data at Z1 and Z3 (p-value > 0.01). (**F**) Black is used for data at Z1 (n=15) and grey for Z3 (n=15). For these WT cross-sections, the ratio between the average total number of cells at the base of the vascular ring at Z1 and at Z3 is 1.2 ± 0.2. (**G**) Violet is used for Z1 (n=7) and grey for Z3 (n=6). For these *bri1-116* cross-sections, the ratio between the average total number of cells at the base of the vascular ring at Z1 and at Z3 is 1.2 ± 0.3.

Recently, auxin polar transport has been shown to be critical to position organs periodically through auxin maxima during the emergence of organ primordia in the shoot, such as the axillary meristems and leaves during the generation of phyllotactic patterns (Reinhardt et al., 2000; Reinhardt et al., 2003). In this context, we hypothesized that auxin maxima promote xylem differentiation and the formation of VBs in the shoot and we investigated whether a periodic distribution of auxin maxima can underlie the formation (*i.e.* number and positioning) of primary VBs along the shoot vascular ring. To this end, we first evaluated whether auxin maxima coincide with VBs. We analyzed the expression pattern of a synthetic auxin-response element DR5::GUS, which has been used as a read-out of auxin levels (Ulmasov et al., 1997). At the base of the inflorescence stem, where completion of the pattern is observed, β-glucuronidase (GUS) activity appeared specifically at the vascular bundles, having a periodic expression in the procambial and differentiating xylem cells (Figures 2D and E). This result indicates that auxin maxima along the provascular ring are correlated with VBs in the WT shoot.

A mathematical model for vascular patterning in the shoot of Arabidopsis

To evaluate whether auxin maxima can control the periodic distribution of VB along the shoot, we formulated a mathematical model for auxin flux across a vascular ring of proliferating cells. This geometry was chosen in concordance with the shoot xylem differentiation pattern (Figure 1 B-E) and following that general, basic pattern, features are preserved among different geometries (Jonsson et al., 2006; Smith et al., 2006). Previous modeling studies of auxin distribution in the shoot and root meristems have supported the relevance of auxin polar transport in creating auxin maxima (de Reuille et al., 2006; Jonsson et al., 2006; Smith et al., 2006; Grieneisen et al., 2007). Based on these studies, our model takes into account auxin polar transport between cells and the apoplast and passive diffusion across the apoplast (Materials and Methods). An analysis of the model shows that appropriate asymmetric localization of efflux carriers is able to elicit auxin maxima as expected (Figure 2F and Figure 3). Such localization drives fluxes that favour auxin accumulation in groups of cells, while depleting auxin in adjacent cells, thereby producing an unequal auxin distribution along the vascular ring

(Figure 2G and Figure 3B). Recently, support for this kind of localization has been reported in both tomato and Arabidopsis where lateral polarization of efflux carrier protein PIN1 toward the developing vasculature has been observed (Bayer et al., 2009). Taken together, these data propose efflux carrier localization as promoters of auxin maxima in shoot vascular bundles.

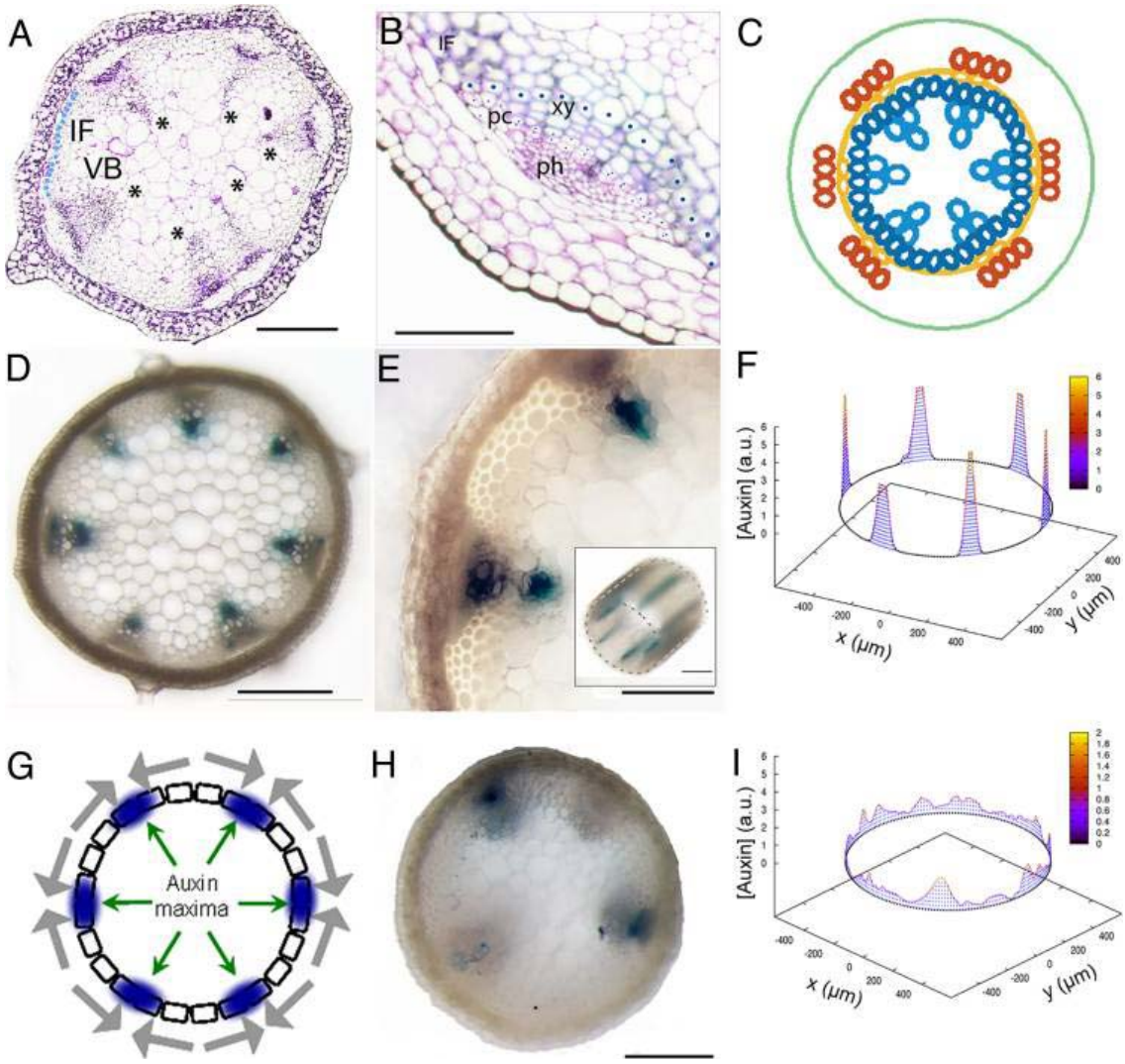

Figure 2. A model for VB spacing in the Arabidopsis shoot inflorescence stem. (*A*) Arabidopsis Col-0 WT transverse-section at the base of the inflorescence stem. IF at the base of the vascular ring (light blue circles) depicted as measured. Asterisks denote VBs. (*B*) Magnification of a VB. Procambial and xylem cells at the base of the vascular ring depicted as measured. Procambial cells (pc), xylem (xy) and phloem (ph) forming a VB and interfascicular fiber (IF) in between. (*C*) Primary VB pattern scheme. Yellow, procambium; blue, xylem and IF; orange, phloem. (*D* and *E*) Radial view of DR5::GUS expression at the base of the inflorescence (*D*) and in a VB (*E*) for the WT. *Inset* in *E* shows a translongitudinal view showing the continuous and periodic expression of DR5::GUS along the shoot inflorescence stem. (*F*) Numerical simulation results for auxin concentration ([Auxin]) in

arbitrary units (a.u.) along a ring of N_F = 210 cells arising from a pool of N_i = 120 progenitors (see Fig. S2 for parameter values). *x* and *y* stand for spatial coordinates (WT average diameter used). (*G*) Auxin maxima (blue), driven by polar transport (gray arrows, plotted outside cells for clarity), position VBs along the vascular ring of cells (boxes). (*H*) Radial view of DR5::GUS expression at the base of the inflorescence for a NPA-treated plant. (*I*) Simulated auxin concentration across a ring of cells as in *F* when the efflux permeabilities are decreased by a factor of 100. [Scale bars: 200 µm (*A* and *D*) and 100 µm (*B* and *E*).]

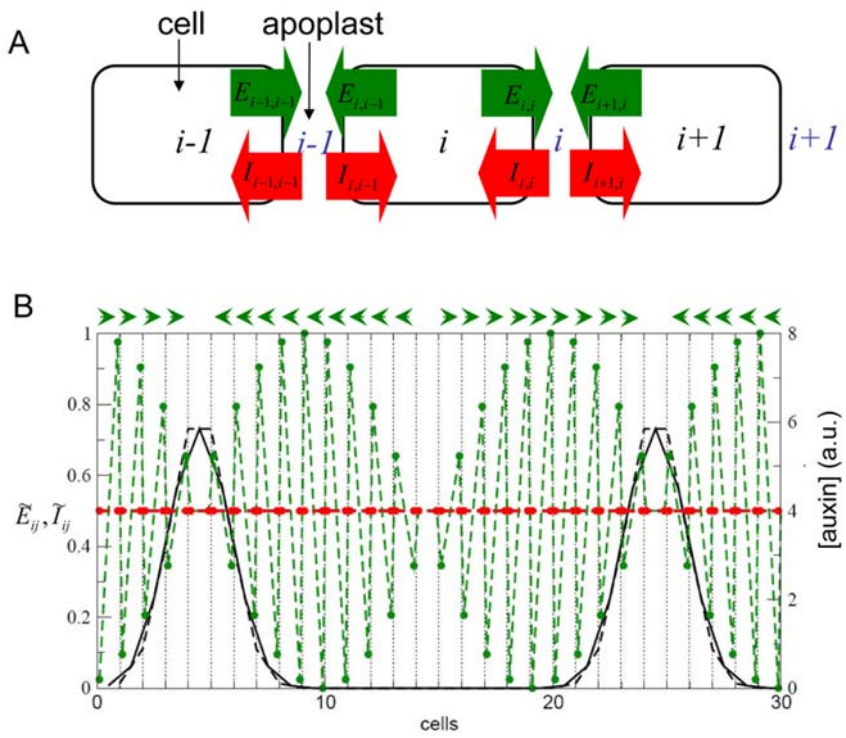

Figure 3. A model for auxin distribution in the inflorescence stem.
(**A**) Schematic representation for clarity of the main elements in auxin polar transport dynamics that are introduced in the model. Efflux permeabilities (E_{ij}) are denoted by green arrows, while influx permeabilities (I_{ij}) are depicted in red. Note, however, that, as denoted by the equations of the model, each cell and each apoplast interspace is indeed modeled as single points. (**B**) Simulation results for the stationary auxin distribution along cells (black continuous line) and in the apoplast (black dashed line) for efflux permeabilities asymmetrically localized and for symmetric influx permeabilities, when cells do not divide. Green arrows at the top depict the direction of auxin transport that is promoted by the efflux and influx permeabilities. Dashed vertical lines are located as a guide to the eye for cell boundaries. Albeit cells are treated as single points in the model, efflux $\tilde{E}_{ij}$ (green dots and line) and influx $\tilde{I}_{ij}$ (red dots and line) permeabilities are plotted near by the dashed lines for visual aid. Parameter values are $\tilde{D} = 0.01$, $l = 20$, $N_i = N_F = 30$, $\varepsilon = 0.01$.

The model reads:

$$\frac{dA_i}{dt} = \sum_{\alpha \in n(i)} a_\alpha I_{i\alpha} - \sum_{\alpha \in n(i)} E_{i\alpha} A_i$$

$$\frac{da_i}{dt} = \sum_{i \in N(\alpha)} E_{i\alpha} A_i - a_\alpha \sum_{i \in N(\alpha)} I_{i\alpha} + D\nabla_\alpha^2 a_\alpha$$

where A_i, a_α stand for auxin in cell *i* and in the apoplast *α*, respectively, and space has been discretized. $E_{i\alpha}, I_{i\alpha}$ are the efflux and influx permeabilities between cell *i* and apoplast *α*, which depend on the level of efflux and influx carriers respectively. $n(i)$ runs over the apoplast neighbouring cell *i,* while $N(\alpha)$ runs over cells surrounding apoplast *α*. *D* represents the effective diffusion rate.

We analysed whether our model could reproduce the phenotypes of plants with defective auxin polar transport (Galweiler et al., 1998; Mattsson et al., 1999). To characterize these phenotypes in further detail, we analysed the vascular phenotype when 2 genes encoding efflux carrier proteins PIN1 and PIN2 are mutated. *pin1pin2* double mutants showed a more disorganized vascular pattern with an increased number of VBs and xylem differentiated cells compared with the WT control (Figure 4 A and C). The xylem differentiation defects were mimicked in plants treated with the auxin transport inhibitor NPA (10 µM, Figure 4B) and are in agreement with previous studies (Galweiler et al., 1998; Mattsson et al., 1999).

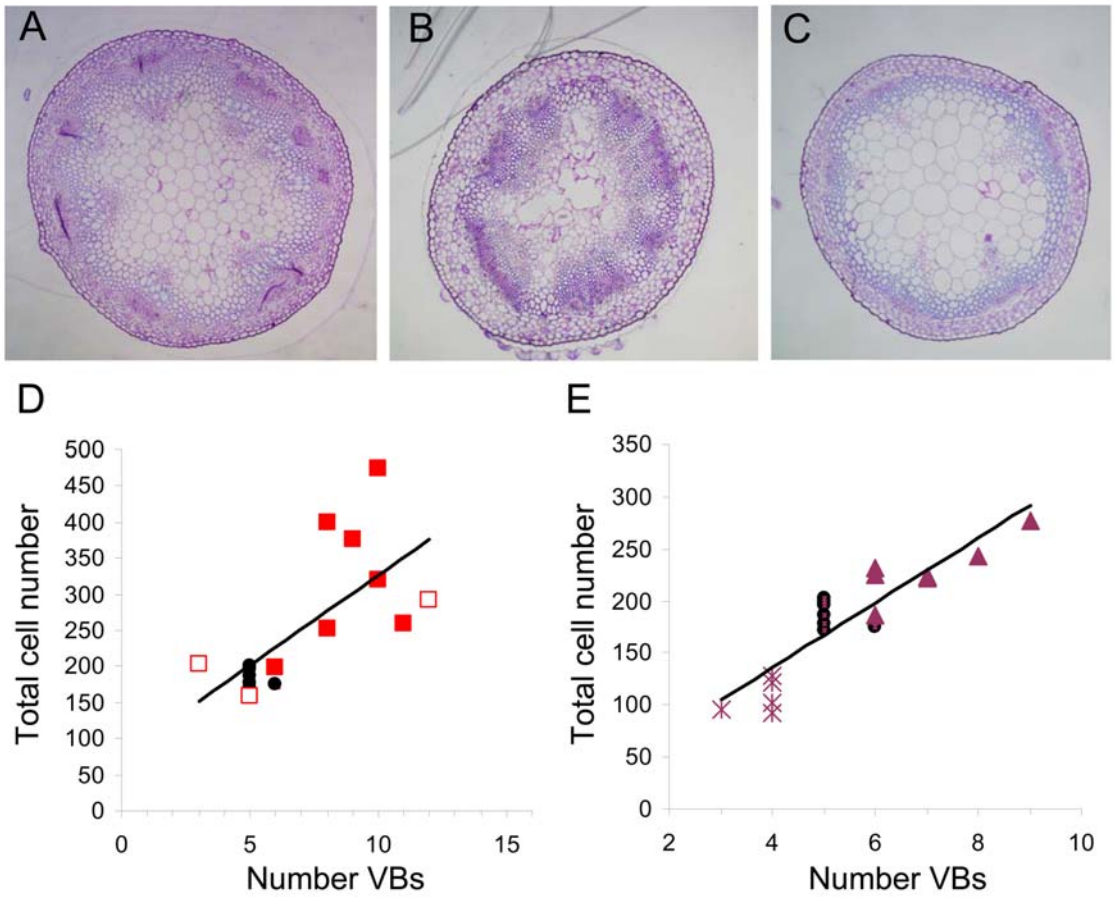

Figure 4. *pin1pin2* double mutants show increased xylem differentiation and VBs.

Cross section at the base of the inflorescence stem from (**A**) homozygous pin1 *pin2* double mutants, (**B**) 10 µM NPA treated plants and (**C**) Col-0 WT plants. (**D,E**) Number of total cells at the base of the vascular ring as a function of the number of vascular bundles for (**D**) *pin1pin2* mutant (full red square), NPA treated plants (empty red square) and Col-0 WT (black circles); and for (**E**) BRs mutants *bri1-116* (stars) and *DWF4-ox* (triangles) and for the WT (black circles). Each point corresponds to a cross-section of a plant being analysed. Empty and full red squares stand for *pin1pin2* double mutant and NPA treated plants respectively. In D, the linear fit yields a correlation coefficient R^2=0.5. In E, the linear fit yields a correlation coefficient R^2=0.8.

We next evaluated whether the vascular pattern of plants with defective auxin transport involves a phenotype in auxin maxima distribution. Accordingly, we analysed the expression pattern of DR5::GUS in plants treated with NPA (10 µM). Our results confirm that auxin maxima are found within VBs although NPA treatment could also lead to a reduced GUS expression in some VBs (Figure 2H). We next evaluated this scenario through computational simulations of the model. When the levels of efflux carriers are strongly reduced, auxin distribution becomes disorganized with larger numbers of auxin maxima, which are less strong and can be broader (Figure 2I). Our theoretical analysis revealed that this auxin pattern arose from a slowing down of the

auxin flux dynamics driven by the decrease in efflux transport rates. For this slow dynamics, initial randomness in the distribution of auxin persists over long times. This result is independent on which mechanism is driving PIN localization. We found the same result in a modified model in which efflux carriers became dynamically reorganized by auxin within the cell. In this case, we set auxin-dependent cycling dynamics for PIN proteins, as proposed for the shoot apical meristem (Jonsson et al., 2006) and took into account that asymmetric endocycling controls the polarization of efflux carriers (Dhonukshe et al., 2008). Taken together, our computational results are in agreement with the observed phenotypes for *pin1pin2* mutants and NPA-treated plants, supporting a model in which auxin flow is driving VB patterning.

Auxin levels appear not to modify the number of vascular bundles

We next challenged this scenario for VB patterning by using mutants that overproduced auxin. Our model predicted that the number of auxin maxima, and not the levels of auxin, determines the number of VBs since the number of auxin maxima did not change when auxin levels were modified (Figure 5A). To test this, we examined the vasculature in an auxin-overproducing mutant, *yucca,* which accumulates ≈ 50% more free indole-3-acetic acid (IAA, the most active auxin) than WT (Zhao et al., 2001). Despite the differences in plant anatomy (Figures 5B and 7A; Zhao et al., 2001), which indicate that the increase in auxin levels in this mutant is significant enough to alter proper plant development, the number of VBs was not modified in *yucca* compared with the WT (Figure 5C and D). As such, our results support the conclusion that auxin levels do not alter the number or arrangement of VBs, as predicted from the model.

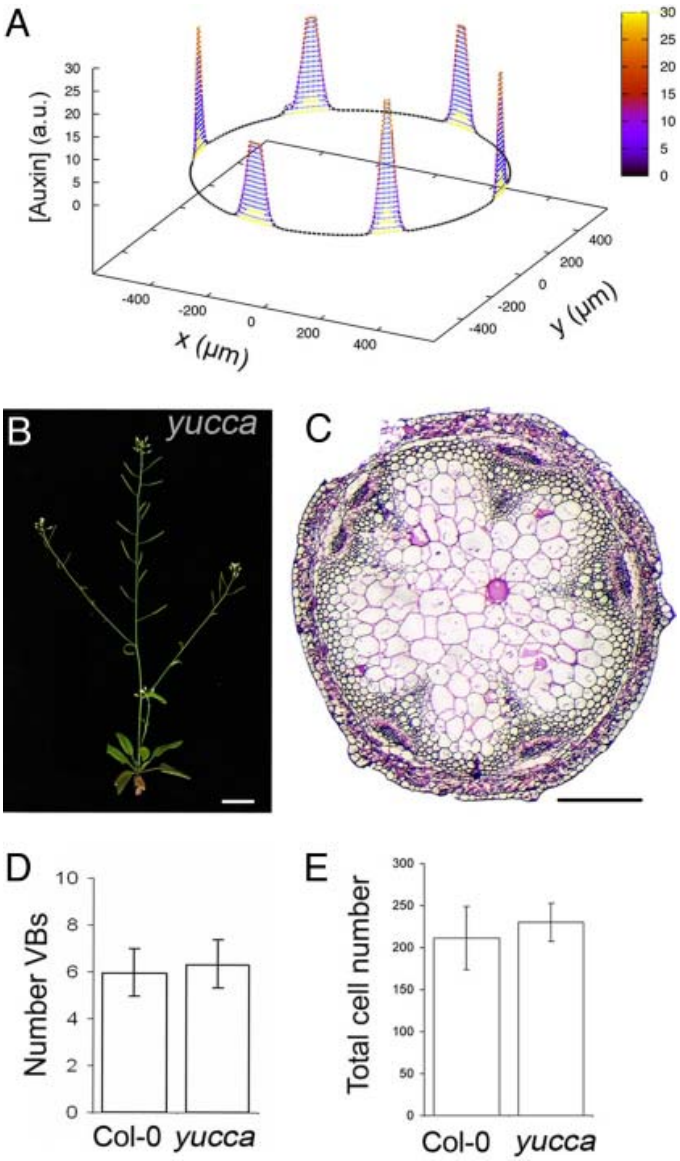

Figure 5. Auxin levels do not change the number of vascular bundles. (*A*) Auxin levels along a ring of provascular cells when the amount of auxin is 5-fold increased. The reference auxin distribution (shown in Fig. 1C) is also plotted (yellow) for comparison. (B) *Yucca* plant. (C) Transverse sections of the inflorescence during primary stem development of *yucca* at the base of the inflorescence. (D) Average number of VBs for Col-0 WT (n = 32) and yucca (n = 21). (E) Average total number of xylem and IF cells (measured as in Fig. 1F) along the vascular ring for Col-0 WT (n = 18) and *yucca* (n = 15). Error bars stand for the standard deviation and P > 0.1 in D and E. (Scale bars: B, 2 cm; C, 200 µm).

BRs control the number of vascular bundle through provascular cell proliferation.

It has been reported that BR-deficient mutants have fewer VBs and reduced xylem compared with WT (Choe et al., 1999b; Caño-Delgado et al., 2004; Savaldi-Goldstein et al., 2007). We first analysed whether this reduction in VBs correlated with a reduction in the number of auxin maxima. We found that DR5::GUS expression in a mutant with reduced BRI1 receptor activity [*bri1-116*, (Li and Chory, 1997)] was localized only within VBs, confirming that a reduction in VB number involves a reduction in auxin maxima as well (Figure 6).

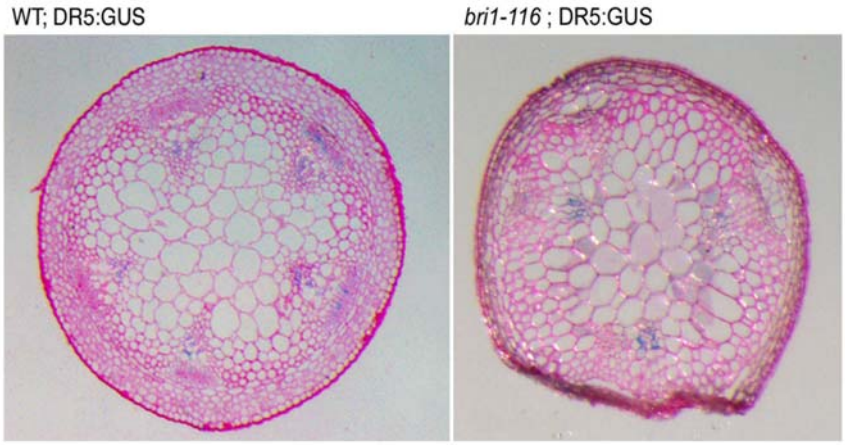

Figure 6. DR5::GUS expression in *bri1-116* mutants. Cross-section at the base of the inflorescence stem of (left panel) a DR5::GUS control plant and (right panel) a F3 plant of DR5::GUS crossed with *bri1-116*. Bars denote 100 µm.

We studied vascular patterning in mutants with impaired BR signaling or synthesis (Table 1 in Material and Methods, Figure 3B). A comprehensive phenotypic analysis revealed that mutants with reduced BR receptor activity [*bri1-116, bri1-301* (Li and Chory, 1997; Li et al., 2001; Xu et al., 2008)], signaling [*bin2* (Li et al., 2001)], or levels [*cpd* (Szekeres et al., 1996)] (Table 1 in Material and Methods) exhibited a reduced number of VBs compared with WT (Figure 7A,D,F,H and J). In contrast, transgenic lines or mutations that increased BR signaling [BRI1-GFP overexpression (Friedrichsen et al., 2000; Wang et al., 2001; Kinoshita et al., 2005), *bes1-D* (Yin et al., 2002), *bzr1-D* (Wang et al., 2002)] or levels [*DWF4-ox* (Choe et al., 2001)] (Table 1 in Material and Methods) led to the formation of a greater number of VBs (Figure 7A,C,E,G and I). Thus, our results show that either impaired BR synthesis or signaling mutants elicit similar alterations of the vascular pattern, implicating a role for BRs in promoting the formation of VBs (Figure 8 and Figure 10 A-C).

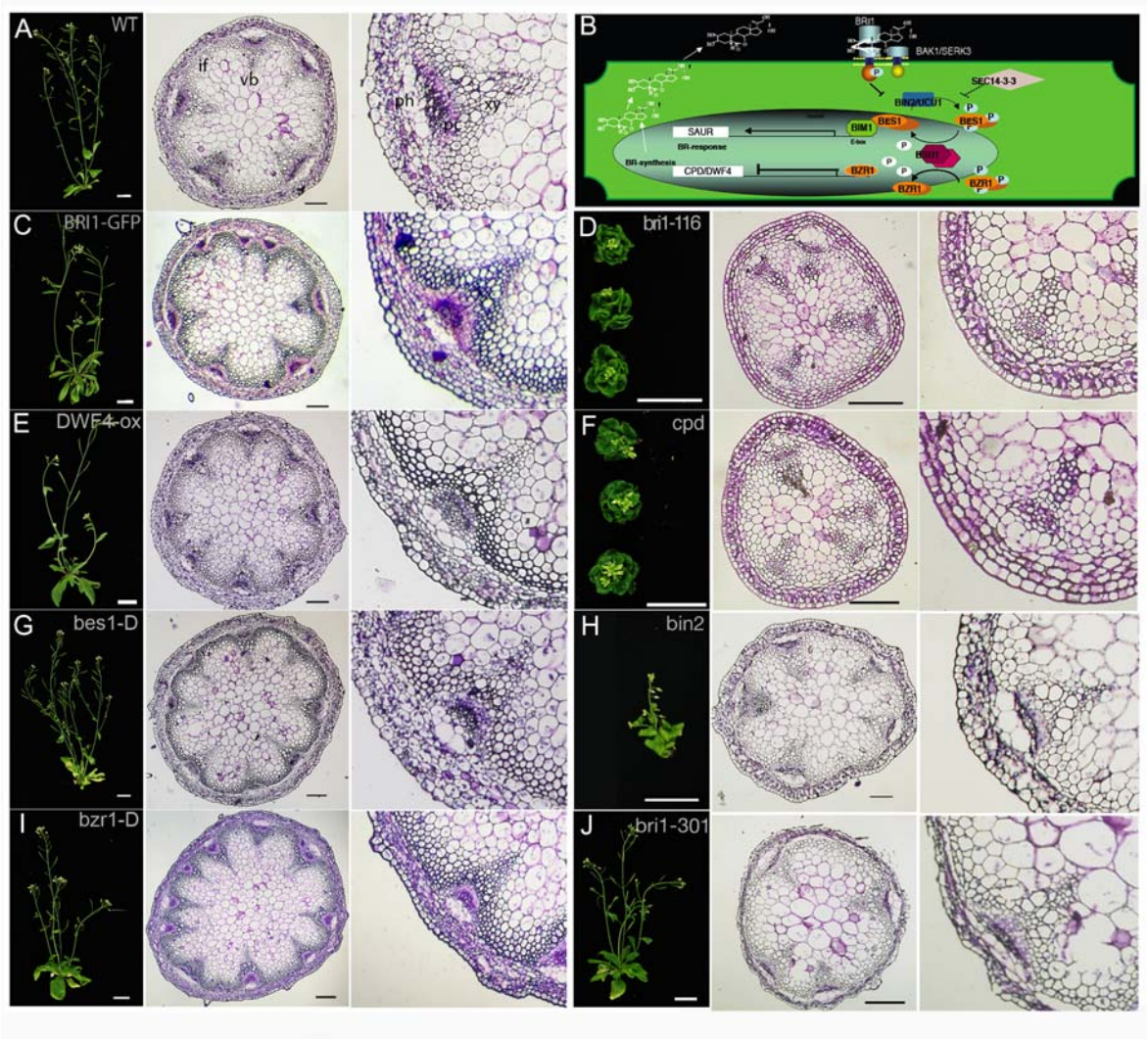

Figure 7. BR signaling mutants modulate the number of vascular bundles. (*A*, *C–J*) From left to right: plant phenotype, cross section at the base of the inflorescence, and a detail of a VB for the WT Col-0 plants (*A*), mutants with enhanced BR signaling and/or synthesis *BRI1-GFP* (*C*), *DWF4-ox* (*E*), *bes1-D* (*G*), and *bzr1-D* (*I*), respectively. The same is shown for mutants with reduced BR synthesis and/or signaling *bri1–116* (*D*), *cpd* (*F*), *bin2* (*H*), and *bri1–301* (*J*). (*B*) Schematic representation of BR signaling pathway showing BR receptor BRI1 at the plasma membrane and downstream signaling component BIN2, a negative regulator that controls the activities of transcription factors BES1 and BZR1. Coordinated action of BZR1, which negatively regulates the expression of BR synthesis genes (CPD and DWARF4), and BES1 transcription factor maintain BR signaling in tune. vb, vascular bundle; if, interfascicular fiber; pc, procambium; ph, phloem; xy, xylem. (Scale bars: 2 cm for plants, 100 µm for stem sections except for *J*, 200 µm).

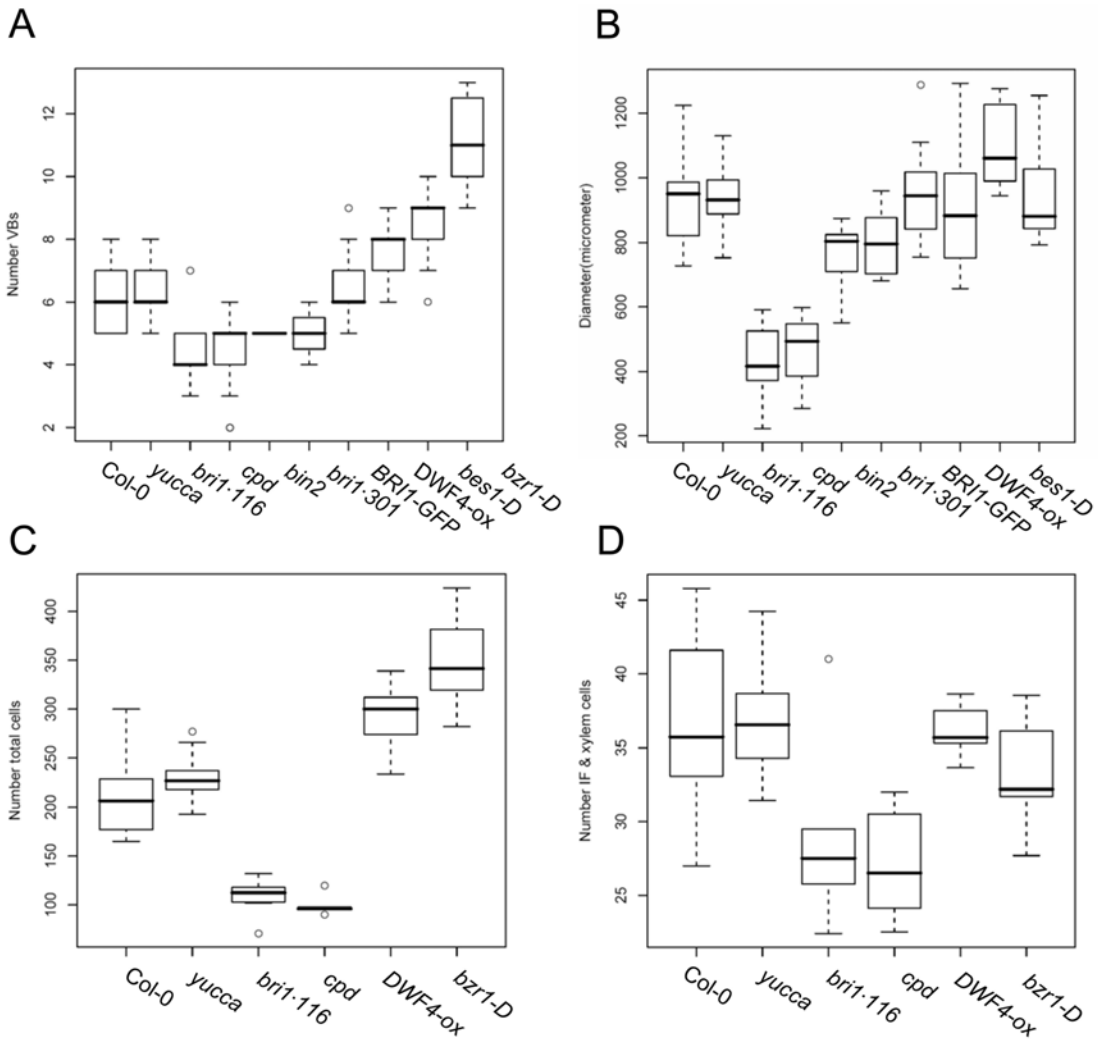

Figure 8. Quartile boxplots of main data sets. Number of VBs (**A**) and stem diameter (**B**) for Col-0, *yucca*, *bri1-116*, *cpd*, *bin2, bri1-301*, *BRI1-GFP* overexpressor, *DWF4-ox*, *bes1-D* and *bzr1-D*. Total number of differentiated cells along the vascular ring (**C**) and number of xylem cells within a VB plus the contiguous interfascicular cells (**D**) for Col-0, *bri1-116*, *cpd*, *DWF4-ox* and *bzr1-D*. Thick horizontal line stands for the median; whiskers show the data within a length of 1.5 time inter-quartile region; dots represent outliers. The size of data sets is indicated in Supplemental Tables 2 and 3.

Furthermore, chemical inhibition of BR synthesis by using brassinazole (BRZ_{220}) or exogenous application of brassinolide (BL, the most active BR) mimicked BR mutants or overexpressing lines, respectively (Figure 9). Exogenous application of BL in *cpd* mutants restored the number of VBs to WT, whereas BRZ_{220} -treated *yucca* plants showed a reduction in the number of VBs (Figure 9), supporting the specific effects of BRs in the control of vascular pattern.

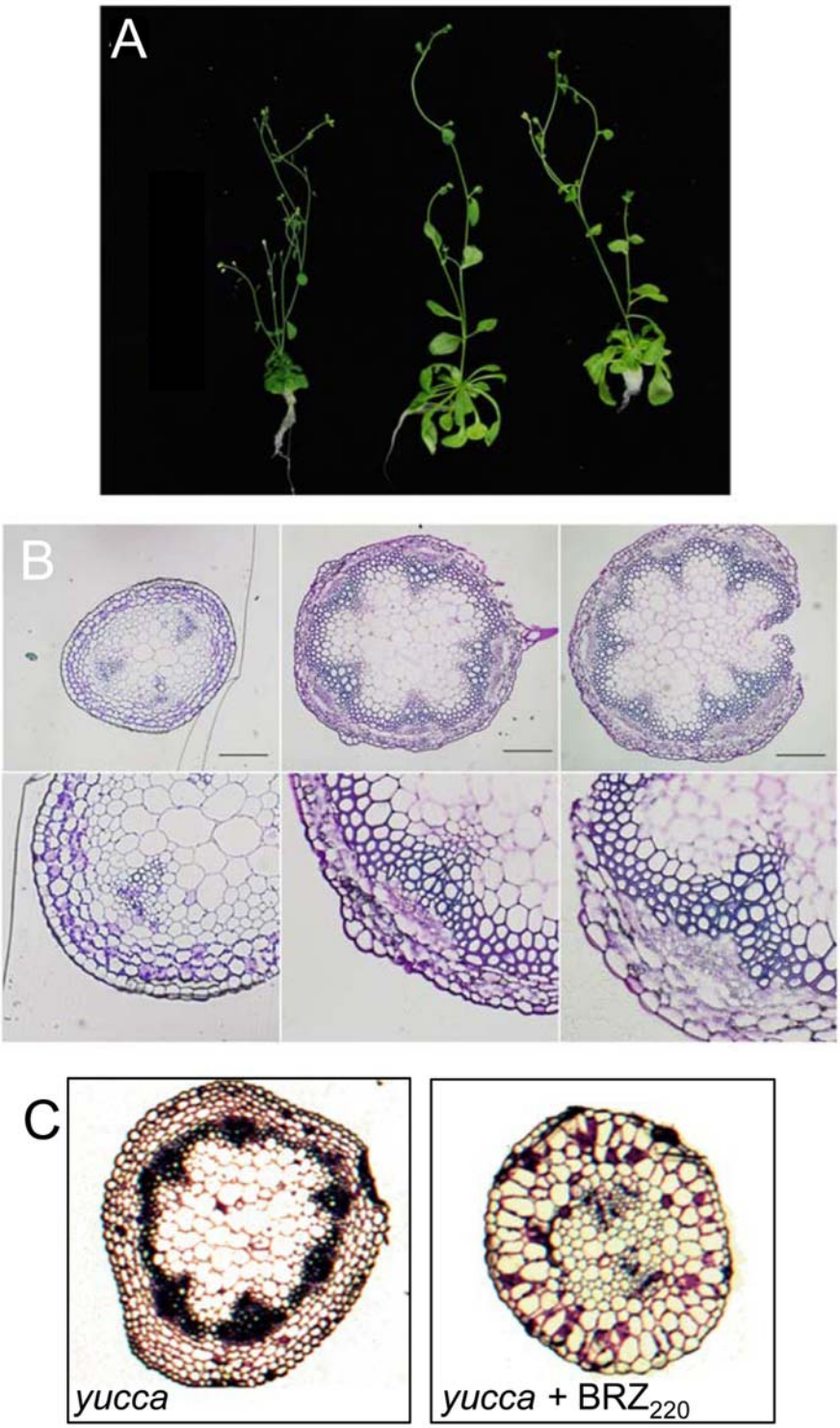

Figure 9. Modulation of vascular bundle number in plants treated with exogenous application of BL and BR-synthesis inhibitor BRZ_{220}.
(**A**) From left to right: plant phenotypes for 1µM BRZ_{220} treated WT plants, non-treated plants WT (Col-0) used as a control and 10 nM BL-treated plants. (**B**) Toluidine-blue stained section at the base of the inflorescence stem and detail of a VB (BRZ_{220}-treated, untreated WT control, and BL-treated plants respectively, from left to right). (**C**) Toluidine-blue stained cross-sections for *yucca* plants and *yucca* after 1µM BRZ_{220} treatment.

To elucidate how the number of VBs is modulated by BRs, we analyzed which factors can change the number of auxin maxima in the model. Our study shows that 2 elements control the number of maxima: the average number of cells from one auxin maximum to the subsequent maximum (*i.e.* the period of the pattern) and the total number of cells when the auxin pattern emerges. Thus, if auxin maxima arise closer to each other in terms of cell numbers, more maxima would be formed within a ring of a fixed cell number. Alternatively, higher numbers of auxin maxima arise as more cells compose the ring when the pattern is being settled down (Figure 10 D and E, Figure 2F).

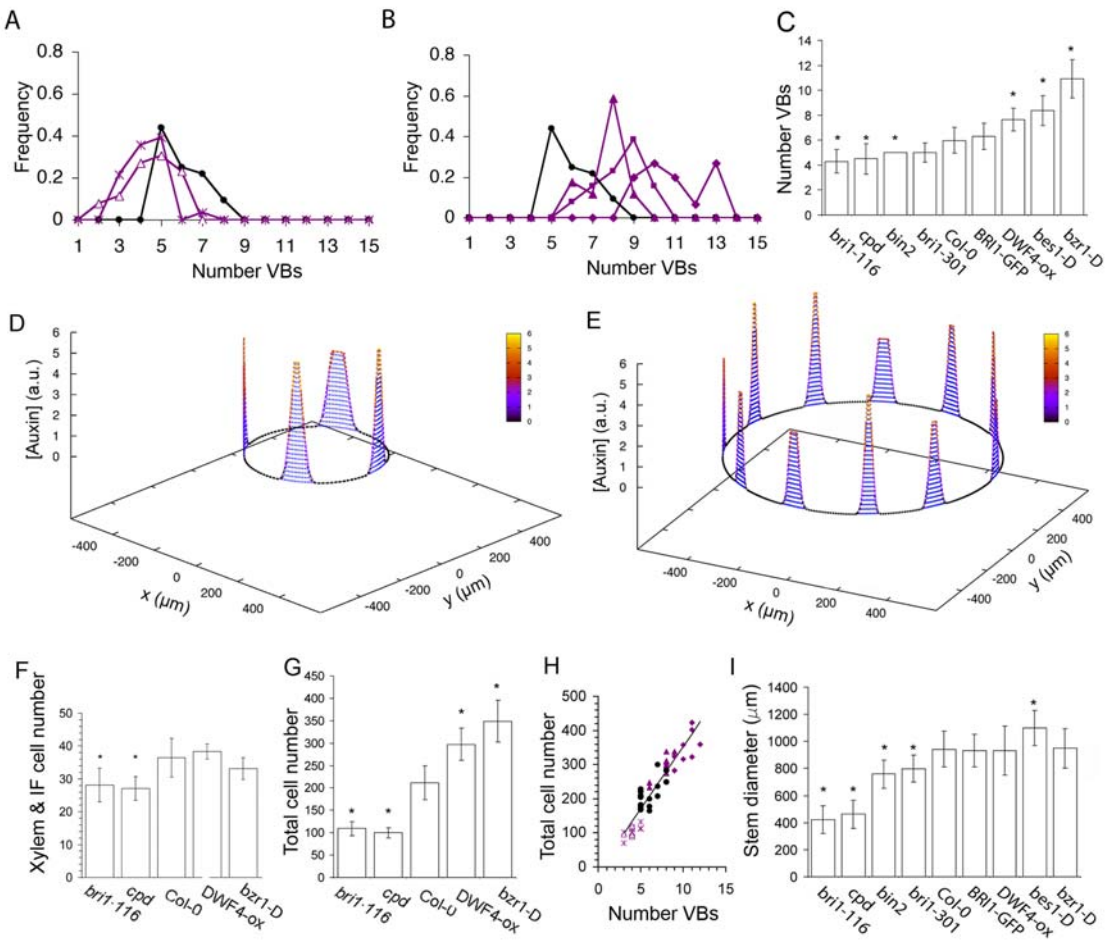

Figure 10. BRs control the number of cells in the vascular ring. (*A* and *B*) Frequency of number of VBs for BR-loss-of-function mutants *bri1–116* (crosses) and *cpd* (triangles) (*A*) and BR-gain-of-function mutants *DWF4-ox* (triangles), *bes1-D* (squares), and *bzr1-D* (diamonds) (*B*) compared with Col-0 WT (black circles). Lines are used as a guide to the eye. (*C* and *I*) Average number of VBs (*C*) and diameter (*I*) at the base of the inflorescence for each mutant genotype.

In *C*, *I*, *F*, and *G*, error bars represent the standard deviation, asterisks stand for*P*-values <0.01 (the data set from each genotype is compared with the WT data; see *Materials and Methods*) and sizes of datasets are found in Table S2 and Table S3. Fig. S6 shows the boxplots of all data in *C*, *I*, *F*, and *G*. In *C*, *bri1–301* has a *P* value <0.05. (*D* and *E*) Simulation results for the auxin concentration along a ring of few (*D*) and many (*E*) cells, mimicking BR-loss- and gain-of-function mutants, respectively. Parameter values as in Fig. 1F with (D) Ni = 80, N_F = 100 and (*E*) N_i = 135, N_F = 250 cells, and average diameter (*I*) for *bri1–116* and *bzr1-D* is being used. (*F* and *G*) Average number of xylem cells within a VB plus the clockwise adjacent interfascicular cells (*F*), and average total number of cells along the vascular ring for BR-mutant genotypes and Col-0 WT (*G*). (*H*) Total number of differentiated cells along the vascular ring as a function of the number of vascular bundles in the stem for each cross section analyzed for different BR-mutant genotypes (*bri1–116*, *cpd*, *DWF4-ox*, and *bzr1-D*) and Col-0 WT (same symbol code used as in *A* and*B*). Linear fit (R^2 = 0.86) shown.

We first evaluated whether the period of the pattern is strongly altered in BR mutants. To this end, we measured the number of cells forming each vascular unit across the ring, *i.e.* the number of procambial and clockwise adjacent contiguous IF cells at the base of the vascular ring for each VB (Figure 2A and B). We observed that procambial cell division occurs centripetally leading to the formation of xylem cells in the VB in such a way that each procambial cell correlated with the first differentiated xylem cell (Figure 2B). To elicit changes in the periodic pattern that would explain the modulation of VB number, we reasoned that fewer cells per vascular unit must be found in gain-of function mutants, while an increase in cells per unit must occur in loss-of-function mutants. Our analysis revealed that the number of xylem and IF cells per vascular unit was similar for gain-of-function mutants and the WT, whereas it decreased slightly for loss-of-function mutants (Figure 10F and Figure 8). These results show that modulation of VB number is not fixed by changes in the periodicity of the pattern.

We next computed the total number of cells, xylem and IF, at the base of the vascular ring in the BR mutants (Figure 2A and B). According to our previous results on the average cell number per vascular unit, we expected the total number of cells to increase in gain-of-function BR mutants, and to be reduced in loss-of-function BR mutants. The analysis confirmed this and revealed a dramatic increase in the number of cells in the vascular ring of gain-of-function BR signaling mutants, whereas loss-of-function BR mutants had fewer cells than the wild type (Figure 10G and Figure 8). Similar features were observed in apical regions of the inflorescence stem (Figure 1 F

and G). Note that an increase in the number of cells forming the vascular ring in BR gain-of-function mutants was not translated to an increase of the stem diameter, as demonstrated by the extreme phenotype of *bzr1-D* mutants (Figure 10G and I). Interestingly, we found that both BR gain-of-function and loss-of-function mutants show a vascular pattern with VBs spaced shorter distances and smaller IF cells (Figure 11).

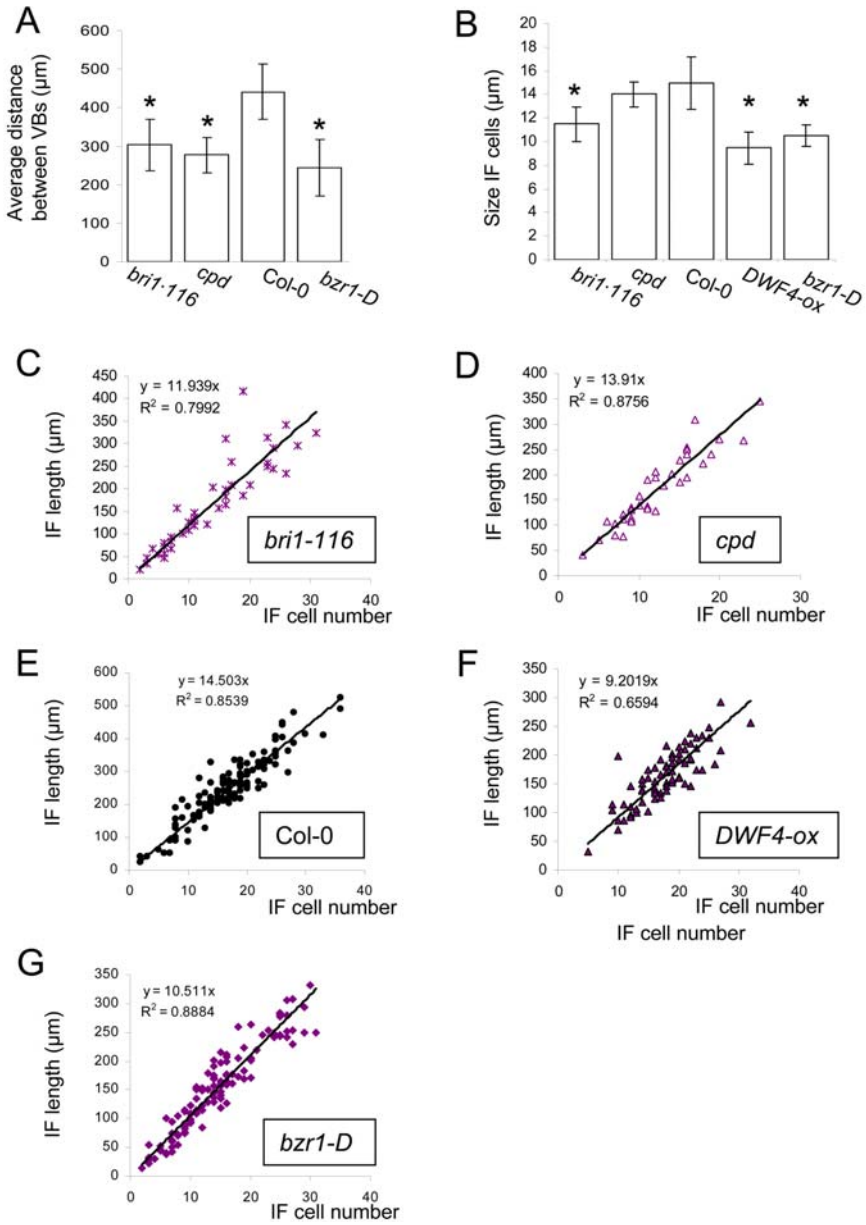

Figure 11. Morphometric changes induced by BRs.
(**A**) Average distance between VBs for BR mutants *bri1-116* (n=11), *cpd* (n=8), and *bzr1-D* (n=15) and for the WT (n=32). The average distance is computed as the perimeter L of the vascular ring divided by the number of VBs. L is obtained as $L = \pi\Phi$ where Φ is the average vascular ring diameter computed from two orthogonal measurements of the vascular ring diameter (Materials and Methods). (**B**) Average size of IF cells at the base of the vascular

ring for BR mutants *bri1-116* (n=11, n_T=42), *cpd* (n=8, n_T=36), and *bzr1-D* (n=15, n_T=122) and for the WT (n=23, n_T=80). This average size is computed as the ratio between the measured length of the IF fiber and the number of IF cells within this length, averaged first for each plant, and then averaged over the sample *n* of plants. Statistical tests are run over the samples of size *n*. (**C** to **G**) Length at the base of the IF fiber (y) as a function of the number of IF cells (x) for *bri1-116* (**C**, n_T=42), *cpd* (**D**, n_T=36), Col-0 (**E**, n_T=80), *DWF4-ox* (**F**, n_T=53) and *bzr1-D* (**G**, n_T=122). The slope of the fitted straight line is an alternative way to quantify the average size of the IF cells. Mutants with increased BR levels have smaller but higher number of IF cells than WT, partially accounting for the small changes in vascular ring diameter observed in these mutants. In A and B, s.d. is shown by line-bars and asterisks stand for *p*-values <0.01 (Materials and Methods).

We found a statistically significant correlation between the number of VBs and the total number of cells in the vascular ring (Figure 10H), consistent with the predictions of the model. Moreover, supporting the different roles of BRs and auxin polar transport in our model for vascular patterning, we did not find such a correlation in plants with defective auxin efflux polar transport (Figure 4 D and E). The specific role for BRs in the patterning process is further supported by the phenotype of auxin-overproducing *yucca* mutants which had a similar number of vascular ring cells to the WT (Figure 5E and Figure 8).

ADDENDUM TO CHAPTER 2

A Systems Biology approach to dissect the contribution of Brassinosteroid and Auxin hormones to vascular patterning in the shoot of Arabidopsis thaliana.

Norma Fàbregas, Marta Ibañes and Ana I. Caño-Delgado

Published as:

A Systems Biology approach to dissect the contribution Brassinosteroid and Auxin hormones to vascular patterning in the shoot of *Arabidopsis thaliana*. Fàbregas N, Ibañes M and Caño-Delgado AI. Plant Signal Behav. 2010 July; 5(7): 903–906.

SUMMARY

Systems biology can foster our understanding of hormonal regulation of plant vasculature. One such example is our recent study on the role of plant hormones brassinosteroids (BRs) and auxin in vascular patterning of *Arabidopsis thaliana* (Arabidopsis) shoots. By using a combined approach of mathematical modeling and molecular genetics, we have reported that auxin and BRs have complementary effects in the formation of the shoot vascular pattern. We proposed that auxin maxima, driven by auxin polar transport, position vascular bundles in the stem. BRs in turn modulate the number of vascular bundles, potentially by controlling cell division dynamics that enhance the number of provascular cells. Future interdisciplinary studies connecting vascular initiation at the shoot apex with the established vascular pattern in the basal part of the plant stem are now required to understand how and when the shoot vascular pattern emerges in the plant.

INTRODUCTION

The plant vascular system is responsible for the long-distance transport of water, solutes and molecules throughout the plant, being essential for plant growth and development. It is formed by two different functional tissues: the xylem, which transports water from roots to aerial organs, and the phloem, through which nutrients and photosynthetic products and signaling molecules are transported.

During embryogenesis, the vasculature is characterized as an undifferentiated procambial tissue in the innermost part of the plant embryo (Esau, 1977). Later in development, the procambium (i.e., a group of pluripotent stem cells (Mahonen et al., 2006)) begins to divide and differentiate into xylem and phloem tissues through oriented cell divisions. In the shoot, procambium generates xylem tissue centripetally and phloem tissue centrifugally, driving the formation of collateral vascular bundles around it (Esau, 1965; Altamura et al., 2001). In the inflorescence stem of the model plant Arabidopsis, the radial pattern of the vasculature exhibits a periodic organization made by the alternation of vascular bundles and interfascicular fibers, which altogether form the vascular ring (Figure 1A).

Previous studies have documented the importance of plant hormones such as auxin and BRs in vascular cell differentiation and patterning (for a recent review see (Dettmer et al., 2009)). Defective polar auxin transport distorts shoot vascular patterning (Galweiler et al., 1998; Mattsson et al., 1999) and BR loss-of-function mutants exhibit few vascular bundles (Choe et al., 2001; Savaldi-Goldstein et al., 2007). But how do these hormones control shoot vascular patterning? In order to answer this question, we used both quantitative measurements of vascular phenotypes and computational modeling (Ibañes et al., 2009).

Auxin Polar Transport, Auxin Maxima and Shoot Vascular Patterning

Auxin is an essential hormone for plant development and it plays important roles in vascular differentiation (Fukuda, 1997; Reinhardt, 2003; Blilou et al., 2005; Scarpella et al., 2006). According to the auxin-flow canalization hypothesis (Sachs, 1981), auxin flow drives continuous strands or paths where the vasculature emerges, by enhancing

its own transport. In leaves, it has been shown that the expression of auxin response marker DR5 and of auxin efflux carrier protein PIN1 precedes vascular induction (Scarpella et al., 2006). Recent work has shown that PIN1 exhibits a dynamic expression pattern that involves its lateral polarization towards the future leaf midvein (Bayer et al., 2009). Furthermore, it is the polar localization of auxin efflux carriers that directs auxin in these cells (Scarpella et al., 2006; Wenzel et al., 2007). Indeed, auxin maxima driven by the polarity of efflux carriers are emerging as a common module for Arabidopsis patterning in leaves, shoots and roots (Scheres and Xu, 2006). In the shoot apical meristem, auxin maxima induce the initiation of organ primordia, such as secondary meristems and leaves during the generation of phyllotactic patterns (Przemeck et al., 1996; Benkova et al., 2003; Reinhardt et al., 2003).

To address how auxin polar transport controls shoot vascular patterning, we formulated a mathematical model for auxin transport dynamics (Ibañes et al., 2009), which partially captured the complexity of previously proposed models (Jonsson et al., 2006; Grieneisen et al., 2007). A hypothesis of the model is that auxin is distributed in maxima, which in turn direct vascular bundle formation in shoots (Figure 1B). To support this hypothesis we analysed the expression pattern of auxin-response element DR5::GUS (Ulmasov et al., 1997) in shoot inflorescence stems. Our results supported the plausibility of the model hypothesis and showed that DR5::GUS expression is within procambial and xylem tissues, colocalizing with vascular bundles (Figure 1A).

To evaluate the role of auxin polar transport we analyzed computationally the effect of reducing active efflux transport rates. Our results showed that auxin dynamics slows down leading to more homogeneous and distorted auxin distributions. In turn, our analysis of the shoot vascular phenotypes of *pin1pin2* double mutants and of plants treated with auxin transport inhibitor NPA revealed disorganization of the shoot vascular pattern with increased vascular bundles in these plants, in agreement with the model predictions.

Another prediction raised by the computational model is that changes in overall auxin levels should not alter the distribution of auxin maxima and, thereby, nor the shoot vascular phenotype. In agreement, we found that the auxin overproducing mutant

yucca (Zhao et al., 2001) exhibits no differences in the number of vascular bundles nor in the number of cells across the vascular ring compared to the wild type.

Brassinosteroids, Vascular Bundle Number and Cell Divisions

BRs have been shown to play an important role in vascular cell differentiation in xylogenic cell cultures from Zinnia (Nagata et al., 2001; Yamamoto et al., 2001). The initial evidences for a role of BRs in Arabidopsis vascular development come from the characterization of BR-deficient (Szekeres et al., 1996; Choe et al., 2001) and perception mutants, (Caño-Delgado et al., 2004) which exhibit a reduced number of vascular bundles (Choe et al., 1998; Savaldi-Goldstein et al., 2007). The identification of novel BRL (BRI1 RECEPTOR LIKE) receptors in Arabidopsis, which are predominantly expressed in the vascular tissues, revealed that BR signal transduction in vascular cells promotes xylem differentiation in the plant shoot (Caño-Delgado et al., 2004).

To investigate the role of BRs on shoot vascular patterning, we carried out a comprehensive vascular analysis at the shoot inflorescence of mutants with reduced BR-signaling or synthesis (Ibañes et al., 2009). Our results confirmed that these mutants exhibit a reduced number of vascular bundles compared to wild-type plants. In contrast, we found that mutations increasing BR-signaling or levels lead to the formation of higher numbers of vascular bundles. Thus, we concluded that BRs control the shoot vascular pattern by modulating the number of vascular bundles.

To further assess how BRs may promote the formation of vascular bundles, we turned into our mathematical model. The model indicated two distinct ways of controlling vascular bundle number: by changing the total number of cells across the vascular ring and by changing the size (measured through number of cells and not distances) of vascular units (i.e. vascular bundle and clockwise contiguous interfascicular cells). The quantification of the number of procambial cells forming the vascular ring in BRs mutants pointed out a strong correlation between vascular bundle and cell numbers, while differences in size could not account per se for the changes in vascular bundle number. Therefore, we concluded that BRs enhance vascular bundle number by increasing the amount of provascular cells. Intriguingly, these results support an important role for BRs in modulating procambial cell divisions.

Shoot Apical Meristem and Vascular Patterning Initiation

Our study unravels how auxin and BRs control shoot vascular patterning by analysing the established vascular pattern at the base of the inflorescence stem of Arabidopsis to. However, when and how the shoot vascular pattern is primarily induced is not yet understood.

The shoot vascular pattern is continuously formed in apical regions of the shoot. The inspection of the vascular pattern along the stem, from apical to basal parts, can provide a spatiotemporal representation of shoot vascular patterning (Guo et al., 2009b). In Col-0 wild-type plants the differentiating xylem cells can be observed at approximately ~100 µm below the shoot apex (Ibañes et al., 2009). Longitudinal sections of the same plants show the connection between the stem vasculature and the vascular strands of secondary stems and floral organs (Figure 1C). Recently, it has been proposed how PIN1 polarization and auxin flow dynamics can drive the connection between leaf midveins and the shoot vasculature (Bayer et al., 2009). Yet, it is not known whether the differentiating shoot vascular tissue is directing vascular patterning in more apical parts or whether the emergence of lateral organs and their vasculature, controlled by the SAM, is dictating shoot vascular patterning. The similarities between the mechanisms proposed for the role of auxin transport in phyllotaxy (Jonsson et al., 2006; Smith et al., 2006) and shoot vascular patterning (Ibañes et al., 2009) suggest to primarily analyse the latter scenario.

One of the limitations in the study of plant vascular patterning is the technical difficulty to observe the vascular tissues since they are the most inner layers in the plant. The use of histological sections has proven to be an excellent tool to observe shoot vascular phenotypes. However, in order to advance in our understanding of shoot vascular patterning, new and more advanced tools (Lee et al., 2006; Truernit et al., 2008) that can depict the spatio-temporal conformation of the stem vasculature by early markers, such as ATHB8 (Kang et al., 2003) and PIN1 (Scarpella et al., 2006) will be very useful. Cell-type specific analyses together with genetic manipulations,

quantitative measurements and modeling will surely facilitate our comprehension of shoot vascular pattern initiation.

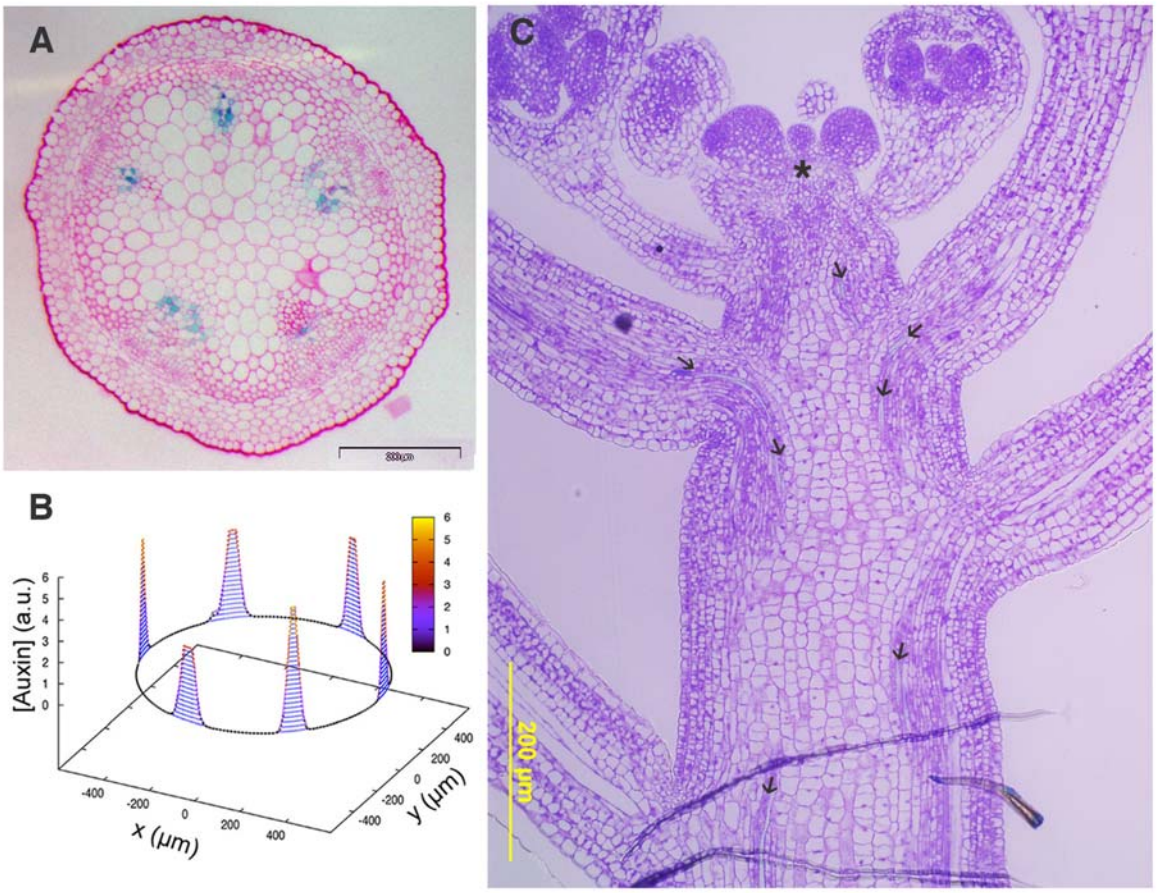

Figure 1. Vascular patterning in Arabidopsis shoot inflorescence stem.
(A) Radial section of DR5::GUS expression at the base of the inflorescence stem in Arabidopsis Col-0 plants.
(B) Computer simulation result for auxin concentration ([Auxin]) in arbitrary units (a.u.) along a ring of cells; x and y stand for spatial coordinates. Auxin is distributed in maxima that according to the model hypothesis, position vascular bundles.
(C) Longitudinal section of an Arabidopsis Col-0 wild-type plant at the most apical zone, immediately below the shoot apical meristem. Arrows point to xylem strains coming from the lateral organs.

CHAPTER 3

Auxin influx carriers play a role in vascular differentiation

Norma Fàbregas*, Pau Formosa*, Ana Confraria, Ana I. Caño-Delgado and Marta Ibañes.

(*Equal contribution)

SUMMARY

Plant hormone auxin is essential for morphogenesis and development of plants. In Arabidopsis, auxin influx carriers carry auxin entrance into the cell while auxin efflux carriers pump it out from the cell. It is well established that auxin efflux carriers play an important role in the shoot vascular patterning by positioning the vascular bundles (VB) along the procambial cell ring (Galweiler et al., 1998; Ibañes et al., 2009), yet the contribution of auxin influx carriers to the shoot vasculature remains unknown. Here, we have combined a theoretical and experimental approach to decipher the role of auxin influx carriers in vascular patterning and differentiation at the shoot inflorescence stem of Arabidopsis. Our theoretical analysis predict an important role for influx carriers in facilitating patterning and modulating the periodicity and intensity of auxin maxima. In agreement, our experimental results unveil a significant reduction in the number of VBs in the influx carriers mutants analysed, indicating that influx of auxin into the cells promotes the periodicity of shoot VBs. Importantly, our experimental analysis uncovered a yet unrecognized novel role for AUX/LAX in promoting of xylem differentiation in the plant shoot inflorescence stem. In conclusion, our results unveil novel roles for auxin influx carriers in plant vascular development.

INTRODUCTION

Auxin is an essential phytohormone in the control of plant growth and development. It is synthesized in the shoot apex and polarly transported to the root and other plant tissues through auxin transporters (Ljung et al., 2001). Auxin efflux carriers enable the hormone to be exported out of the cell to the apoplast. The paramount condition for proper auxin transport is the polarized localization of the auxin efflux carriers PIN and PGP (PIN-FORMED and P-GLYCOPROTEIN) within the cell. Consequently, their biological function has been deeply explored and they have been associated to many biological processes such as emergence of new organ primordia (Benkova et al., 2003; Smith et al., 2006), phyllotaxis (Reinhardt et al., 2003; Smith et al., 2006), root apical meristem maintenance (Blilou et al., 2005; Grieneisen et al., 2007), root gravitropism (Muller et al., 1998; Friml et al., 2002; Abas et al., 2006), lateral root development (Benkova et al., 2003) and shoot vascular patterning (Galweiler et al., 1998; Ibañes et al., 2009).

In Arabidopsis, auxin entrance into the cell is carried by auxin influx carriers, which comprise a multi-gene family containing four highly conserved genes: *AUX1* and the *AUX1*-like genes *LAX1*, *LAX2*, and *LAX3. AUX1* has been the most studied and novel roles for AUX1 in promoting gravitropism and lateral roots development have been demonstrated (Marchant et al., 1999; Marchant et al., 2002). *LAX3* was also shown to promote lateral root initiation and hook development (Swarup et al., 2008; Vandenbussche et al., 2010). The analysis of *aux1 lax* mutants has revealed that AUX1 LAX influx carriers act redundantly to stabilize and maintain the phyllotactic patterning under short-day conditions, suggesting that AUX/LAX transporters may be particularly relevant under less favourable conditions (Bainbridge et al., 2008).

Despite the redundancy reported, AUX1/LAX family members have distinct tissue-specific expression patterns and functions, suggesting that those genes underwent sub-functionalization and therefore they are likely providing additional mechanisms of regulation to the plant (Bainbridge et al., 2008; Peret et al., 2012). Recent work showed that auxin controls petal initiation in Arabidopsis through AUX1 influx carrier (and not LAX) (Lampugnani et al., 2013). In regard to vascular patterning, LAX2 influx carrier has been recently shown to participate in the cotyledons vascular development

(Peret et al., 2012), but the relevance of AUX/LAX proteins in the vascular patterning of the shoot remains unknown.

Here we provide theoretical and experimental evidence reporting that auxin influx carriers regulate vascular patterning in the shoot inflorescence stem of Arabidopsis. In particular, our study unveils a novel role for AUX/LAX transporters in the control of VB number by promoting larger distances between auxin maxima. In addition, our experiments show that AUX/LAX promote xylem differentiation, what depletes procambial cell state in Arabidopsis shoots.

RESULTS

Auxin influx carriers modulate the pattern periodicity

We have previously demonstrated that periodic distributions are relevant for VB patterning (Ibañes et al., 2009). To further investigate how auxin transport drives periodic auxin distribution in the plant, a theoretical and computational analysis was done. We reformulated a model for polar auxin transport (Material and methods) that takes into account auxin inside cells and in the apoplast, enabling the distinction between efflux and influx carriers, which is essential for our study (Material and methods). The model predicts that the amount of influx carriers controls the periodicity of the pattern, and in particular the distance between auxin maxima measured in number of cells (Figure 1). Before being imported into cells, auxin is located in the apoplast (after it has been exported by efflux carriers), where it diffuses. Hence, albeit the transient distribution of auxin would be asymmetric, its stationary distribution will be homogeneous, and no pattern will arise. Therefore, decreasing influx carriers potentiates the role of diffusion (see equations in Material and Methods). Accordingly, the distance between periodic units is enlarged as influx carrier level is diminished, as shown in Figure 1. Furthermore, the simulation results indicate that influx impairment drives higher apoplastic auxin peaks while lower cytosolic auxin peaks (Figure 1A). Our analysis predicts that auxin influx carriers promote periodic patterning of auxin maxima just when the passive income of auxin is low (Figure 1C). Moreover, our analysis shows that influx carriers act as pattern stabilizers (Figure 1C), in agreement to what was previously reported for phyllotaxis (Bainbridge et al., 2008).

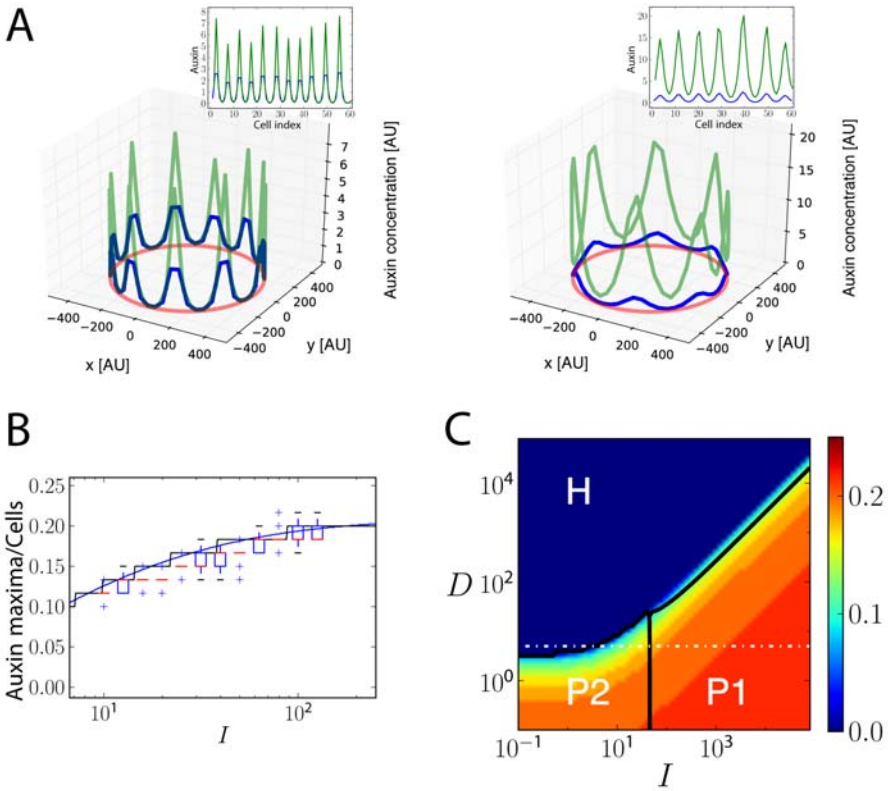

Figure 1. Theoretical and simulation results predict that auxin influx carriers modulate the pattern period and facilitate patterning.
(A) Snapshots of simulation results showing distribution of auxin inside and outside cells for higher (left, I=79.4) and lower (right, I=10) influx carriers levels along a ring of vascular tissue. Blue and green lines denote cellular and apoplastic auxin profiles, and red line is a drawing of the ring of vascular tissue. Insets depict the same results projected into a 2D plane. (B) Theoretical and simulation results of number of cells between cytosolic auxin maxima. Each point in the boxplot corresponds to simulation results of 30 simulations. Black and blue lines are the corresponding theoretical estimation for a ring of 60 and 1200 cells, respectively. (C) Phase diagram showing theoretical results from linear stability analysis. The color scale shows an estimation of the number of cells between cytosolic and apoplastic auxin maxima. Three different regions in the parameter space are found: P1, where a typical Turing instability would lead to patterning; P2 a region where patterning is possible due to a non-turing instability, involving longer characteristic wavelength in the pattern emergency, so that more peak fusions are expected to happen; and H, where the homogeneous characteristic wavelength is the fastest to grow, so no patterning is expected. Horizontal white line depicts the line along which simulations are presented in panels A and B. Main parameter values: E=100, D=10 and D_{ca}=10.

The model predicts that influx impairment will have an effect on the auxin maxima pattern, and ultimately on the formation of the vascular pattern. In particular, our results predict that plants with impaired influx carriers will undergo an increase of the characteristic distance between VB in number of cells (Figure 1). Consequently, plants having the same number of cells in the shoot vascular ring are expected to show less VBs. Pattern destabilization could lead to peak fusion, and therefore more phenotypic variability of the distance between VBs within the same plant. Furthermore, weaker cytosolic auxin peaks could impair different effects downstream auxin signaling. For instance, if vascular differentiation is impaired, shoots will display deficient xylem development (Fosket and Torrey, 1969; Sachs, 1981; Fukuda, 2004). Alternatively, low levels of auxin may decrease cell proliferation (Perrot-Rechenmann, 2010) leading to smaller shoots. Additionally, cell proliferation in combination with pattern instability could result in a disrupted pattern and a more diversified plant phenotype.

Loss-of-function mutations in AUX/LAX resulst in reduced number of vascular bundles

VB patterning in Arabidopsis shoots depends on auxin transport dynamics (Galweiler et al., 1998; Ibañes et al., 2009; Caño-Delgado et al., 2010). Recently, we have shown that a model of auxin transport predicts that efflux carriers can distort the regularity of the pattern as observed experimentally (Ibañes et al., 2009; Fàbregas et al., 2010). Because our theoretical and computational analysis predicts that influx carriers can alter the period of a regular pattern, analysis of VB patterning in Arabidopsis inflorescence stem of auxin influx mutants was done to test the model prediction. Thus, the pattern of VBs in the shoot inflorescence stem of triple *knock-out* (ko) mutants in auxin influx carriers *aux1lax1lax2* and quadruple *aux1lax1lax2lax3* mutant combinations was analysed. In agreement with the model prediction, we found that depletion of auxin influx carriers in the plant resulted in a significant reduction of VBs as compared to the WT (Figures 2A-E). This quantitative analysis revealed that WT plants have many more VBs (12 in average) than WT plants grown in long day conditions (6 in average). We next evaluated whether the reduction in VB number observed in *aux1lax1lax2lax3* quadruple mutants was caused by a reduction in the

total number of procambial cells in the vascular ring (less units, equally distant to those of WT can arise) or whether it was produced by an increase in the distance between vascular units. We defined a vascular unit as each vascular bundle (VB) together with its adjacent interfascicular fiber (IF) zone, limited by the next VB. Our results show that the vascular number reduction is accompanied by both a reduction in total procambial cell number (Figure 2F) and an increase in the vascular unit size (Figure 2G), what would correspond to an increased distance between auxin maxima.

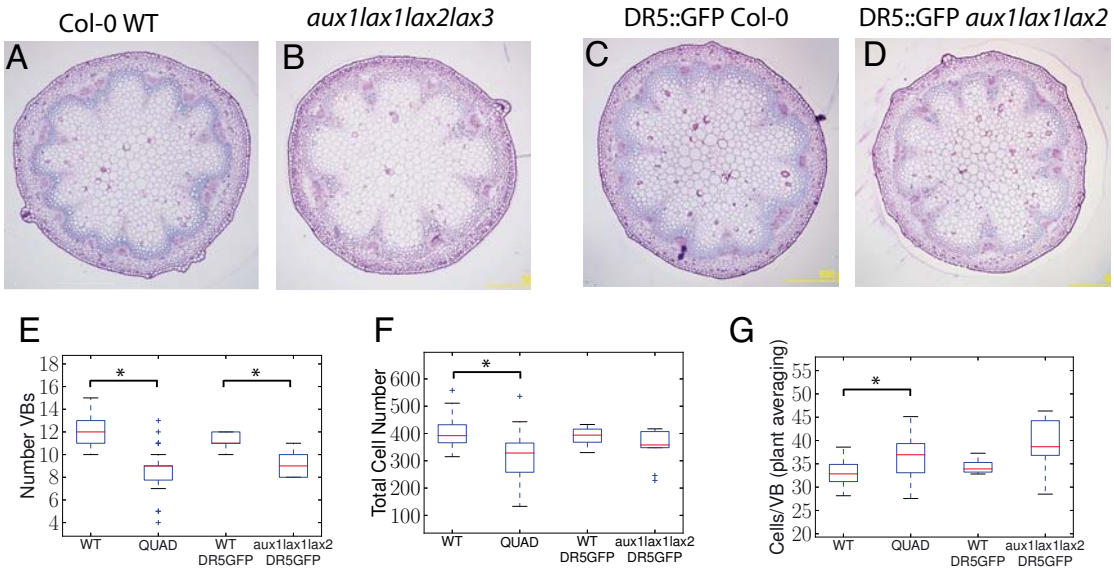

Figure 2. Auxin influx carrier mutants show less vascular bundles and reduced auxin response

(A) Basal shoot transverse section of Col-0 WT (SD). (B) Basal shoot cross section of *aux1lax1lax2lax3* quadruple mutant (SD). (C) Basal shoot cross section of DR5::GFP in Col-0 background (SD). (D) Basal Shoot Cross section of DR5::GFP in *aux1lax1lax2* triple mutant background (SD). (E-G) Boxplots of VB number (E), total cell number (F) and vascular unit λ (cells/VB) (G) for WT, *aux1lax1lax2lax3* mutant, WT DR5::GFP and *aux1lax1lax2* DR5::GFP influx mutant plants. (H-I) Cross section GFP fluorescence of (H) WT DR5::GFP and (I) a*ux1lax1lax2* DR5::GFP plants (J,K) 3D density plots showing the GFP intensities in GFP fluorescence of (J) WT DR5:GFP and (K) *aux1lax1lax2* DR5::GFP plants. Scale bar: 250 µm. Abbreviations: QUAD (Quadruple *aux1lax1lax2lax3* mutant); AU (Arbitrary Units).

The increase in distance between vascular units observed in the *aux1lax1lax2lax3* quadruple mutants is in agreement with the theoretical prediction that influx levels shorten the periodicity of the vascular pattern (Figure 1). Importantly, we noticed that quadruple auxin influx mutants *aux1lax1lax2lax3* also exhibit higher phenotypic variability in the vascular units at both individual plant and population levels (Figure 3)

supporting a stabilizing role for auxin infux carriers. This variability for auxin influx mutants has been addressed previously (Bainbridge et al., 2008) and it was also visible at the adult plant phenotype level (Figure 4). In conclusion, all these results confirmed the model predictions and propose that AUXIN INFLUX CARRIERS are important regulators of vascular patterning in the plant shoot.

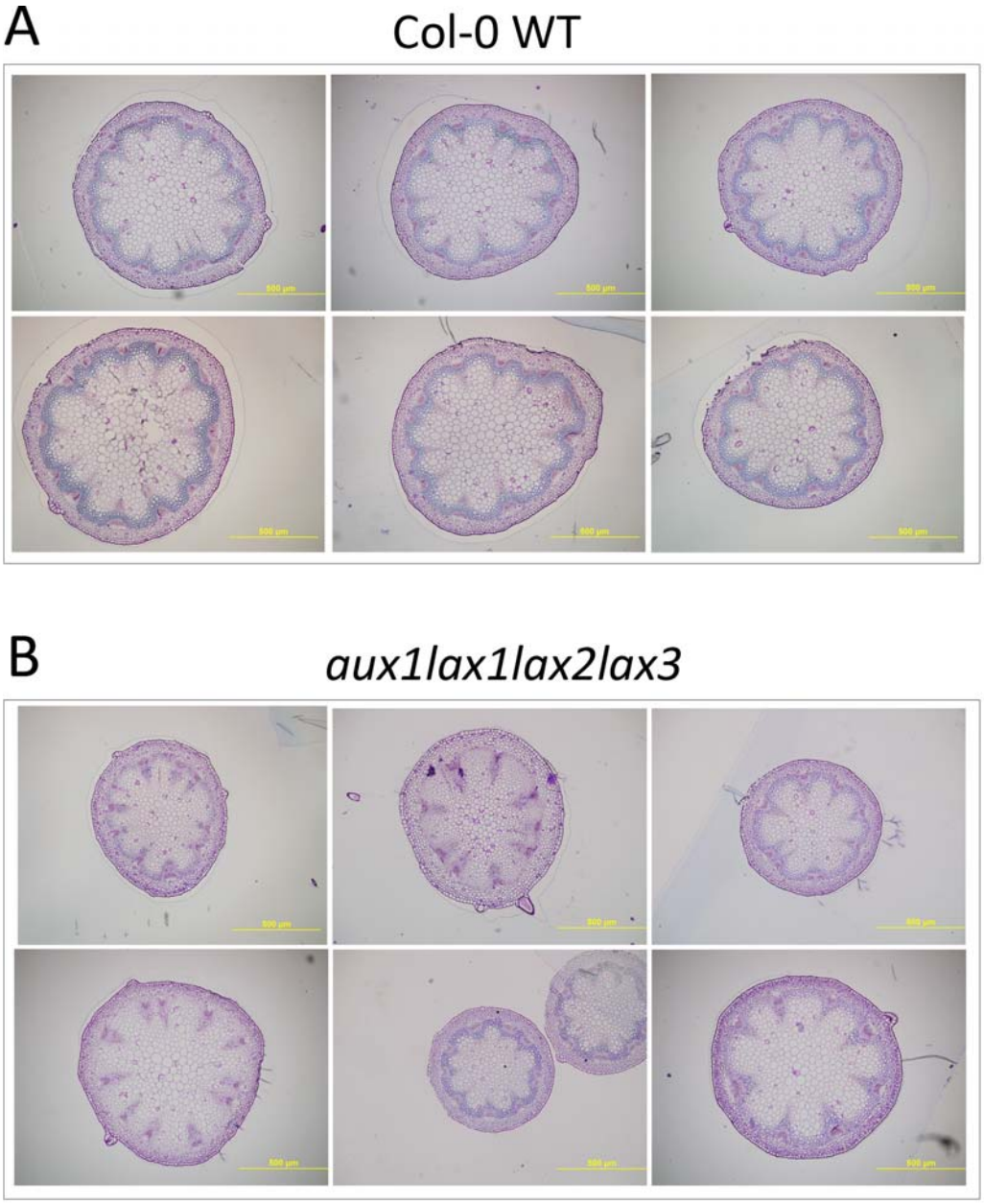

Figure 3. Phenotypic variability of influx mutants in vascular patterning.
(A) Toluidine-blue stained sections of basal inflorescence stems of Col-0 plants
(B) Toluidine-blue stained sections of basal inflorescence stems of quadruple *aux1lax1lax2lax3* mutant plants.

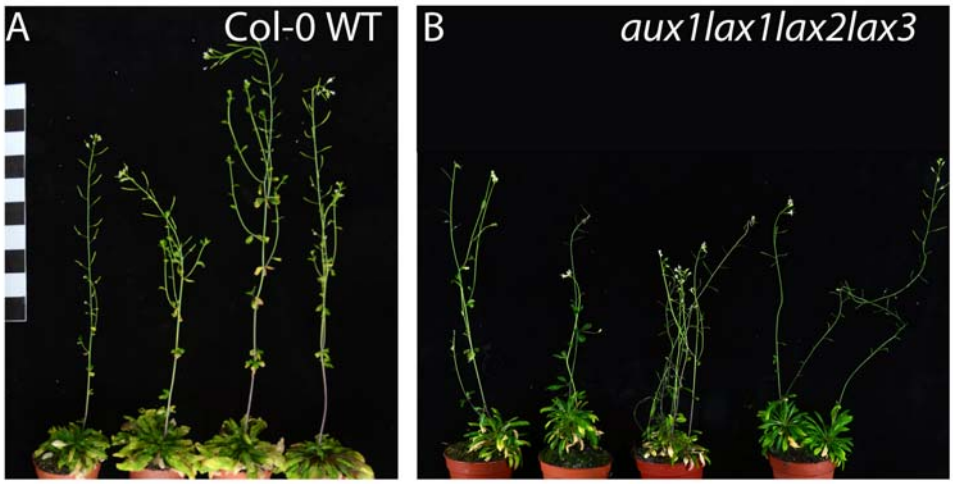

Figure 4. *aux1lax1lax2lax3* quadruple mutants adult display shorter stems than WT plants.
(A) 14-weeks-old Col-0 WT plants grown in SD conditions.
(B) 14-weeks-old *aux1lax1lax2lax3* plants grown in SD conditions.

Auxin influx carriers promote xylem differentiation within the vascular bundle

Because of our simulation results showed a reduced level of auxin inside the cells of when influx transport is impaired (*i.e.* at low I values; Figure 1A), we next tested whether auxin signaling in influx carrier mutants was attenuated by analysing the expression of the auxin response reporter DR5::GFP (Ulmasov et al., 1997) in the *aux1lax1lax2* mutant backgrounds. Compared to the WT DR5::GFP lines, which auxin response appeared within the VBs as reported (Ibañes et al., 2009), *aux1lax1lax2* mutants stem sections showed a dramatic decrease in DR5::GFP fluorescence (Figure 2H,I,J,K) supporting that auxin influx carrier mutations impaired auxin response inside the VB cells**.** In particular, the auxin peaks in *aux1lax1lax2* mutants were narrower, meaning that a smaller ratio of cells harbour auxin maxima in the mutants than in the DR5::GFP control plants (Figure 2 J and K), in agreement with the model predictions (Figure 1A). Since auxin signaling mediates vascular differentiation processes (Fosket and Torrey, 1969; Fukuda and Komamine, 1980; Sachs, 1981; Fukuda, 2004; Perrot-Rechenmann, 2010) we examined whether vascular differentiation was impaired in *aux1lax1lax2lax3* mutants. Compared to WT, *aux1lax1lax2lax3* mutants clearly show undifferentiating of the interfascicular fibers and reduced differentiation of xylem cells within the VB (Figure 5A-F; Figure 3).

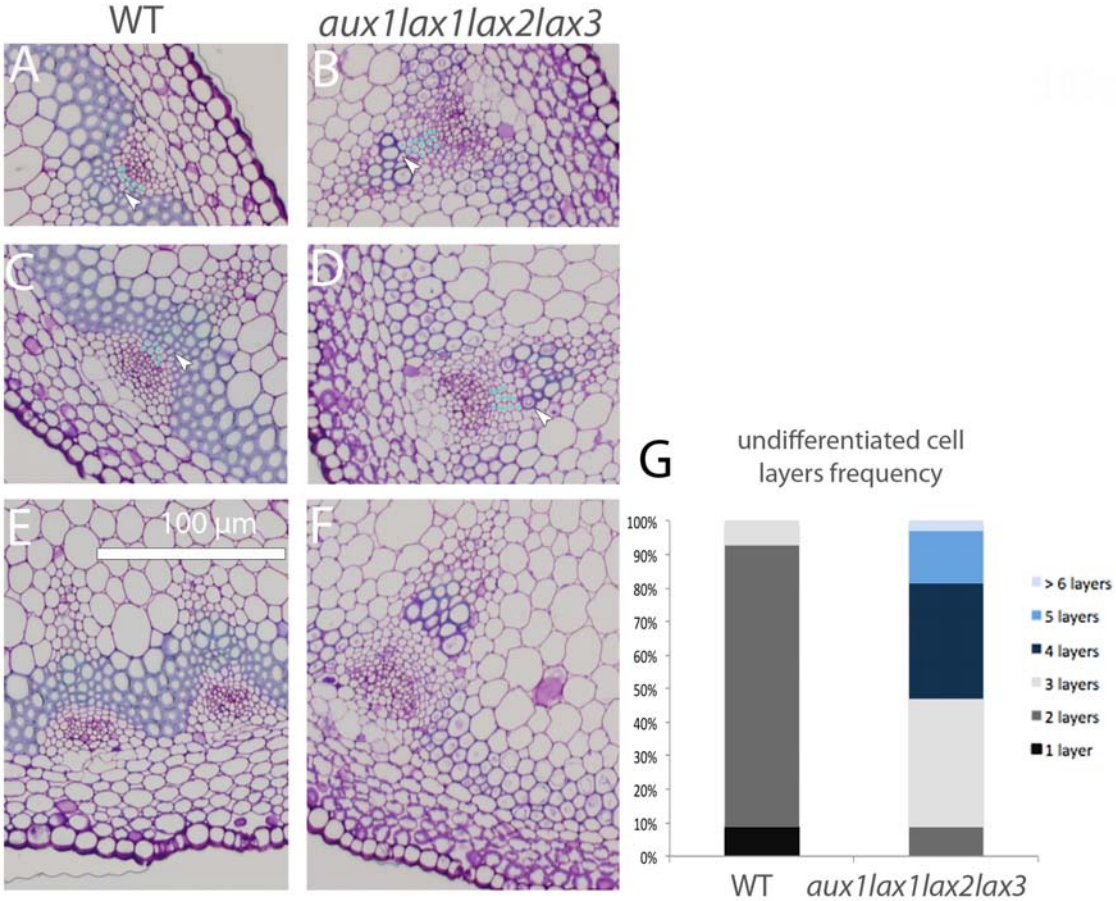

Figure 5. Influx carrier mutants show impaired xylem differentiation in Arabidopsis shoot stem.
(A-F) VB magnification of a shoot basal cross-section for WT (A, C and E) and quadruple mutants *aux1lax1lax2lax3* (B, D and F) (blue dots indicate undifferentiated cell layers between phloem and xylem differentiated cells. First differentiated xylem cell is indicated by white arrow. (G) Distribution of the number of cell layers in procambium, for WT and *aux1lax1lax2lax3* within two biological replicas (n=24). Scale bar: 100 µm.

This lack of differentiation was accompanied by a significant increase of undifferentiated (procambial) cells layers within the VB (Figure 5A-F). All procambial cell layers within the VBs of auxin influx mutants were quantified within two biological replicates, consistently showing 2 undifferentiated cell layers on average in the WT while 3.6 undifferentiated cell layers in the influx mutants. Thus, we plotted the frequency of undifferentiated cell layers number within the observed population (n=25). We observed that 83% of WT plants displayed 2 undifferentiated cell layers while less than 10% of *aux1lax1lax2lax3* showed 2 layers. In fact, 40% of *aux1lax1lax2lax3* mutants showed 3 undifferentiated cell layers while around 50% showed at least 4 undifferentiated cell layers (Figure 5G). In agreement, it has been

previously shown that auxin efflux carrier mutants *pin1pin2* display increased xylem differentiation in the inflorescence shoot stem (Galweiler et al., 1998; Ibañes et al., 2009).

In conclusion, our results reveal a novel role for auxin influx carriers in shoot vascular differentiation and patterning in Arabidopsis plants.

CHAPTER 4

Specific roles for BRL3 signalosome complex in Arabidopsis root development

Norma Fàbregas, Na Li, Sjef Boeren, Sacco de Vries and Ana Caño-Delgado

Specific roles for BRL3 signalosome complex in Arabidopsis root development
Fàbregas N, Li N, Boeren S, de Vries S and Caño-Delgado AI[+] (2013).
The Plant Cell. (submitted June 2013)

SUMMARY

Brassinosteroid (BR) hormones are primarily perceived at the cell surface by the LRR-RLK BRASSINOSTEROID INSENSITIVE 1 (BRI1). In Arabidopsis, BRI1 has two close homologs, BRL1 and BRL3 (BRI1-like 1 and 3 respectively) expressed in the vascular tissues and regulating shoot vascular development. Here we identify components of the BRI1 and BRL3 receptor complexes *in planta* and determine common and different signaling elements for both BR-perception complexes. BRL3 interacting proteins included BAK1 and several other proteins present in BRI1 receptor complexes, although BRL3 was not identified within BRI1 immunoprecipitates, suggesting the formation of different BR receptor complexes in distinct cellular domains. In addition to BRL3, BAK1 interaction with BRL1 receptor was further confirmed by co-immunoprecipitation (co-IP) and fluorescence microscopy analysis. Importantly, genetic analysis of *brl1brl3bak1-3* triple mutants revealed a non-redundant role for BRL3 signalosome in root growth and development by contributing to the cellular activities of provascular and quiescent centre (QC) cells. This provides functional relevance to the observed protein-protein interactions at the BRL3 signalosome. Overall, our study demonstrates that cell-specific BR-receptor complexes are assembled in different cellular activities during plant root growth, while highlights that immunoprecipitation of LRR receptor kinases in plant is a powerful approach for unveiling signaling mechanisms with cellular resolution in plant development.

INTRODUCTION

Plant steroid hormones brassinosteroids (BRs), are perceived by the plasma membrane localized BRASSINOSTEROID INSENSITIVE 1 (BRI1; (Li and Chory, 1997)). BRI1 is one of the best-characterized Leucine-Rich-Repeat Receptor-Like-Kinase (LRR RLK) proteins in plants. Brassinolide (BL) binding occurs at the BRI1 extracellular domain. This domain is made of 24 LRRs interrupted by a 70-amino-acid island domain (ID) placed between 20th and 21st LRR that creates a surface pocket for ligand binding (Wang et al., 2001; Kinoshita et al., 2005; Hothorn et al., 2011; She et al., 2011). Ligand-mediated BRI1 receptor activation results in mutual transphosphorylation events with one or several of the SERK (SOMATIC EMBRYOGENESIS RECEPTOR KINASE) coreceptors, one of which is SERK3/BAK1 (Li et al., 2002; Russinova et al., 2004; Wang et al., 2005; Karlova et al., 2006). Recent evidence suggests that SERKs coreceptors are essential for the BRI1-mediated signaling (Gou et al., 2012). Downstream of BRI1 and SERKs, members of the BSK cytoplasmic kinase family are subject to BRI1-mediated phosphorylation (Tang et al., 2008) and subsequently the signal is transmitted to BES1 and BRZ1 transcription factors (Wang et al., 2002; Yin et al., 2002).

Many of the components of the BRI1 pathway have been identified using forward or reverse genetic approaches (Wang et al., 2012b) while more recently structural studies of the extracellular domain of BRI1 confirmed the behaviour of BRI1 mutant alleles (Hothorn et al., 2011; She et al., 2011). As an alternative approach we have previously employed immunoprecipitation of the GFP–tagged SERK1 coreceptor (Karlova et al., 2006; Smaczniak et al., 2012). This resulted in the identification of BRI1 as well as BAK1, suggesting that at least in part, protein-protein interactions mirror genetic evidence.

In Arabidopsis, there are two closely related members of the small BRI1-like family, BRASSINOSTEROID RECEPTOR LIKE 1 and 3 (BRL1 and BRL3 respectively) that share the overall structure of BRI1 including the ligand-binding ID, and can bind to BL with higher (BRL1) or similar (BRL3) binding affinity that the main BRI1 receptor (Caño-Delgado et al., 2004; Kinoshita et al., 2005). While BRI1 is expressed in most if not all cells (Friedrichsen et al., 2000), the expression of BRL1 and BRL3 is enriched in the vascular tissues. The analysis of *bri1brl1brl3* mutant in the inflorescence stem suggested a

redundant role with BRI1 for these two receptors in controlling cell proliferation during vascular bundle patterning (Caño-Delgado et al., 2004). Since then, the discrete localization of BRLs together with the dramatic phenotype of triple BR-receptor mutants has hampered the identification of novel specific roles for BRL receptors in plant growth and development. In this study, it was of interest to investigate whether the BRI1 and the BRL3 receptors share common downstream elements or are indeed part of a larger BR signalosome complex.

Here, we report the identification of proteins associated with BRI1 and BRL3 receptors using immunoprecipitation and LC-MS/MS techniques (Karlova et al., 2006; Smaczniak et al., 2012). We found that BRI1 and BRL3 complexes shared the BAK1 coreceptor and other previously described BR-signaling components, while no biochemical evidence was found that support a direct interaction between BRI1 and BRL3 in native conditions. BRs control the normal cell cycle progression of root meristematic cells including the rarely divided QC cells during root growth (González-García et al., 2011), yet a role of BRLs in the root has not been reported. The genetic analysis of *brl1brl3* mutants in combination with *bak1-3* confirms a novel cell-specific role of the BRL3 complex in regulating QC cells renewal in response to BRs. Our study unveils the functional relevance of BR-receptor complexes for the control of BR-mediated responses with cellular resolution in plant development.

RESULTS

Protein expression of BRI1-like family members

In Arabidopsis, expression of BRL1 and BRL3 is enriched in the vascular tissues in contrast to that of BRI1 that appears in most plant cells (Caño-Delgado et al., 2004). To reveal the localization of BRL1 and BRL3 receptors, the full-length genomic sequences of *BRL1* and *BRL3* were fused to yellow fluorescent protein (YFP) under the control of the native promoters consisting of 2Kb upstream of the start codon for BRL1 and BRL3 (*ProBRL1:BRL1-YFP* and *ProBRL3:BRL3-YFP*). Localization of these receptor fusions in stable T4 homozygous plants was compared to the one of *ProBRI1:BRI1-GFP* plants, previously shown to complement *bri1* null mutants (Geldner et al., 2007). Root analysis of 6-day-old plants revealed the presence of BRI1-GFP in all cell files of the root apical

meristem (Figure 1A), similar to reported by (Friedrichsen et al., 2000; Geldner et al., 2007; van Esse et al., 2011). Further up in the meristem, a transversal confocal microscopy view showed a predominant BRI1 localization at the outer cell files (epidermis/cortex) at the differentiation zone (Figure 1E). In contrast to BRI1, the localization pattern for BRL1 and BRL3 was specific to a few cell files. At the root apex BRL1 and BRL3 are similarly localized at the quiescent center (QC), columella stem cells (CSC) and a group of provascular cells including vascular initials cells located right above the QC (Figure 1B, C). Transverse view at the differentiation zone of the root showed the presence of BRL3 at the phloem-pole pericycle (PPP) cells (Figure 1F), whereas BRL1 was absent from these cells (Figure 1G).

Since the expression of BRL1 and BRL3 receptors under their native promoters was lower than that of *ProBRI1:BRI1-GFP* lines, additional *35S:BRL3-GFP* overexpressing plants were established in order to increase the amount of BRL3 protein in the plant (Figure 1D, H; Figure 2). The analysis of *35S:BRL3-GFP* plants revealed a localization pattern similar to the *ProBRL3:BRL3-YFP* native lines (Figure 1B, D), suggesting an additional spatial control at the protein level for BRL3. At the elongation and differentiation zone of the root, a stele-specific localization was found in *35S:BRL3-GFP* plants (Figure 1H).

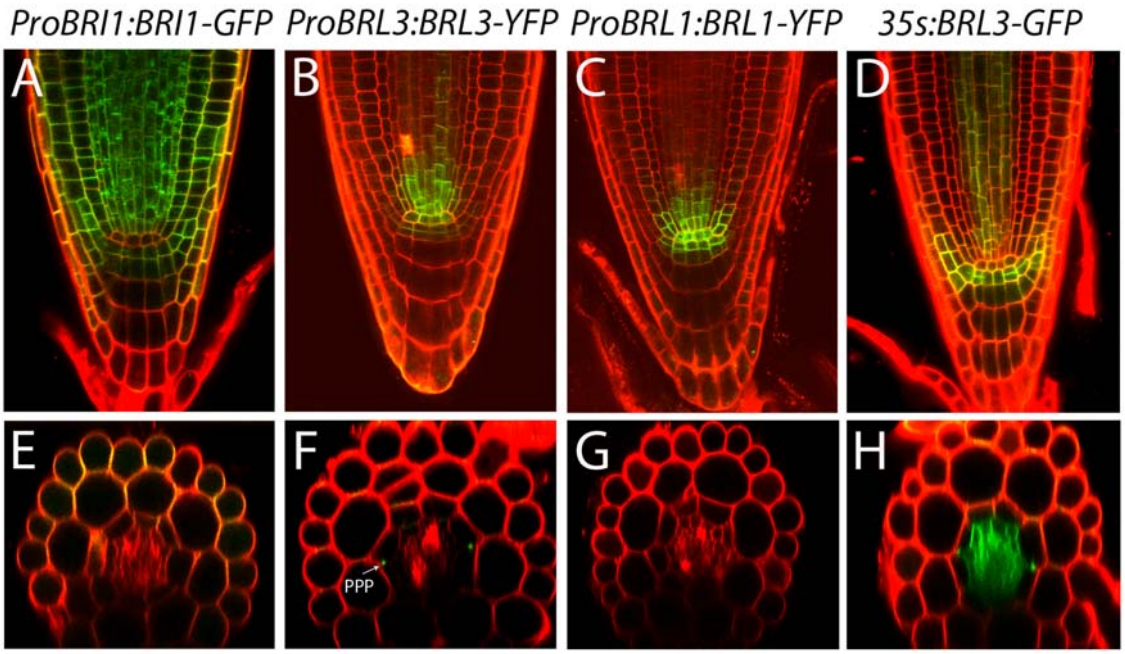

Figure 1. Spatial localization of BRI1-like family receptors in Arabidopsis.

(A-H) 6-day-old seedlings expressing *ProBRI1:BRI1-GFP* (A,E), *ProBRL3:BRL3-YFP* (B,F), *ProBRL1:BRL1-YFP* (C,G) and *35S:BRL3-GFP* (D,H) in the MZ of the primary root. (A) *ProBRI1:BRI1-GFP* plants ubiquitous expression at the MZ. (B) *ProBRL3:BRL3-YFP* expression in the QC, CSC and vascular initials of the MZ. (C) *ProBRL1:BRLI1-YFP* plants show provascular expression overlapping with *ProBRL3:BRL3-YFP* in the MZ. (D) *35S:BRL3-GFP* plants show a similar localization pattern to plants expressing *ProBRL3:BRL3-YFP*. (E) Confocal radial sections of *ProBRI1:BRI1-GFP* expression in the epidermis and cortex at the (DZ) of the root. (F) *ProBRL3:BRL3-YFP* localization in the Phloem Pole Pericylce (PPP) , compared to (G) *ProBRL1:BRLI1-GFP* that is absent at the DZ of the root. (H) A confocal radial view of *35S:BRL3-GFP* denotes BRL3 localization in the stele of the DZ of the root. Abbreviates: MZ (Meristematic Zone), DZ (Differentiation Zone), QC (Quiescent Center), CSC (Columella Stem Cells), PPP (Phloem Pole Pericycle). Scale bar 100 µm.

In mature plant organs, BRL1 and BRL3 were predominantly localized at leaf veins and associated to phloem tissues in the vascular bundles of the shoot inflorescence stem (Figure 2). While *35S:BRL3-GFP* plants showed a strong localization in the vascular tissues, GFP protein was also present at the epidermis where BRI1 is predominantly localized (Figure 3).

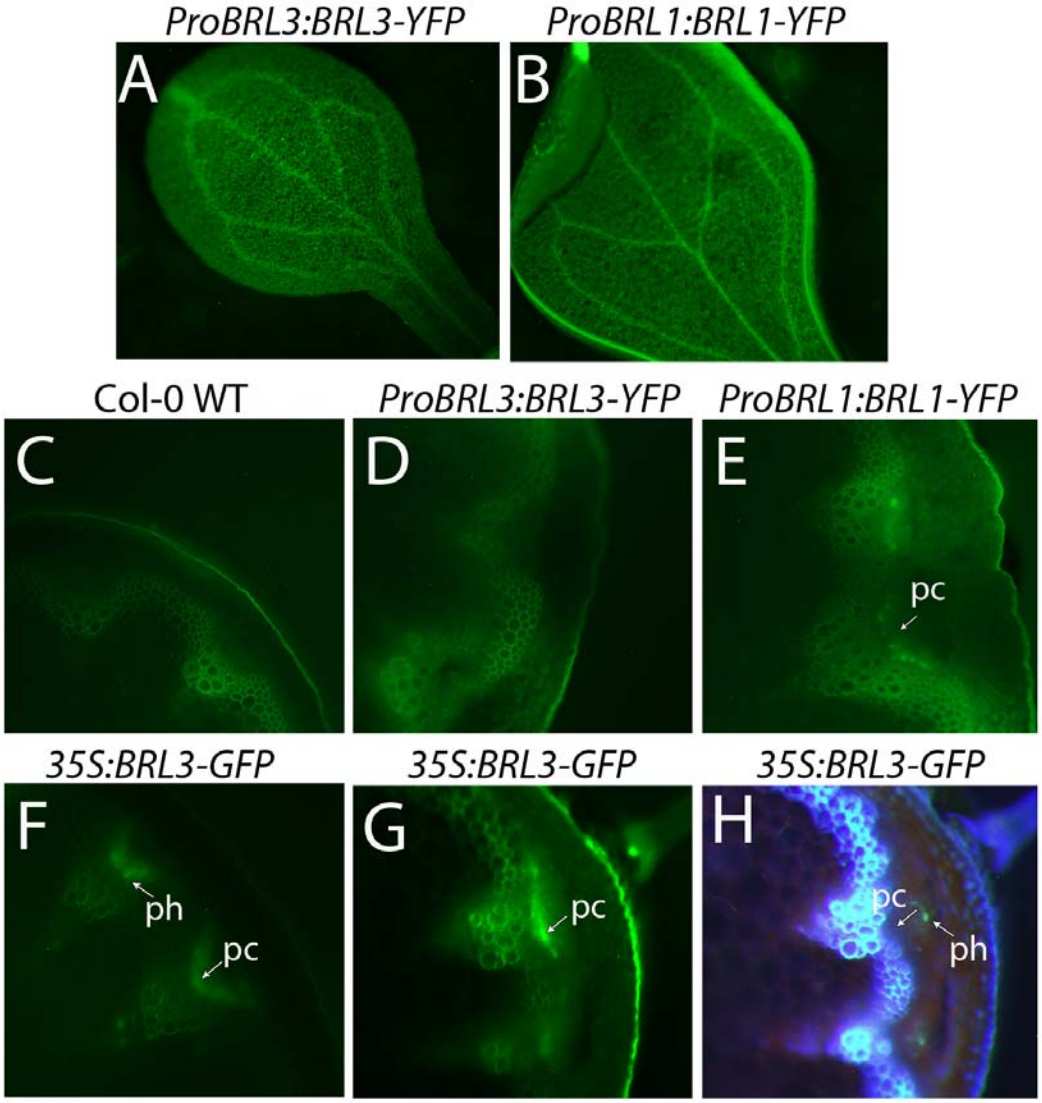

Figure 2. Vascular expression pattern of BRI1-like receptors family in other plant organs
(A, B) *ProBRL3:BRL3-YFP* (A) and *ProBRL1:BRLI1-GFP* (B) native lines show BRL3 and BRL1 receptor proteins predominantly localized at leaf venation. (C, D) Col-0 WT and *ProBRL3:BRL3-YFP* shoot stem radial hand-cuts respectively (in green xylem autofluorescence). (E) *ProBRL1:BRL1-YFP* shoot stem hand cut sections showing expression in the phloem tissues of the vascular bundles. (F) *35S:BRL3-GFP* plants showed vascular expression in the phloem and procambial cells of shoot stem radial handcuts. (G, H) *35S:BRL3-GFP* is localized in the procambial and phloem cells of the shoot vascular bundles (H) Aniline blue mark phloem cells. Green autofluorescence background is visualized in Col-0 WT xylem cells unspecific fluorescence. Abbreviates: pc (procambium), ph (phloem).

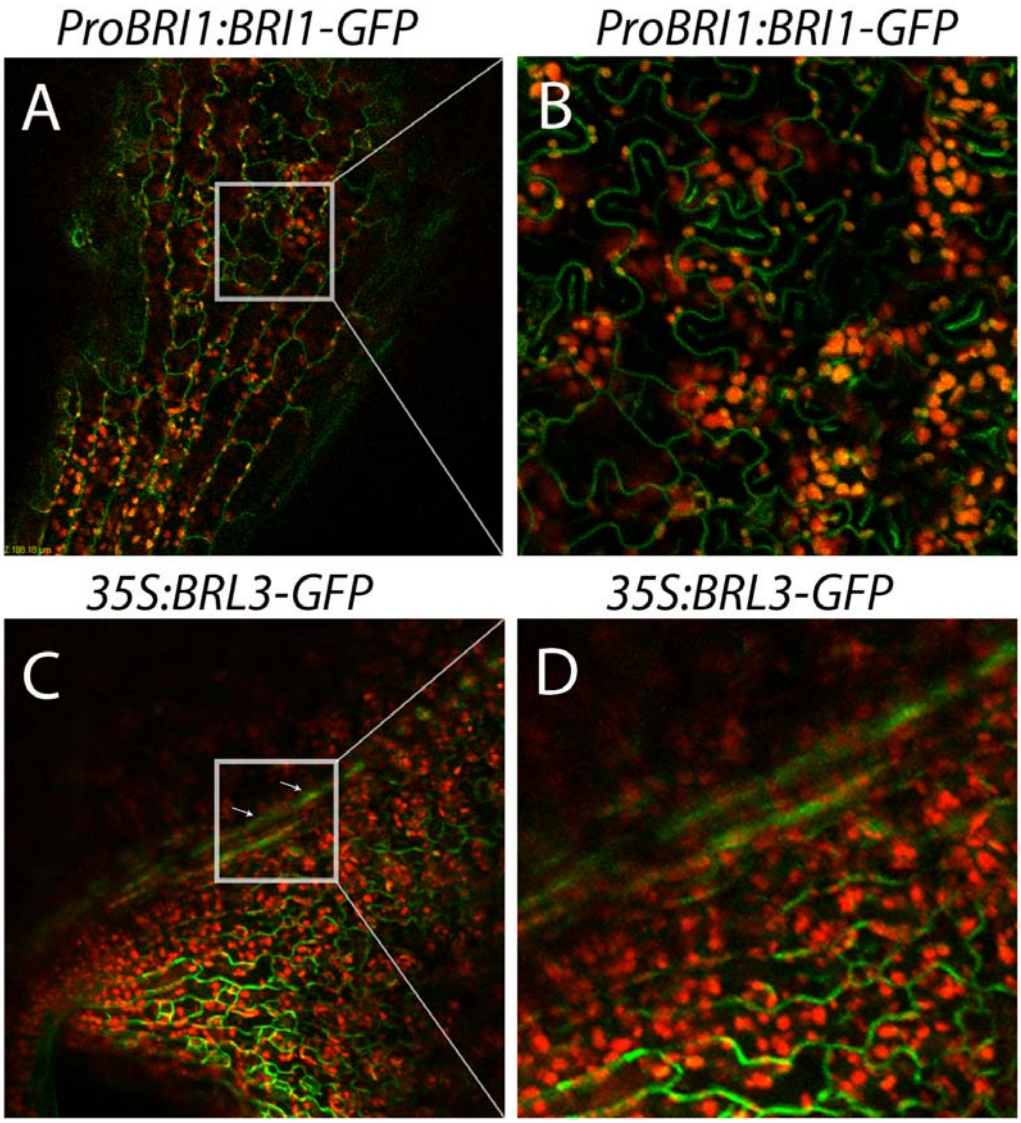

Figure 3. *ProBRI1:BRI1-GFP* and *35S:BRL3-GFP* show different and overlapping localization patterns in the leaves
(A, B) *ProBRI1:BRI1-GFP* lines show BRI1 localization predominantly localized in the epidermal cells of the leaves. (C, D) In *35S:BRL3-GFP* lines, expression in leaves showing partially overlapping localization with BRI1 receptor in those cells but not in the vasculature where BRL3 is highly expressed.

Identification of BRI1-interacting proteins

Previously identified BRI1 interactors have been essential for understanding BR signal transduction in the plant, yet the nature of the native BRI1 complex has not been revealed. Here, 10-day-old *ProBRI1:BRI1-GFP* seedlings were used to purify the native BRI1 complex by immunoprecipitation (IP) using immobilized anti-GFP antibodies (see

Material and Methods). Wild-type Col-0 (WT) seedlings were used as a control to clean out proteins binding non-specifically to the anti-GFP beads. A total of three independent biological replicates were done for BRI1 and WT complexes purified in pairs. The resulting peptides were measured by liquid chromatography mass spectrometry (nLCMS) (see Material and Methods). Quantitative analyses selected a total of 327 statistical significant BRI1 candidate interactors (FDR <= 0.0005, S0=1; dots above the green curve in the right hand side of Figure 4A). A complete list of BRI1 interactors is provided in Supplemental Table S1 annexed.

Our analysis identified BRI1 and its tag GFP, the vacuolar ATPases VHA-A2 and VHA-A3 (Dettmer et al., 2006) and the ATPase 2 between the most enriched proteins in the IP (Log Protein ratio [BRI1/WT] > 4); (Figure 4B). Furthermore, known BRI1-interacting membrane proteins were also present including BAK1 coreceptor (Li et al., 2002; Nam and Li, 2002) and the AHA1 plasma membrane ATPase (Witthoft et al., 2011). Additional proteins previously related to BR signaling such as DET3 (Schumacher et al., 1999), the sec14-like protein PATL2 (Deng et al., 2007), the LRR-RLKs THESEUS, FERONIA, HERCULES (Guo et al., 2009a) and the PP2AA1/RCN1 phosphatase (Wu et al., 2011) were identified as candidate BRI1 interactors (Figure 4B, See Supplemental Table S1 annexed). These results demonstrate the efficacy of the immunoprecipitation technique for the identification of key BRI1 interactors and signaling components in the plant.

Interestingly, a number of uncharacterized signaling proteins including several LRR-RLKs, kinases and phosphatases (Mora-García et al., 2004) were identified among the most significant BRI1 interactors (Figure 4B, See Supplemental Table S1 annexed). The presence of membrane trafficking components such clathrins and other elements of the endocytic machinery, several ABC transporters (Sanchez-Fernandez et al., 2001), auxin efflux carriers PIN3 and PIN7 (Friml et al., 2002; Friml et al., 2003) that appeared significantly represented in the native BRI1 IPs, supports the different compartmentalization of the BRI1 receptor among the signaling cascade (Irani et al., 2012). Interestingly, a large number of the total proteins found after IP were integral membrane proteins (aprox. 15%) previously identified as BES1 and/or BZR1 targets

that might imply a feedback control of these proteins by BR signaling (Figure 4B; Sun et al., 2010; Yu et al., 2011).

A

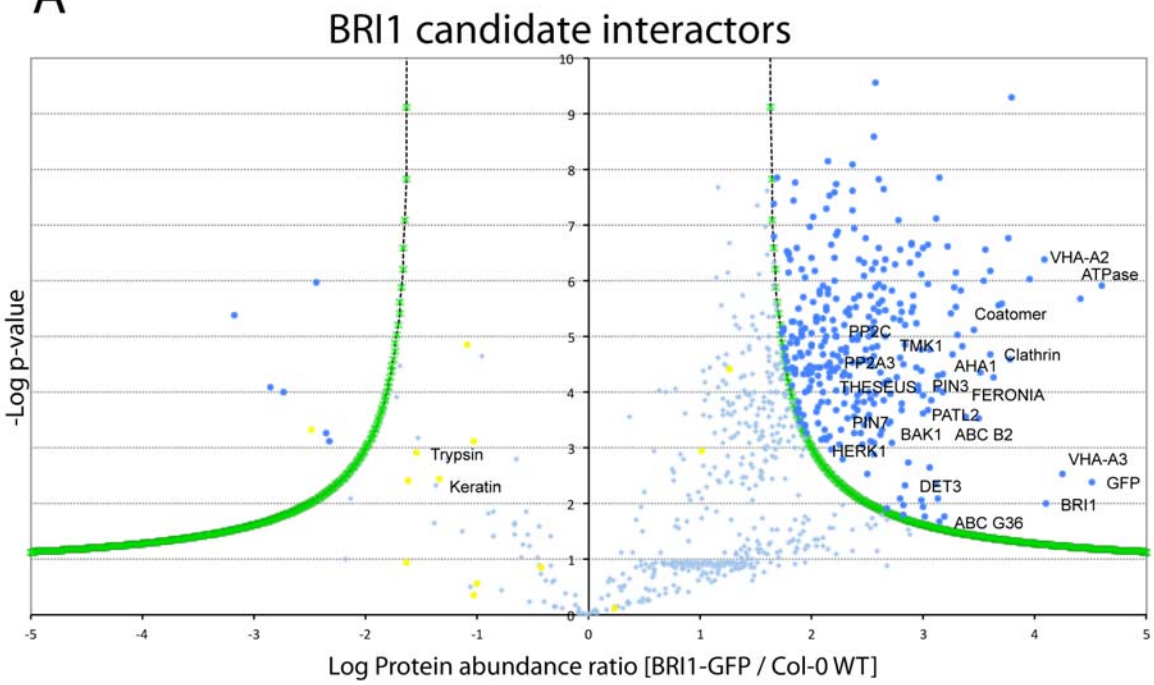

B

Gene Locus	Protein name	Localization	Type	BZR/BES1 target	ratio
Brassinosteroids					
At4g39400	BRI1 Protein BRASSINOSTEROID INSENSITIVE 1	plasma membrane	LRR-RLK	yes / yes	4.10
At1g22530	PATL2 Patellin-2	plasma membrane	transporter	yes (low)	3.07
At1g12840	DET3 Putative uncharacterized protein (Fragment)	membrane, vacuole	LRR-RLK	no / yes	2.84
At4g33430	BAK1 BRASSINOSTEROID INSENSITIVE 1-associated receptor kinase 1	plasma membrane	LRR-RLK	yes / yes	2.32
At3g51550	FERONIA Receptor-like protein kinase	plasma membrane	LRR-RLK	yes (low)	3.00
At5g54380	THESEUS 1 Receptor-like protein kinase	plasma membrane	LRR-RLK	yes (low)	2.22
Signalling					
At2g37050	LRR-RLK Putative receptor-like protein kinase	plasma membrane	LRR-RLK		2.73
At5g46330	FLS2 LRR-RLKH Leucine-rich repeat receptor-like protein kinase (Fragment)	plasma membrane	LRR-RLK	yes	2.69
At1g66150	TMK1 Probable receptor protein kinase TMK1	plasma membrane	LRR-RLK	yes	2.54
At3g28040	Probably inactive leucine-rich repeat receptor-like protein kinase	plasma membrane	LRR-RLK		2.22
At3g58500	PP2A3 Serine/threonine-protein phosphatase PP2A-3 catalytic subunit	cytoplasm	phosphatase		2.16
At2g20050	PP2C Protein phosphatase 2C and cyclic nucleotide-binding/kinase domain	cytoplasm	phosphatase		2.20
Transport					
At4g39080	VHA-A3 Putative proton pump	vacuole, tonoplast	ATPase	yes	4.25
At2g21410	VHA-A2	vacuole, tonoplast	ATPase		4.08
At4g30190	AHA1 ATPase 1 plasma membrane-type	vacuole	ATPase	yes	4.19
At1g23080	PIN7 Auxin efflux carrier component 7	plasma membrane	transporter	yes / yes	2.47
At4g25960	ABCB2 ABC transporter B family member 2	membrane	transporter	yes (low)	2.99
At1g59870	ABCG36 ABC transporter G family member 36	membrane	transporter	yes	3.15
At1g70940	PIN3 Auxin efflux carrier component 3	membrane, vesicles	transporter	yes	2.95
Trafficking					
At3g08530	CLAH2 Clathrin heavy chain 2	cytoplasm, membrane	structural	yes (low)	3.60
At4G34450	Coatomer subunit gamma	cytoplasm, membrane	binding		3.29

Figure 4. Immunoprecipitation of the BRI1 receptor complex from Arabidopsis seedlings.
(A) Plot shows protein abundance ratios of BRI1 candidate interactors proteins (x axis) compared to the negative control Col-0 WT (WT). The intensity of these values has been calculated by MaxQuant software. Quantitative analyses selected a total of 322 statistical significant BRI1 candidate interactors with FDR <= 0.0005 represented as blue dots above the

green curve (A). The remaining 553 proteins did not meet the cut-off p-value and therefore were considered to be less likely BRI1 interactors (A; light blue dots).
(B) Summary table of BRI1 candidate interactors. Abbreviates: (False Discovery Rate) FDR.

Identification of BRL3-interacting proteins

To investigate whether BRL receptors may confer BR perception specificity for a group of cells, BRL3 interacting proteins were identified using the same methods as above. First, the *ProBRL3:BRL3-YFP* line was used. In this line, the amount of BRL3-YFP protein was undetectable in total protein extracts by direct Westerns, yet successfully enriched after IP (Figure 5A; Figure 10A). Peptide measurement by nLCMS of native BRL3 IPs only yielded a few proteins besides the BRL3 bait that included BRL1, DET3 and clathrin-binding protein At4g18060 (Figure 5B).

A

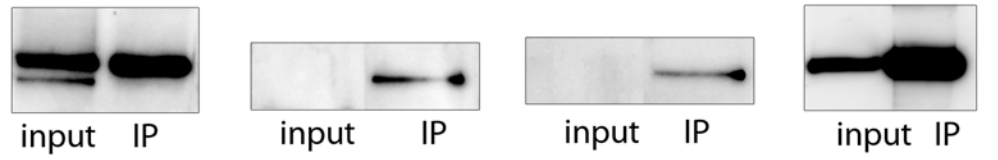

B

Protein	Peptide	MH+	DeltaM (ppm)	P (pro) P (pep)	Sf Sf	Score XC	Coverage DeltaCn	MW Sp	Peptide (Hits) Ions
BRL1	-.KGGIYLN#WAAR.-	1249.66878	-4.03232	1.49E-01	0.30	2.42	0.43	403.2	10/20
At1g55610	-.RPTMIQLM*AMFK.-	1482.76296	-5.82653	9.88E-01	0.14	2.23	0.44	257.5	9/22
DET3	R.LQEQISK.H	845.47272	-1.31533	9.46E-01	0.68	2.16	0.09	410.3	10/12
At1g12840	R.VAEYNNIR.G	978.50031	-0.20087	2.74E-03	0.80	2.17	0.43	482.5	10/14
	K.LVQDQESLR.S	1087.57422	-3.88467	9.43E-06	0.92	2.54	0.44	809.2	14/16
	K.HSFDTPVYR.F	1121.53748	0.15127	3.51E-05	0.78	2.16	0.49	286.3	11/16
	K.SNSFVEGVSQK.I	1181.57971	-1.19946	7.54E-05	0.93	2.84	0.52	887.5	16/20
	K.EVVDNIQSQVAK.I	1329.70093	-2.71830	4.56E-05	0.93	2.95	0.52	986.2	16/22
	R.DFEQSVEAQETR.K	1438.64453	4.10592	6.14E-05	0.94	2.78	0.56	1163.3	16/22
	R.DLSNLVKPEDIVESEHLVTLLAVVPK.Y	2857.59204	0.22083	5.66E-07	0.95	5.18	0.67	1114.9	35/150
Clathrin binding	R.LVAMVEGEK.N	975.51794	-2.39133	6.84E-03	0.90	2.56	0.51	567.9	13/16
At4g18060	R.IAAILSDIEAEMVTEK.Q	1732.90369	-4.62175	1.50E-07	0.97	3.82	0.60	1495.5	20/30

Figure 5. Immunoprecipitation of the BRL3 receptor complex in *ProBRL3:BRL3-YFP plants*
(A, left panel) Western blot (input) for *ProBRI1:BRI1-GFP* plants and immunoprecipitation (IP) by antiGFP antibodies detecting with antiBRI1 antibodies.
(A, middle and right panels) *ProBRL3:BRL3-YFP, ProBRL1:BRL1-YFP* and *35S:BRL3-GFP* immunoprecipitation by antiGFP antibodies blotting with antiGFP antibodies. 10 grams of seedlings as initial material were used in all the experiments and the same volume of protein extract was loaded in each well of the gel. (B) Table of specific and unique peptides identified

for BRL1, DET3 and clathrin by immunoprecipitation coupled to MS and analysed with Bioworks software for *ProBRL3:BRL3-YFP* line.

To increase the sensitivity of our approach, *35S:BRL3-GFP* lines were subsequently used for IP (Figure 1C, D, G, H; Figure 2A, Figure 6).

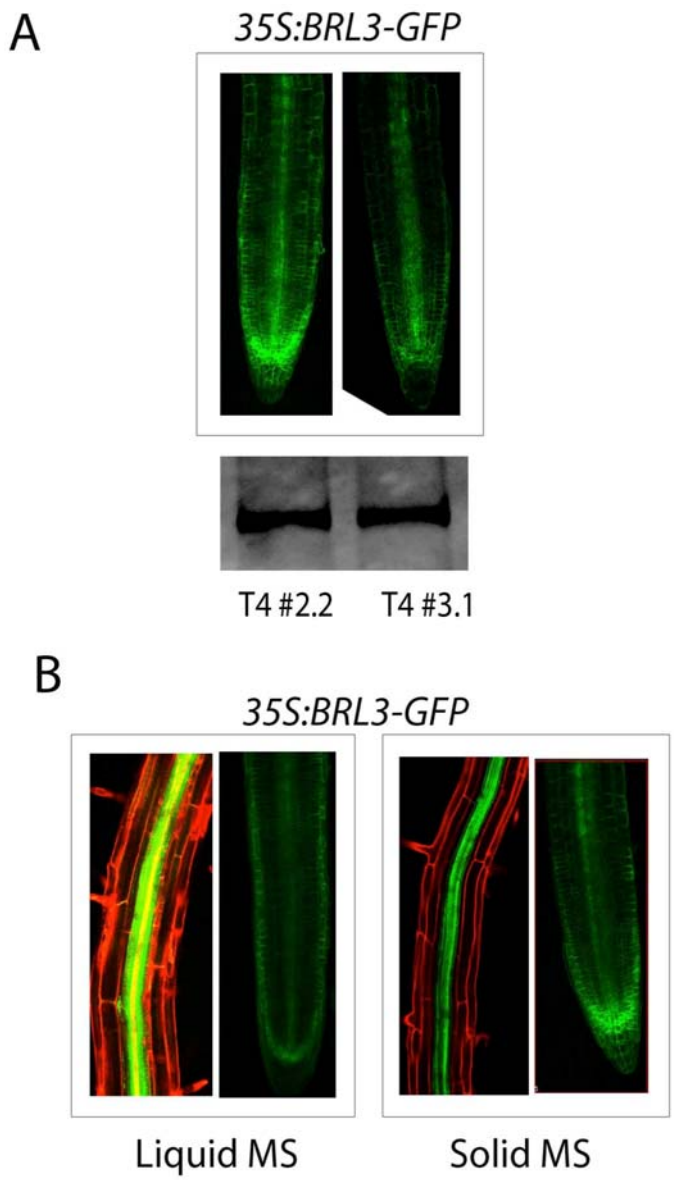

Figure 6. BRL3 protein localization of *35S:BRL3-GFP* lines is not altered in MS liquid under agitation conditions
(A) *35S:BRL3-GFP* lines were generated and T4 #2.2 line showing most vascular enriched GFP expression was used for further experiments. (B) 10-day-old plants grown in MS1 liquid shaking culture (used for IPs) show the same expression pattern than plants grown vertically in MS1 agar plates during 10 days (used for confocal imaging).

Thus, a total of 270 candidate BRL3 interactors were significantly enriched (FDR<=0.005, S0=1; green dots above the blue line in the right hand side of Figure 7A). A complete list of the proteins identified is shown in Supplemental Table S2 annexed. The specific peptides found for BRL1 in the IPs of both *ProBRL3:BRL3-YFP* and *35S:BRL3-GFP* lines strongly supported the in vivo interaction between BRL1 and BRL3 receptors in Arabidopsis.

Previously described components of BR signaling such as BSK1, BSK3 (Kim et al., 2011) and DET3 as well as the BR biosynthesis protein Diminuto (DWF1) (Klahre et al., 1998) were found among the most-likely interactors of BRL3 (Figure 7B). Indeed, the coreceptor BAK1 was purified as a highly significant interactor of BRL3. In contrast, BRI1 itself was not detected among the significant BRL3 interactors.

The VHA-A3 and AHA1 ATPases were enriched in BRL3 IPs as well as a group of uncharacterized LRR-RLKs and phosphatases (See Supplemental Table S2 annexed). Trafficking and transport related proteins such as clathrins, ABC transporters, sugar transporters and PIN3 efflux carrier were also present, confirming the presence of BRL3 in similar general trafficking pathways compared to BRI1.

A

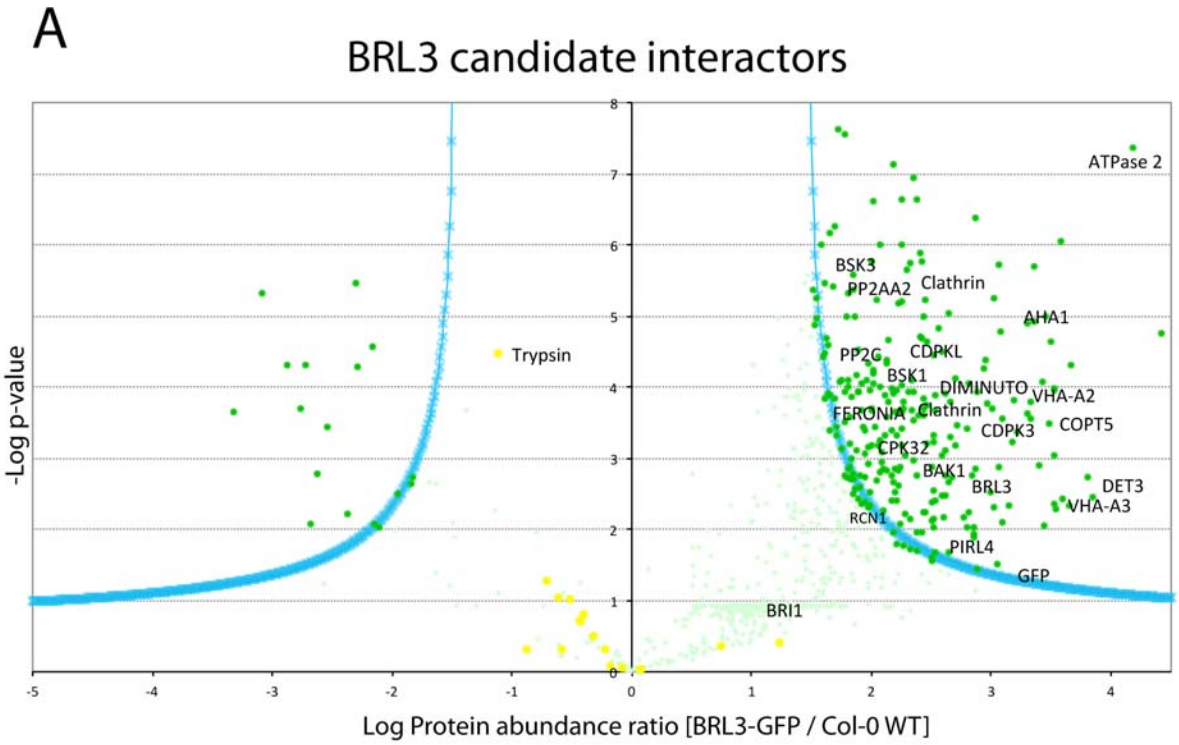

B

Gene Locus	Protein name	Localization	Type	BZR/BES1 target	ratio
Brassinosteroids					
At3g13380	BRL3 Receptor-like protein kinase BRI1-like 3	plasma membrane	LRR-RLK	yes / yes	2.05
At1g55610	BRL1 Receptor-like protein kinase BRI1-like 1	plasma membrane	LRR-RLK	yes / yes	2.05
At3g19820	DIMINUTO Delta(24)-sterol reductase	plasma membrane	BR synthesis		2.43
At4g00710	BSK3 BR-signalinG kinase 3	plasma membrane	kinase	yes (low)	1.61
At4g35230	BSK1 Probable serine/threonine-protein kinase BR-signaling kinase 1	plasma membrane	kinase	yes	2.01
At4g33430	BAK1 BRASSINOSTEROID INSENSITIVE 1-associated receptor kinase 1	membrane, endosome	LRR-RLK	yes / yes	2.25
At1g12840	DET3 Putative uncharacterized protein (Fragment)	membrane, vacuole	LRR-RLK	no / yes	3.85
At3g51550	FERONIA Receptor-like protein kinase FERONIA	plasma membrane	LRR-RLK	yes (low)	2.20
Signalling					
At4g23650	CDPK3 CPK3 Calcium-dependent protein kinase 3	cytoplasm, membrane	kinase	yes (low)	2.79
At1g63500	Protein kinase protein with tetratricopeptide repeat domain	plasma membrane	kinase	yes (low)	2.42
At4g35470	PIRL4 Plant intracellular Ras-group-related LRR protein 4	plasma membrane	LRR-RLK		2.38
At1g27190	LRR-RLK Leucine-rich repeat receptor-like protein kinase (Fragment)	plasma membrane	LRR-RLK		2.14
At3g57530	CDPKW CPK32 Calcium-dependent protein kinase 32	cytoplasm, membrane	kinase	yes	2.21
At3g25800	PP2AA2 Serine/threonine-protein phosphatase 2A 65 kDa regulatory subA	cytoplasm	phosphatase		1.68
At1g78200	PP2C 17 Probable protein phosphatase 2C 17	cytoplasm	phosphatase		1.81
Transport					
At4g39080	VHA-A3 Putative proton pump	vacuole, tonoplast	ATPase	yes	3.52
At2g21410	VHA-A2	vacuole, tonoplast	ATPase		3.09
At4g30190	AHA1 ATPase 1 plasma membrane-type	vacuole	ATPase	yes	4.19
At5g20650	COPT5 Copper transporter 5	cytoplasm, vacuole	transporter		3.32
At1g70940	PIN3 Auxin efflux carrier component 3	membrane, vesicles	transporter	yes	2.35
At3g19930	STP4 Sugar transport protein 4	plasma membrane	transporter	yes	1.88
Trafficking					
At2g20760	CLC2 Clathrin light chain 1	cytoplasm, membrane	structural	yes (low)	2.09
At3g60190	DRP1E Dynamin-related protein 1E	membrane, cell plate	GTPase	yes	2.36

Figure 7. Immunoprecipitation of the BRL3 receptor complex from Arabidopsis seedlings.
(A) Plot showing BRL3 triplicates results analysed by MaxQuant software with the same parameters that BRI1 IPs. Green dots above the curve represent 253 candidate BRL3 interactors significantly enriched in the BRL3 sample compared to the WT with a FDR <= 0.005. The remaining 589 proteins were considered to be less likely BRL3 candidate interactors (A; light green dots).

(B) Summary table of enriched BRL3 candidate interactors showing previously described components of BR signaling, some ATPases, some uncharacterized LRR-RLKs and phosphatases and trafficking and transport related proteins. Abbreviates: (False Discovery Rate) FDR.

Comparison of BRI1 and BRL3 receptors complexes

To address to what extent the BR receptor complex composition was distinct in the different cellular domains where BRL3 is present, a comparative analysis between both BRI1 and BRL3 pull down lists was carried out (Figure 8A and 8B). The analysis yielded a total of 146 potential interactors (54% of the BRL3 interactors) unique for BRL3 (Figure 8A and 8B, See Supplemental Table S3 annexed) of which half were membrane proteins by GO analysis. Significantly, a total of 124 common proteins (46% of the BRL3 interactors), including the coreceptor BAK1, were present in both BRI1 and BRL3 IP results (Figure 8A and 8B, See Supplemental Table S4 annexed) suggesting several common and overlapping functions between the two BR pathway receptors.

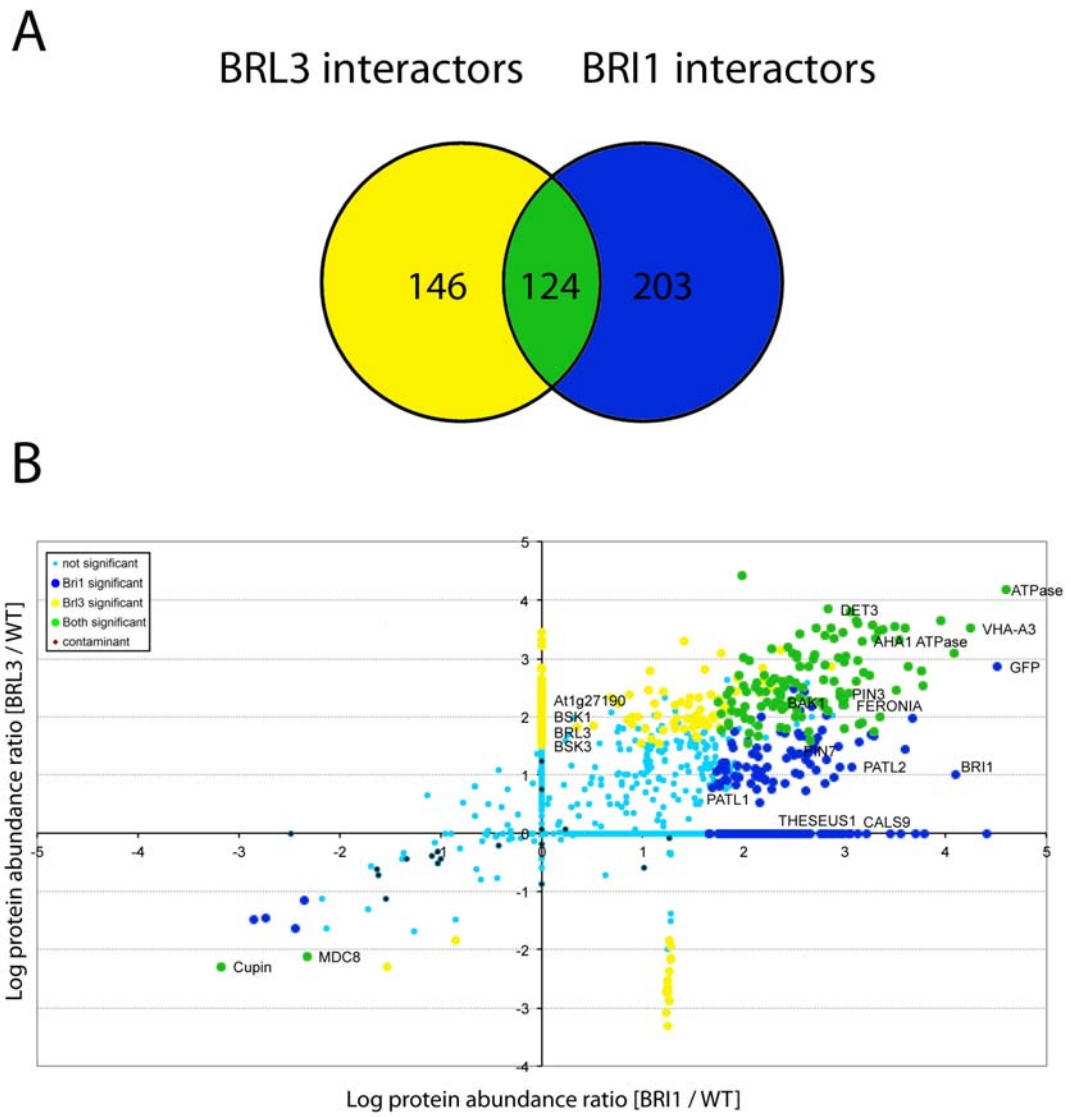

Figure 8. Comparison of BRI1 and BRL3 receptors complexes.
(A) Venny diagram representing the statistical significant BRL3 receptor interactors in blue with the significant candidate interactors detected for BRI1 receptor in yellow (A). (B) Plot showing protein abundance ratios of BRI1 candidate interactors proteins (x axis) compared to protein abundance ratios of BRL3 candidate interactors proteins (y axis). Color legend for common or specific interactors is represented in the upper left side of the plot.

Furthermore, a list of 203 BRI1-specific partners was generated (Supplemental Table S5 annexed) that included BR related proteins such as the PATL2 and THESEUS (Figure 9). A summary list showing up some of the significant signaling proteins after the comparison between BRL3 and BRI1 IP results is shown in Figure 9. A new group of LRR membrane proteins identified may unveil potential candidates to be associated directly or in close proximity to BRI1.

Taken together, our results show that only half of BRL3 interactors are shared with BRI1 and that BRI1 receptor is absent from the significant interactors list for BRL3 complex.

Gene Locus	Protein name	BZR/BES1	type	localization	BRI1	common	BRL3
Brassinosteroids							
At4g39400	BRI1 Protein BRASSINOSTEROID INSENSITIVE 1	yes / yes	LRR-RLK	membrane	x		
At1g22530	PATL2 Patellin-2	yes (low)	transporter	membrane	x		
At1g12840	DET3 Putative uncharacterized protein (Fragment)	no / yes		membrane, vacuole	x		
At3g13380	BRL3 Receptor-like protein kinase BRI1-like 3	yes / yes	LRR-RLK	membrane			x
At3g19820	DIMINUTO Delta(24)-sterol reductase		BR synthesis	membrane			x
At4g00710	BSK3 BR-siGnalinG kinase 3	yes (low)	kinase	membrane			x
At4g35230	BSK1 Probable serine/threonine-protein kinase BR-signaling kinase 1	yes	kinase	membrane			x
At4g33430	BAK1 BRASSINOSTEROID INSENSITIVE 1-associated receptor kinase 1	yes / yes				x	
At3g51550	FERONIA Receptor-like protein kinase FERONIA	yes (low)				x	
Signalling							
At2g37050	LRR-RLK Putative receptor-like protein kinase		LRR-RLK	membrane	x		
At4g23180	CRK10 Cysteine-rich receptor-like protein kinase 10	yes	CRR-RLK	membrane	x		
At5g46330	LRR-RLKH Leucine-rich repeat receptor-like protein kinase (Fragment)	yes	LRR-RLK	membrane	x		
At1g66150	TMK1 Probable receptor protein kinase TMK1	yes			x		
At5g65700	BAM1 Leucine-rich repeat receptor-like serine/threonine-protein kinase	no / yes	LRR-RLK	membrane	x		
At3g28040	Probably inactive leucine-rich repeat receptor-like protein kinase		LRR-RLK	membrane	x		
At3g58500	PP2A3 Serine/threonine-protein phosphatase PP2A-3 catalytic subunit		phosphatase		x		
At5g48380	BIR1, BAK1 interacting receptor-like kinase1	yes (low)	LRR-RLK	membrane			x
At5g62390	BAG7 BCL-2-associated athanogene 7	yes	LRR-RLK	membrane			x
At4g04720	CDPKL CPK21 Calcium-dependent protein kinase 21		kinase	cytoplasm, membrane			x
At4g23650	CDPK3 CPK3 Calcium-dependent protein kinase 3		kinase	cytoplasm, membrane			x
At1g63500	Protein kinase protein with tetratricopeptide repeat domain	yes (low)	kinase	membrane			x
At4g35470	PIRL4 Plant intracellular Ras-group-related LRR protein 4		LRR-RLK	membrane			x
At1g27190	LRR-RLK Leucine-rich repeat receptor-like protein kinase (Fragment)		LRR-RLK	membrane			x
At5g50000	Protein kinase		kinase	membrane			x
At3g57530	CDPKW CPK32 Calcium-dependent protein kinase 32	yes	kinase	cytoplasm, membrane			x
At1g06700	PtI11 PtI1-like tyrosine-protein kinase 1			membrane			x
At5g12480	CDPK7 CPK7 Calcium-dependent protein kinase 7		kinase	cytoplasm, membrane			x
At3g25800	PP2AA2 Serine/threonine-protein phosphatase 2A 65 kDa regulatory subA		phosphatase	cytoplasm			x
At1g78200	PP2C 17 Probable protein phosphatase 2C 17		phosphatase	cytoplasm			x
At5g07300	BON2 Protein BONZAI 2			membrane			x
AT3g52400	SY1P22 Syntaxin-122 O	yes		membrane			x
At5g16590	LRR-RLK Leucine-rich repeat receptor-like protein kinase (Fragment)	yes (low)				x	
At4g08850	LRR-RLK LRR receptor-like serine/threonine-proTein kinase	yes				x	
At3g02880	LRR-RLK Leucine-rich repeat receptor-like protein kinase (Fragment)	yes				x	
AT3G17840	RLK902 Leucine-rich repeat receptor-like protein kinase (Fragment)					x	
At3g14840	LRR-RLK Probable leucine-rich repeat receptor-like	yes				x	
At3g23750	LRR-RLK Leucine-rich repeat receptor-like protein kinase (Fragment)	yes (low)				x	
At3g01290	HIR3 Hypersensitive-induced response protein 3	yes (low)				x	
At5g49760	LRR-RLK Leucine-rich repeat receptor-like protein kinase (Fragment)	yes (low)				x	
At2g26730	LRR-RLK Leucine-rich repeat receptor-like protein kinase (Fragment)	yes (low)				x	
At3g08680	LRR-RLK Leucine-rich repeat receptor-like protein kinase (Fragment)	yes (low)				x	
At1g10860	Q56ZA8_ARATH Receptor-kinase isolog					x	
At3g24550	PERK1_ARATH Proline-rich receptor-like protein kinase PERK1	yes (low)				x	
At5g16050	14335_ARATH 14-3-3-like protein GF14 upsilon					x	
AT3G08510	PLC2 PhosphoinosiTide phospholipase C 2					x	
At3g14350	SRF7 Protein STRUBBELIG-RECEPTOR FAMILY 7	yes (low)				x	
At1g48480	RKL1 Leucine-rich repeat receptor-like protein kinase (Fragment)					x	
At1g53730	SRF6 STRUBBELIG-receptor family 6					x	

Gene Locus	Protein name	BZR/BES1	type	localization	BRI1	common	BRL3
Transport							
At1g23080	PIN7 Auxin efflux carrier component 7	yes / yes			x		
At1g51500	ABCG12 ABC transporter G family member 12				x		
At2g39480	ABCG6 ABC transporter G family member 6				x		
At1g30400	ABCC1 ABC transporter C family member 1				x		
At2g39480	ABC6B_MDR6 ABC transporter B family member 6				x		
At1g11260	STP1 Sugar transport protein 1	yes			x		
At3g48740	SWEET11 Bidirectional sugar transporter SWEEt11			endomembrane			x
At5g20650	COPT5 Copper transporter 5			vacuole			x
At1g71880	SUC1 Sucrose transport protein SUC1	yes / yes		membrane, vacuole			x
At1g61250	SCAMP3 Secretory carrier-associated membrane protein 3			cytoplasm, membrane			x
At3g54140	PTR1 Peptide transporter PtR1			membrane			x
At3g19930	STP4 Sugar transport protein 4	yes		membrane			x
At4g25960	ABCB2 ABC transporter B family member 2	yes (low)				x	
At2g47000	ABCB4 ABC transporter B family member 4	yes / yes				x	
At3g62700	ABCC14 ABC transporter C family member 14	yes				x	
At1g59870	ABCG36 ABC transporter G family member 36	yes				x	
At1g70940	PIN3 Auxin efflux carrier component 3	yes				x	
Trafficking							
At3g08530	CLAH2 Clathrin heavy chain 2	yes (low)			x		
At4G34450	Coatomer subunit gamma				x		
At1g71820	SEC6 Protein SEC6				x		
At3g13870	RHD3 Protein ROOT HAIR DEFECtIVE 3				x		
At3g46060	RABE1C Ras-related protein RABE1c				x		
At5G46860	SYP22 Syntaxin-22				x		
At5g65020	ANXD2 Annexin D2				x		
At2g40060	CLC2 Clathrin light chain 2			membrane, cell plate			x
AT3g60190	DRP1E Dynamin-related protein 1E	yes		membrane			x
At5g12370	SEC10 Exocyst complex component 5					x	
At3g17440	NPSN13 Novel plant SNARE 13	yes (low)				x	
At2g20760	CLC1 Clathrin light chain 1	yes (low)				x	
At3g11130	CHC1 Clathrin heavy chain 1	yes (low) / yes				x	
At1g30630	COPE1 Coatomer subunit epsilon-1					x	
At4g31490	COPB2 Coatomer subunit beta-2					x	
At2g21390	COPA2 Coatomer subunit alpha-2					x	
At1g10290	DRP2A Dynamin-2A					x	
At2g45820	REMO Remorin	yes (low)				x	
At5g08080	SYP132 Syntaxin-132					x	
Enzymes							
At2g31960	CALS2 Callose synthase 2				x		
At5g64740	CESA6 Cellulose synthase A catalytic subunit 6 [UDP-forming]	yes			x		
At2g22125	Cellulose synthase-interactive protein 1				x		
At5g40810	Cytochrome c1				x		
At3g07160	CALS9 Callose synthase			membrane			x
At2g36850	CALS10 Callose synthase 10	no / yes		membrane			x
At4g32410	CESA1 Cellulose synthase A catalytic subunit 1 [UDP-forming]					x	
At4g03550	CALS12 Callose synthase 12	yes				x	
At5g05170	CESA3 Cellulose synthase A catalytic subunit 3 [UDP-forming]					x	
At2g06850	XTH4 Xyloglucan endotransglucosylase/hydrolase protein 4					x	
At3g23300	PMT1 Probable methyltransferase PMT1					x	
At3g66654	Cyclophilin-like peptidyl-prolyl cis-trans isomerase family protein					x	
Others							
At2g20990	SYTA Synaptotagmin A			membrane			x
At5g44130	FLA13 Fasciclin-like arabinogalactan protein 13	yes		membrane			x
At2g23810	TET8 Similar to senescence-associated protein			membrane			x
At5g64330	RPT3 Root phototropism protein 3	yes (low)				x	
At5g06320	Q9FNH6_ARATH Harpin-induced protein-like	yes (low)				x	
At2g47650	AT2G47650 protein	yes				x	
At3g51050	FG-GAP repeat-containing protein	yes (low)				x	

Figure 9. BRI1 and BRL3 candidate interactors summary table
A summary list showing up some of the significant signaling proteins after the comparison between BRL3 and BRI1 IP results with their corresponding localization. BES1 and BZR1 targets are indicated.

BRL3 assemble hetero-oligomers complexes with BAK1 in vivo

In order to confirm the newly identified BRL3 complex interactions, transient expression in Arabidopsis protoplasts of selected CFP and YFP-tagged receptors was done and Fluorescence Resonance Energy Transfer (FRET) combined with Fluorescence Lifetime Imaging (FLIM) technique was used. Positive co-localization of CFP-tagged

BRL3 was observed in protoplasts expressing BAK1, BRL1 and BRL3 proteins fused to YFP. FLIM microscopy allowed the selection of certain membrane fluorescence areas where CFP lifetime was imaged (Figure 10A). The average lifetimes of the BRL3-CFP fluorescence of all double-transfected protoplasts combinations were measured and compared to the control BRL3-CFP protoplasts. Significantly reduced CFP lifetimes were found between the BRL3-CFP and BAK1-YFP receptor pairs (Figure 10B) confirming their in vivo interaction properties. Positive interaction was also detected for BRL3-CFP / BRL3-YFP homodimers, as well as BRL3-CFP / BRL1-YFP receptors (Figure 10B). Overall, these results confirm BAK1 and BRL1 as two new BRL3 interactors in live protoplasts.

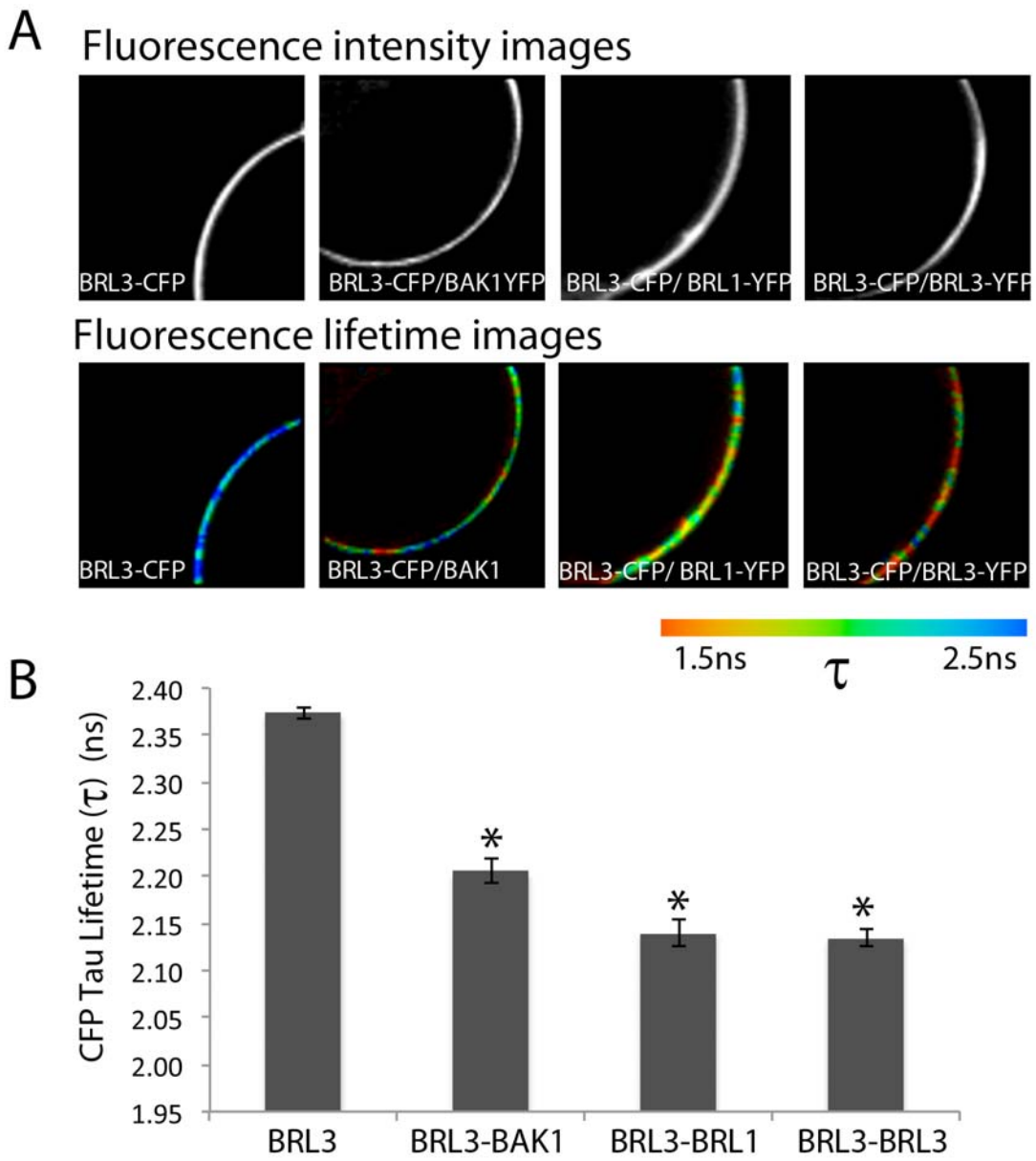

Figure 10. FRET/FLIM validation analysis in Arabidopsis protoplasts.
(A-B) Fluorescence Resonance Energy Transfer (FRET) combined with Fluorescence Lifetime Imaging (FLIM) in Arabidopsis protoplasts transfected with BRL3-CFP alone or co-expressing BRL3-CFP with BAK1-YFP, BRL3-YFP and BRL1-YFP. (A, upper panel) Fluorescence intensity images show expression along all the membrane. (A, lower panel) Fluorescence lifetime images show tau lifetime for CFP represented by coloured scale.
(B) Graphical representation for significantly reduced CFP Tau lifetimes between the BRL3-CFP and BAK1-YFP receptor pairs confirming their in vivo interaction. (B) Reduced lifetime also significant for protoplasts co-expressing BRL3 with BRL3 and BRL1 membrane proteins. Student's t-test indicates that differences are statistically significant between BRL3-CFP and BAK1-YFP as well as between BRL3-CFP homodimers and BRL1-YFP heterodimers (* p-value <0.01).

To further confirm the observed interactions, co-immunoprecipitation in vivo was done in double tagged Arabidopsis plants co-expressing *ProBAK1:BAK1-HA* and *ProBRL3:BRL3-YFP* constructs. BAK1 was successfully detected in an immunoprecipitated BRL3-YFP sample demonstrating the heterodimerization of BRL3/BAK1 receptors in planta (Figure 11A). Similar results were obtained for BRL1-BAK1 (Figure 11B). In contrast, BRI1 receptor was not detected in immunoprecipitates from *ProBRL3:BRL3-GFP* plants (Figure 11C). Nonetheless, the capability for BRI1/BRL3 heterodimerization was only detected in *35S:BRL3-GFP* immunoprecipitates and by FLET/FLIM analysis (Figure 12).

In conclusion, our data shows that BRL3 receptors interact with BAK1 in planta, while question BRI1/BRL3 interactions in vivo.

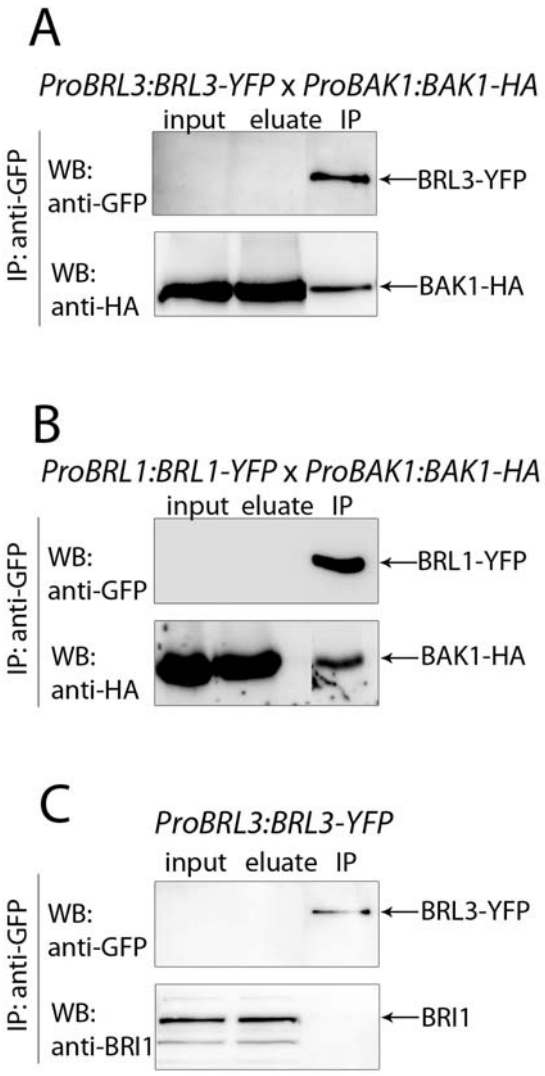

Figure 11. BRL3 forms stable hetero-oligomers with BAK1 but not BRI1 *in vivo.*
(A, upper panel) co-immunoprecipitation using double tagged transgenic plants co-expressing *ProBAK1:BAK1-HA* and *ProBRL3:BRL3-YFP*. In these plants, the amount of BRL3-YFP protein is almost undetectable in total protein extracts by direct Western (input), yet successfully enriched after antiGFP IP. (A, lower panel) BAK1 is successfully detected by using antiHA antibodies in both, direct Western (input) and immunoprecipitated sample, demonstrating a positive heterodimerization between both receptors *in planta*.
(B, upper panel) In *ProBRL1:BRL1-YFP* line, the amount of BRL1-YFP protein is undetectable in total protein extracts by direct Western (input), yet successfully enriched after antiGFP IP. (B, lower panel) BAK1 is successfully detected by using antiHA antibodies in BRL1-YFP protein immunoprecipitated fraction.
(C, upper panel) In *ProBRL3:BRL3-YFP* line, the amount of BRL3-YFP protein is

undetectable in total protein extracts by direct Western (input), yet successfully enriched after antiGFP IP. (C, lower panel) Western Blot with antiBRI1 native antibodies do not detect BRI1 receptor in *ProBRL3:BRL3-GFP* immunoprecipitated fraction.

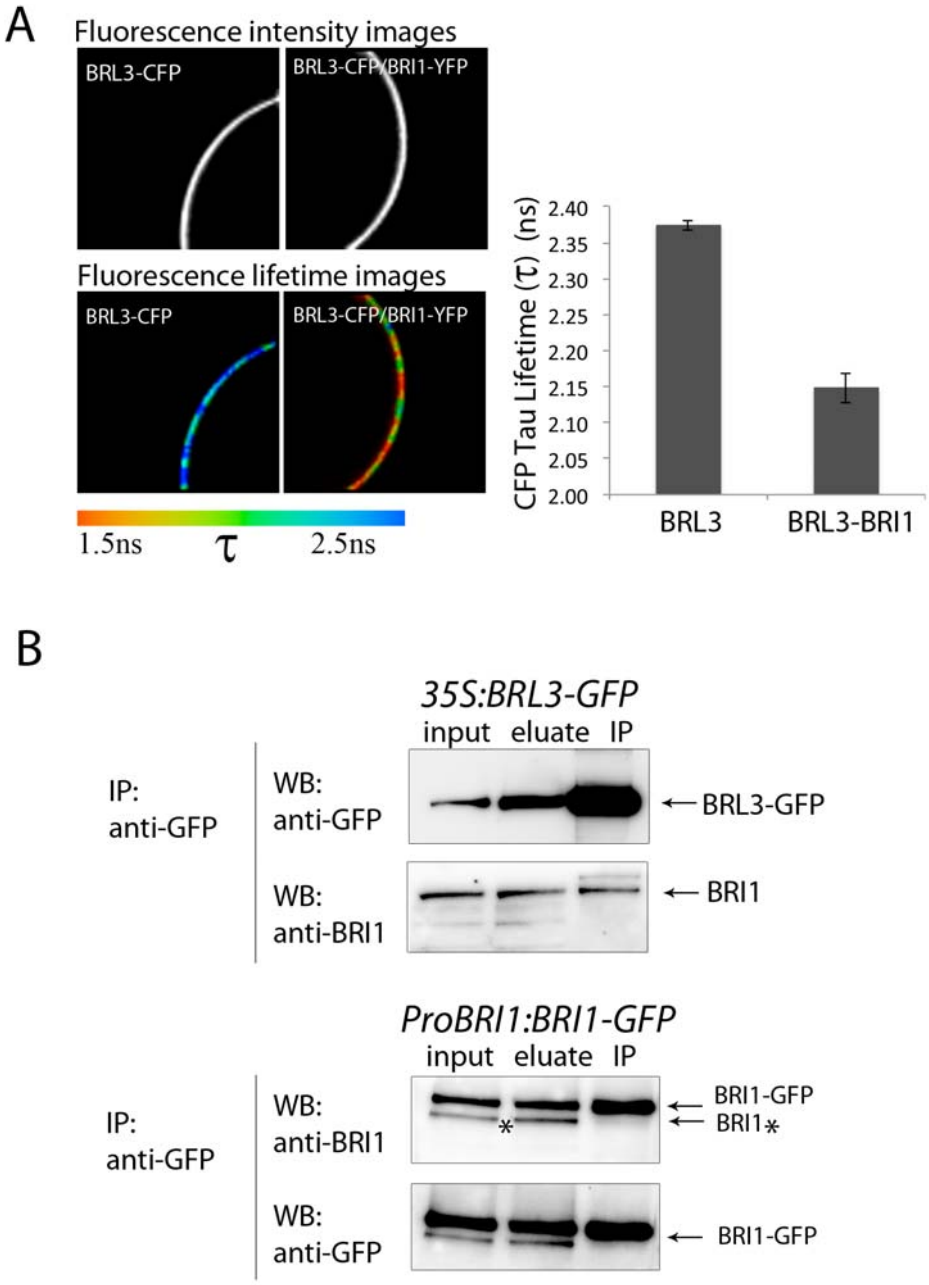

Figure 12. BRL3 and BRI1 have the capacity of heterodimerize in overexpression but not in native conditions

(A) Graphical representation for significantly reduced CFP Tau lifetimes between the BRL3-CFP and BRI1-YFP receptor pairs. (B) (upper panel) In *35S:BRL3-GFP* line, the amount of BRL3-GFP protein is shown in total protein extracts (input) and enriched after IP by using antiGFP antibodies. (D, lower panel) BRI1 protein is detected in total protein extract as well as in BRL3-GFP immunoprecipitated fraction. (D) In *ProBRI1:BRI1-GFP* line, BRI1 native antibody recognises BRI1 specifically the BRI1-GFP receptor in the immunoprecipitated fraction.

The BRL1/BRL3/BAK1 receptor complex accounts for root growth and QC organization

BRs control the normal cell cycle progression of root meristematic cells including the rarely divided QC cells during root growth (González-García et al., 2011), yet a role of BRLs in the root has not been reported. To address the biological relevance of the observed BRL1 and BRL3 interactions with BAK1, a genetic analysis was done using multiple combinations for the BRI1-like receptors with the BAK1 coreceptor. Root length analysis for 6-day-old seedlings showed that *bak1-3* roots have significantly shorter roots than Col-0 WT plants, in agreement with ((Nam and Li, 2002; Albrecht et al., 2008, Figure 13A and 13B), whereas *brl1brl3* double mutant roots were similar to the WT ones. Strikingly, *brl1brl3bak1-3* triple mutants enhanced the *bak1-3* short root phenotype (Figure 13A and 13B), supporting the notion that biochemical interaction between BRL1/BRL3 and BAK1 is required for BR-mediated root growth. In contrast, the root of *bri1-301brl1brl3* (Figure 13A and 13B) and *bri1-116brl1brl3* (Figure 14A) were similar to those of their respective bri1 parental.

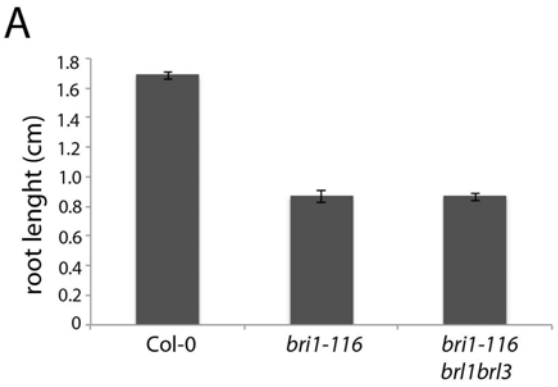

B

	1layer	1>layer>2	2layers	n
Col-0	58	32	10	50
Col-0 + 0.1nM	17.85714286	37.5	44.6428571	30
Col-0 + 1nM	15.38461538	25	59.6153846	43
Col-0 + 10nM	0	17.1428571	82.8571429	32
brl1brl3	70	26.6666667	3.33333333	56
brl1brl3 + 0.1nM	31.42857143	42.8571429	25.7142857	45
brl1brl3 + 1nM	30.43478261	36.9565217	32.6086957	78
brl1brl3+ 10nM	12	12	76	68
bak1-3	72.09302326	25.5813953	2.3255814	52
bak1-3 + 0.1nM	55.12820513	23.0769231	21.7948718	46
bak1-3 + 1nM	40.29850746	23.880597	35.8208955	67
bak1-3 + 10nM	4	16	80	65
brl1brl3bak1-3	71.875	28.125	0	35
brl1brl3bak1-3 + 0.1nM	58.82352941	27.9411765	13.2352941	25
brl1brl3bak1-3 + 1nM	49.23076923	23.0769231	27.6923077	25
brl1brl3bak1-3 + 10nM	14.28571429	33.3333333	52.3809524	25

Figure 14. *bri1-116brl1brl3* shows the same mutant root phenotype than *bri1*
(A) Root length assay for WT, *bri1-116* and *bri1-116brl1brl3* measured in 6-day-old seedlings. Experiment was repeated three times with similar results. Results are average of three replicates experiments +/- S.E. (n=35). (B) Quantification of mPS-PI-stained root tips of WT, *brl1brl3, bak1-3* and *brl1brl3bak1-3* in response to a BL dose curve. Frequency distribution of the number of QC layers corresponding to the graphical representation in Figure 8.: 1 layer (1L; white), 1<layer<2 (1<L2; grey) and 2 layers (2L; black). Results are average of among three independent biological replicates where n shows the total number of roots analysed.

BR sensitivity of *brl1brl3bak1-3* mutants was analysed in a dose-response curve. WT plants significantly reduced the root length while increasing BL concentrations (Figure 13C; in agreement with (González-García et al., 2011). At 0.1nM BL a 20% reduction of root growth was observed in the WT plants that was not observed in *brl1brl3, bak1-3*, and *brl1brl3bak1-3* (Figure 13C). In response to 1nM BL the root length of *brl1brl3* double and *bak1-3* single mutant was similar to the WT, whereas in the same conditions *brl1brl3bak1-3* triple mutants showed a significantly reduced sensitivity to the BR-mediated root shortening (Figure 13C).

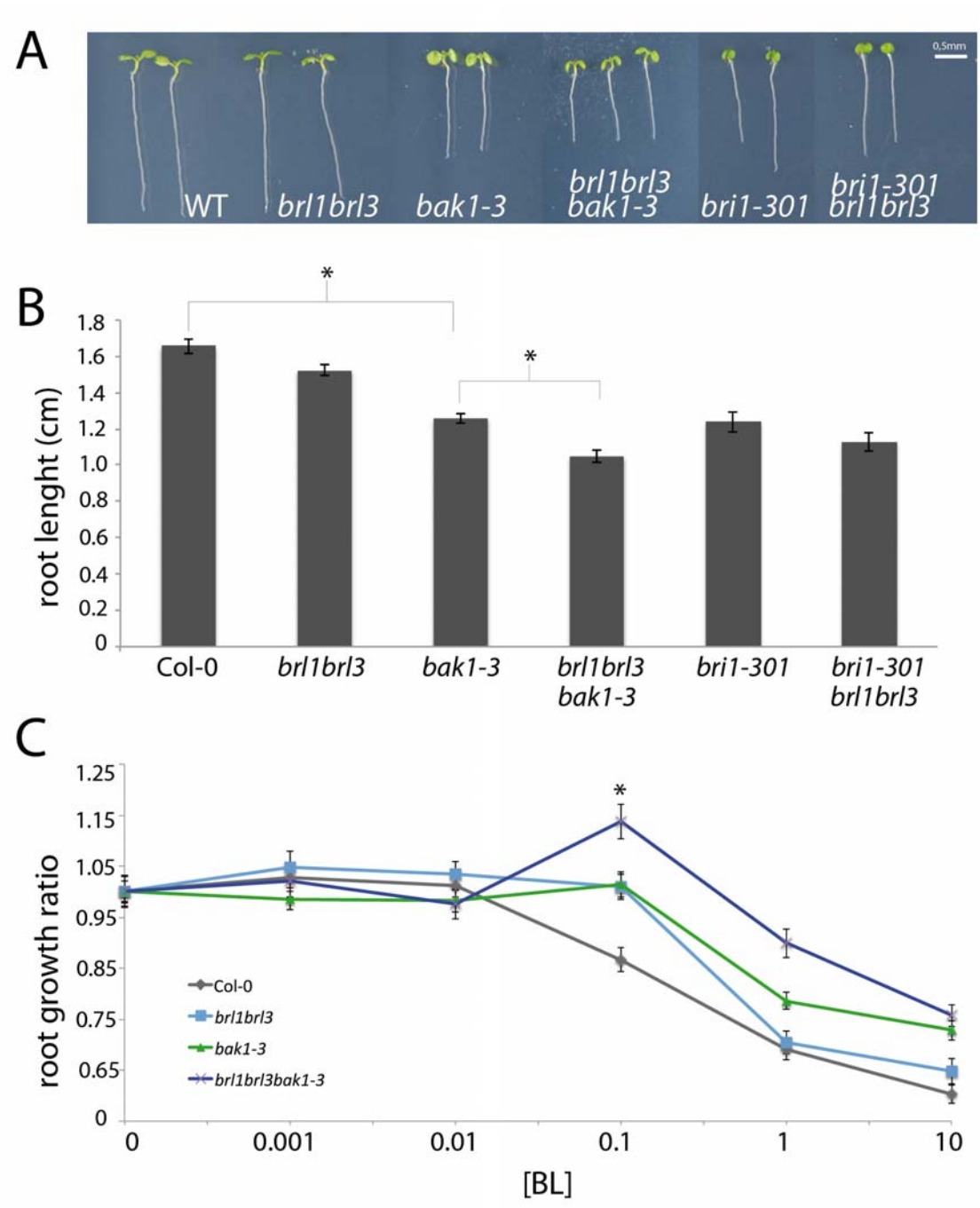

Figure 13. *brl1brl3bak1-3* triple mutant enhances the root and BR insensitivity phenotypes of *bak1-3* mutant.

(A) Phenotype of 6-day-old WT, *bak1-3*, *brl1brl3*, *brl1brl3bak1-3*, *bri1-301* and *bri1-301brl1brl3* mutants (B) Root length assay for WT, *bak1-3*, *brl1brl3*, *brl1brl3bak1-3*, *bri1-301* and *bri1-301brl1brl3* measured in 6-day-old seedlings. (C) Dose response curve by exogenous BL treatments at 0,001 0,01 0,1 1 and 10nM in 6-day-old seedlings. Results are average +/- S.E. (n=40). Results are average of three independent replicates experiments +/- S.E. (n=85). Student's t-test indicates that differences are statistically significant between Col-0 WT and *bak1-3* as well as between *bak1-3* and *brl1brl3bak1-3* triple mutant (*p-value<0.01).

Previous mutant analysis has shown that BRs are required to maintain the quiescence at the root stem cell niche (González-García et al., 2011). Since we found BRL receptors localized in these cells, we asked whether BRL3 complex is necessary to preserve the competence of QC cells to divide at the root apex. Confocal microscopy and quantitative analysis of QC cells in a WT population showed 58% plants with 1 layer of QC cells (1L), whereas 10% show 2 layers (2L; Figure 15A, 8E). The remaining 32% of the roots analysed exhibited an intermediary phenotype, where only part of cells in the QC cell layer were divided. This transition state was referred as (1<L<2). Analysis of QC organization was studied in different mutant combinations. Compared to WT plants (Figure 15A and 15E), a reduction in the frequency of QC division was observed in *brl1brl3* (Figure 15F and 15J), *bak1-3* (Figure 15K and 15O) and *brl1brl3bak1-3* (Figure 15P and 15T) mutants, showing 70% plants with 1 layer of QC cells. Strikingly, treatment with 0,1nM BL enhanced the observed insensibility to BL in *brl1brl3* double mutants (25% 2L; Figure 15G and 15J) and *bak1-3* mutant (20% 2L; Figure 15L and 15O) compared to the WT (45% 2L; Figure 15B and 15E) in the QC cells. This phenotype was even stronger in the *brl1brl3bak1-3* triple mutants (13% 2L; Figure 15Q and 15T) in agreement with our previous results in the BL dose-response curve.

Similar to what observed in the root analysis for in the BL dose-response curve (Figure 7C) this phenotype was dose specific and 1nM BL promoted QC division in WT plants (60% 2L; Figure 15C and 15E) whereas QC cells *brl1brl3* and *bak1-3* plants retain some insensitivity to this hormone concentration (35% 2L; Figure 15H, 15J and 15M, 15O). This insensitivity was stronger on *brl1brl3bak1-3* mutants treated with 1nM BL (28% 2L; Figure 15R and 15T) that was confirmed when these plants were treated with 10nM BL (Figure 15S and 15T). In agreement, *brl1brl3bak1-3* mutants show an increased number of plants with one QC layer compared to the rest of genotypes in all the BL concentrations analysed (Figure 15E, 15J, 15O, 15T).

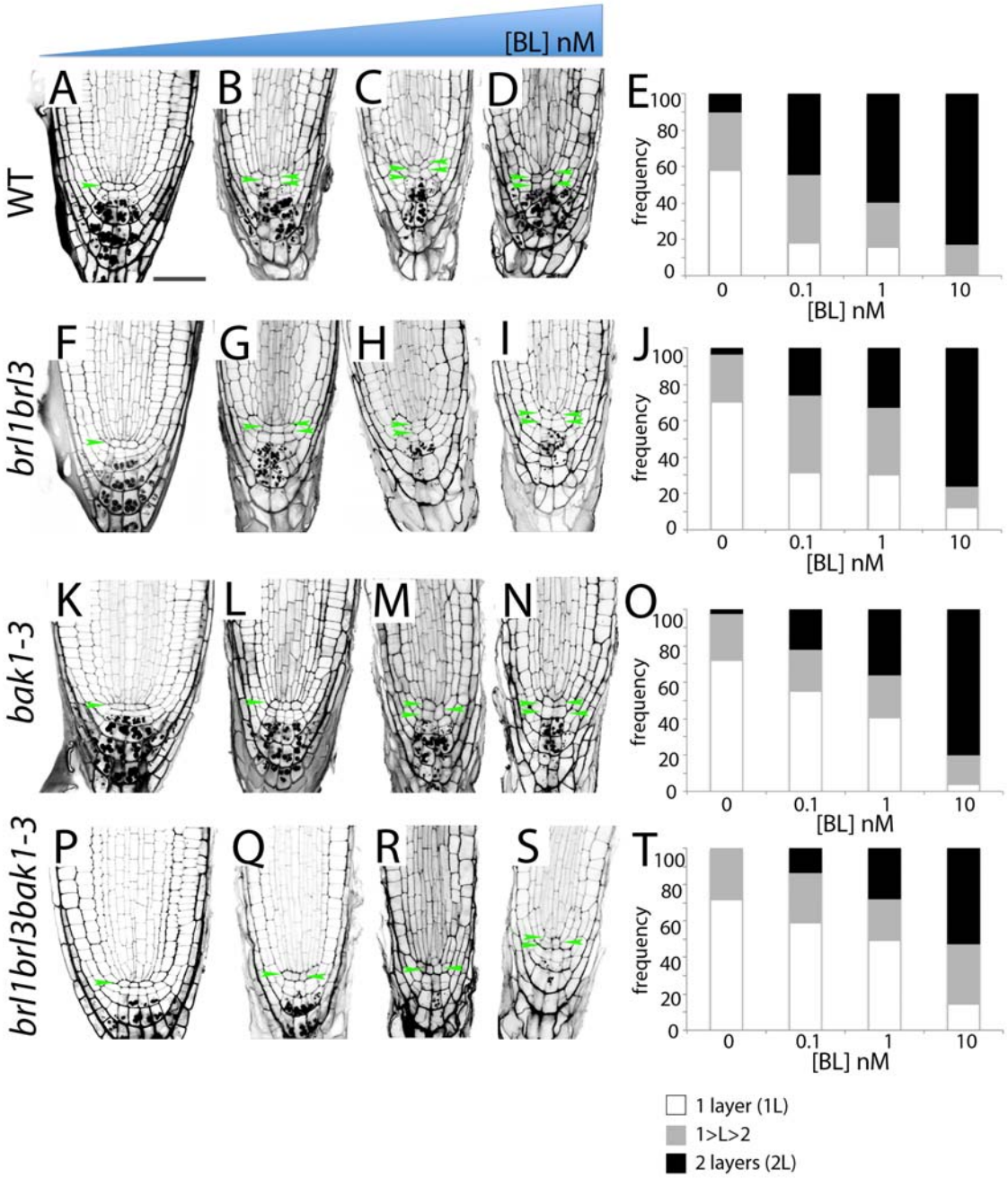

Figure 15. BRL3/BRL1/ BAK1 complex contribute to activity of QC cells in the primary root. Effect of exogenously applied BL on mPS-PI-stained root tips of WT (A-E), *brl1brl3* (F-J), *bak1-3* (K-O) and *brl1brl3bak1-3* (P-T) in response to a BL dose curve. Images illustrate longitudinal median confocal images of 6-day-old primary Col-0 roots treated with the indicated amounts of BL. WT root tip control (A), treated with 0,1nM BL (B), 1nM BL (C) and 10nM BL continuous treatment. *brl1brl3* control (F) and treated with 0,1nM BL (G), 1nM BL (H) and 10nM BL continuous treatment (I). *bak1-3* root tip without (K) and after 0,1nM BL (L), 1nM BL (M) and 10nM BL continuous treatment (N). *brl1brl3bak1-3* without (P) and with 0,1nM BL (Q), 1nM BL, (R) and 10nM BL continuous treatment (S). Quantitative analysis of the effects of exogenous BL treatment at different concentrations (from left to right: 0; 0.1; 1 and 10nM of BL) in QC division for WT, *brl1brl3*, *bak1-3* and *brl1brl3bak1-3* triple mutant respectively (E, J, O, T). Frequency distribution of the number of QC layers: 1 layer (1L; white), 1<layer<2 (1<L2; grey)

and 2 layers (2L; black) of QC cells for the different BL treatments. Green arrowheads indicate QC cells layer. Scale bar 50 µm.

The complete quantitative analysis for three independent biological replicates is shown in Figure 14B. Furthermore, we observed that the *brl1brl3bak1-3* mutants showed hypersensitivity to BR in the stele when compared to *bak1* or *brl1brl3* mutants (Figure 16). These results unveil a concerted action of these receptors in BR-mediated QC activity provascular cells and provide a biological significance to the observed biochemical interactions. In conclusion, our analysis shows that BRLs control BR-mediated responses of a specific cellular environment at the innermost located tissues of the plant.

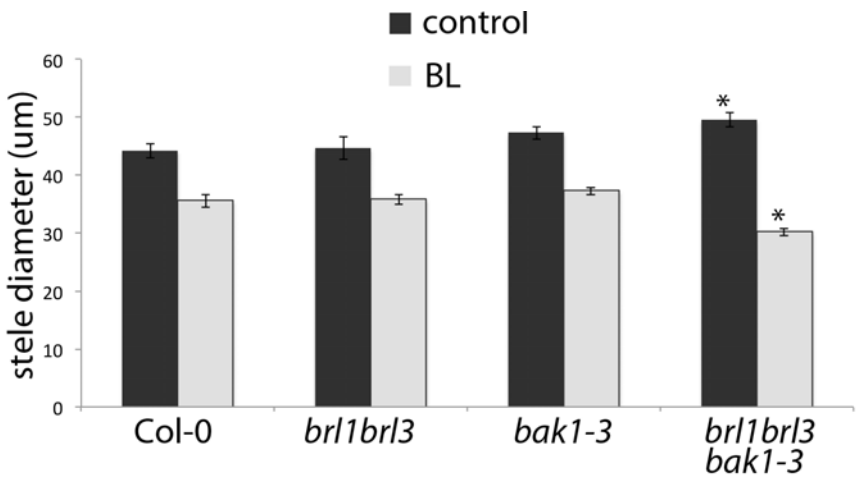

Figure 16. *brl1brl3bak1-3* mutant shows hypersensitivity to BR in the stele
Root stele diameters for WT, *brl1brl3*, *bak1-3* and *brl1brl3bak1-3* mutants measured in 6-day-old mPS-PI-stained root tips. Stele diameter was calculated at 50µm distance from the QC. Experiment was repeated three times with similar results. Results are average of two replicates experiments +/- S.E. (n=30) (*p-value<0.01).

CHAPTER 5

GENERAL DISCUSSION

The present PhD thesis dissertation describes the composition of BRI1 and BRL3 receptor protein complexes in Arabidopsis. These results represent a conceptual advance for the molecular understanding of BR signaling pathways that control plant growth and development, and disclose several elements for understanding BR signaling beyond the current state of the art.

First, a role for BRs in regulating vascular development in the shoot inflorescence stem of Arabidopsis has been demonstrated. The quantitative analysis of BRs mutants revealed a promoting role for BRs in shoot vascular bundle (VB) number. Through computational and modeling predictions, it was found that BRs alone were not sufficient to create the VB patterning, suggesting the requirement of auxin transport for VB formation. These results proposed a promoting role for auxin polar transport in shoot vascular development, in agreement with in other studies demonstrating that auxin in phyllotactic pattern and root cell fate positioning previously reported (Reinhardt et al., 2003; Jonsson et al., 2006; Smith et al., 2006; Grieneisen et al., 2007). Thus, mathematical modeling provided an unbiased direction to our study while permitted to unveil coordinated roles for auxin and BRs in establishing the vascular patterning within Arabidopsis shoots.

Second, experimental evidence for two different BR perception complexes, BRI1 and BRL3 complexes, operating at distinct and specific cell types is provided. Several BRI1 interactors and downstream signaling components have been identified by extensive proteomic studies (Wang and Chory, 2006; Deng et al., 2007; Tang et al., 2008; Tang et al., 2010; Kim et al., 2011; Tang et al., 2011) while no evidence for the composition of the native BRI1 receptor complex has been so far reported. Additionally, BRL receptors have been described to be active BR receptors that play specific roles in Arabidopsis (Caño-Delgado et al., 2004; Zhou et al., 2004) yet the composition of BRL signalosome remain unknown. The identification of BRI1 and BRL3 receptor complexes provided here identifies known and novel candidate interactors in the BR signaling field. Of note, identification of the BRL3 receptor complex composition in combination with high-resolution microscopy and genetic analysis reveals a novel function for BAK1 and BRL1 proteins through interaction with BRL3 in BR-mediated root development.

Collectively, these results highlight the power of using multidisciplinary approaches for the study of signaling pathways within specific cellular domains in the plant.

A breakthrough in the BRL receptor field

The molecular understanding of BR signaling pathway has advanced greatly from the characterization of downstream BRI1 signaling components (Wang et al., 2012b). More recently scientists have started to search for specific cell-type components of BRs in regulating plant development (chapter 1; Bell et al., 2012; Gudesblat et al., 2012; Kim et al., 2012; Wang et al., 2012b; Caño-Delgado and Blazquez, 2013). Despite their cellular specificity and their role as functional BR receptors (Caño-Delgado et al., 2004; Zhou et al., 2004), the study of BRL receptors has been neglected and no reports have been published on them. Several barriers may have hampered the study of BRL pathways in the plant. Despite BRL being functional BR receptors, obstacles in: (i) the visualization of vascular inner tissues, (ii) the biological variability that exists within the shoot stem vasculature where BRL proteins are localised, and (iii) the lack of an apparent phenotype for the *brl* mutants, altogether might have hampered the study of these receptors. This PhD thesis challenges the study of the functional role of BRL receptors by using multidisciplinary approaches ranging from systems biology to quantitative biochemistry and high-resolution microscopy. The purification and identification of BRL3-receptor protein complex has permitted to assign a specific role for BRL3 receptor *in planta*, independently from the BRI1 main receptor (also reported in this study). This is important not only for BR pathway, but for the general understanding of LRR-RLK proteins in plants. Transmembrane receptor kinases play critical roles in both animal and plant signaling pathways regulating growth, development and differentiation responses. In Arabidopsis, there are at least 223 LRR-RLKs, representing the largest protein subfamily in Arabidopsis (Shiu and Bleecker, 2001). Although functional roles for a group of LRR-RLKs have been revealed, the functions of the majority of members within this protein family have not been elucidated.

Instead, BAK/SERK receptors family has been deeply characterized (Rienties et al., 2005; Karlova et al., 2006) and specific and redundant roles for SERKs in BR mediated signaling have been assessed (Albrecht et al., 2008; Gou et al., 2012). Thus, our results revealing the BRL3 signalosome composition and validating the biological relevance of BRL3 interaction with the BAK1 co-receptor position BRL3 receptor among the more comprehensives studies on LRR-RLK homologues in Arabidopsis.

In summary, results presented here disclose novel roles and interactions for BR signaling in plant development, and BR cell-type specificity functions uncover a spatial regulation for BR signaling in plants.

BR control vascular patterning by modulating procambial cell number

Plant vascular tissues enclose distinct cell-types, which are organized in a complex manner displaying different patterns. Arabidopsis shoot inflorescence stems display a radial vascular pattern composed by VBs that are spaced regularly within a ring of procambial cells. Previously it has been reported that BR mutants show less VBs (Choe et al., 1999b; Savaldi-Goldstein et al., 2007) yet specific role for BRs in vascular development of Arabidopsis shoot was unclear. We report an exhaustive and accurate quantitative analysis of a vast number of BR signaling and synthesis mutants that have elucidated a novel role for BRs in shoot vascular development.

First, we have characterized the shoot vascular patterning of WT plants by setting standard vascular parameters. These parameters accounted for the number of VB and procambial cells, the stem diameter and the interfascicular fibres spacing between the VBs. Second, the analysis of vascular parameters for several BR loss-of-function and gain-of function mutants, has revealed a promoting role for BRs in the number of VBs. Third, we found a statistically significant correlation between the number of VBs and the total number of procambial cells along the vascular ring, suggesting a role for BRs in procambial cell divisions. Previous studies have documented the role of BRs in promoting cell expansion (Gudesblat and Russinova, 2011), but little information has been published concerning a role for BRs in cell division (González-García et al., 2011;

Hacham et al., 2011; Zhiponova et al., 2013). These distinct functions of BRs, in cell expansion in vegetative shoot tissues or in the control of cell division during vascular pattern formation, may be the result of cell-type specific BR signaling conferred by the BRL1 and BRL3 receptors, which are specifically expressed in provascular cells (Caño-Delgado et al., 2004). Unlike BRI1, which is ubiquitously expressed and it is known to promote cell expansion, the downstream signaling components for BRL1 and BRL3 will contribute to further understand the role of BRs in vascular development (chapter 4).

Based on our experimental results, mathematical modeling (in collaboration with Physicists at the group of Dr. Ibañes, UB) was mutually beneficial to jointly establish the role of auxin in plant vascular patterning. Our initial experimental approach accounted for exhaustive analysis of BRs mutants while did not concern auxin hormone action. Through computational and modeling predictions, it was found that BRs alone were not sufficient to create the VB patterning, suggesting the requirement of auxin transport for the VB formation. Auxin polar transport is critical to position organs periodically through auxin maxima during the emergence of organ primordia in the shoot, such as the axillary meristems and leaves during the generation of phyllotactic patterns (Reinhardt et al., 2000; Reinhardt et al., 2003). Previous studies have used mathematical and computational modeling to show the importance of auxin polar transport in creating auxin maxima that are essential for phyllotactic patterning (Jonsson et al., 2006; Smith et al., 2006), leaf vascular development (Reinhardt, 2003) and cell fate positioning in Arabidopsis primary root (Grieneisen et al., 2007). In this context and based on the vascular defects of *pin1pin2* double mutants (this study) and *pin1* (Galweiler et al., 1998), together with the phentoypes of plant in which auxin polar transport was chemically inhibited using NPA (this study; Mattsson et al., 1999), we propose that auxin maxima, established by asymmetric auxin polar transport, position the VBs across the vascular ring. We showed that *yucca* mutants do not show a significant alteration of the pattern, which confirmed in turn another prediction of the model.

Our results point at auxin maxima as a common element between lateral organ positioning and shoot vasculature formation and show that early xylem differentiating cells are observed at the shoot apex concurrent with lateral organ primordia outgrowth. Thus, it is tempting to propose that early signaling events at the shoot apex control the initiation of shoot vascular pattern in the plant, although whether these arise from central and/or peripheral zones of the meristem and whether these are linked with organ primordia positioning remains to be investigated. Future studies using local auxin and BRs response during vascular primordia initiation and differentiation may reveal additional interactions of these two signaling pathways underlying VB patterning and plant development.

A new role for influx and efflux auxin carriers in vascular differentiation of Arabidopsis shoots

Auxin transport is required to establish proper periodic shoot stem radial vascular patterning as shown in chapter 2 of this thesis. Our study in this chapter revealed that BRs modulate the number of VBs potentially by altering the number of procambial cells. However, further studies should be done to uncover the molecular mechanism that connects BRs and auxin pathways within procambial and xylem cells in Arabidopsis shoot.

While efflux transport was addressed in chapter 2, the role of auxin influx carriers AUX/LAX, which are membrane localized proteins that import auxin inside the cell (Rubery and Sheldrake, 1973), was addressed in chapter 3. Our results showed that influx carriers modulate the radial shoot vascular patterning in a totally different way to BR modulation. While auxin efflux carriers are essential for the VBs formation (chapter 2), the VB phenotype of auxin influx carrier mutants show sharp VBs, suggesting that AUX/LAX proteins are not required for the VBs formation *per se.* Our results revealed that triple *aux1lax1lax2* and quadruple *aux1lax1lax2lax3* mutants showed less VB compared to the WT plants, less procambial cells and a reduced number of cells between VBs. This change of the periodicity of the pattern confirmed a prediction from a mathematical model for auxin transport constructed by our collaborators. Remarkably, BRs modulate VB number by modulating procambial cell

number (chapter 2) whereas auxin influx carriers change the periodicity of the pattern within the same number of procambial cells (chapter 3), which indicate distinct mechanisms of VB patterning control for each hormone.

Additionally, *aux1lax1lax2lax3* mutants showed impaired xylem differentiation (Figure 3 in chapter 3) in contrast to extra differentiation of xylem cells previously observed in *pin1pin2* mutants (Figure 4 in chapter 2) and NPA-treated plants (Mattsson et al., 1999). Auxin efflux carrier mutants show defective vascular patterning (i.e. VB peaks are not sharp nor defined since auxin maxima are dissolved within the procambial cell ring) and aberrant xylem formation in both interfascicular and VB areas (chapter 2; Galweiler et al., 1998). These results suggest that retained auxin inside the cell promotes xylem differentiation, while inhibiting auxin entrance impairs xylem differentiation. Whether activation of cell differentiation processes is initiated uniquely inside the cell or either accumulation of auxin concentration levels in the apoplast could regulate cell differentiation, remains unknown. Further studies on vascular differentiation of *yucca* auxin over-expressor mutants (Zhao et al., 2001) may contribute to better address this question. It is important to remark that BR loss-of-function mutants also display reduced xylem differentiation (*bri1, cpd* mutants in chapter 2; Choe et al., 1999a) while gain-of-function BR mutants show a slightly increased vascular differentiation (BRI1ox, DWARF4ox, chapter 2) suggesting an additional level for BRs and auxin crosstalk in controlling xylem cells differentiation**.**

Remarkably, this work has permitted us to approach BRs and auxin crosstalk from a theoretical perspective, revealing that BRs control VB position by modulating procambial cell number while auxin control VB formation by creating auxin maxima within the procambial cell ring. In conclusion our approach unveils the importance of auxin and BRs coordination in the elaboration of the shoot vascular patterning.

Genetic redundancy may facilitate signal transduction within distinct cell-types

It is a fact that high number of BR signaling components belongs to gene families that show functional redundant genes in Arabidopsis (Vilarrasa-Blasi et al., 2012; Wang et al., 2012b), although biological relevance for such high homolog proteins operating at

the same signaling pathway remains unknown. In fact, redundant isoforms of kinases, phosphatases and other posttranscriptional regulators occur in most signal transduction pathways. Recent study in *S. cerevisiae* reported that 28% of redundant genes are associated with signal transduction such as Ser/Thr receptor tyrosine kinases (DeLuna et al., 2008). At the perception level, BRL receptors share high homology to BRI1 and most downstream components of the BR signaling pathway also present high homolog genes, including SERKs, BSKs and GSKs kinases, BZRs transcription factors and BSUs phosphatases, which are described in chapter 1 of this thesis. Although BRs are present at very low levels (traces) *in planta*, genetic alterations on BR transduction pathway components usually display dramatic developmental defects (Vilarrasa-Blasi et al., 2012; Wang et al., 2012b). Thus, one explanation for such redundant proteins playing at the same hormone pathway may be that BR levels must be strictly fine-tuned to maintain optimal levels in each cell-type. Another hypothesis is that evolutionary duplication of these genes may occur when new cell-type or tissue specific BR functions emerged, to carry specific and localized functions among the different cell types.

Supporting this, studies on vertebrate developmental pathways show redundant regulators with spatially or temporally distinct expression patterns (Kafri et al., 2006). Furthermore, it has been suggested that genetic redundancy may have a role to facilitate signal transduction within cells that have evolved to produce precisely fine-tuned responses to a wide variety of signals (Kafri et al., 2009). Thus, the high homology that exists between BRI1 and BRL3 receptors converts BR signalling pathway in a good model system to further understand genetic redundancy in plants. How signaling specificity is maintained when multiple pathways share the same components and whether homologue components are functional in the same pathways, is a question for future study. In this thesis, we unveil several candidate interactors for both BRI1 and BRL3 receptors (kinases and other signalling components) that will shed some light in their common and specific functions during plant responses.

Specific BR perception complexes for specific cell types

As discussed above, it has been suggested that genetic redundancy may facilitate signal transduction within cells that have evolved to produce precisely fine-tuned responses to a wide variety of signals. As the existing knowledge regarding spatial regulation for BRs was limited, we generated translational fusions for the different BR receptors to better understand how and where the BR signaling starts within the plant. BRI1 receptor has been reported to show ubiquitous expression in Arabidopsis roots and leaves, and it is the most abundant BR receptor in the plant. In this thesis we differ on the wide expression previously reported for BRI1 receptor, based on our results from accurate analysis of BRI1-GFP roots, which revealed that BRI1 is not homogenously localized along the entire root (chapter 4). Differentiation and elongation zones showed reduced expression of the BRI1 when compared to the meristematic zone. Therefore, we report a predominant expression in the meristematic zone of the root while almost absent expression in the differentiation zone. Further analysis unveiled that BRLs receptors are low expressed in the plants, since they are localized in a very reduced number of cells within the plant. In Arabidopsis roots, both BRL1 and BRL3 receptors are co-localized in the stem cell niche. Thus, we searched for specific functions of the BRL3 receptor within the stem cell niche where it localizes specifically and complementary to BRI1 (van Esse et al., 2011; Fàbregas et al., under revision) to test whether BRL3 fine-tunes BR responses in those specific cell types.

Next, we used advanced biochemical techniques that permitted a successful purification of the BRL3 and BRI1 membrane receptor complexes in plants. To investigate the signal transduction pathway associated BRI1 family receptors, both BRI1 and BRL3 receptor complexes were isolated *in vivo* and analysed by mass spectrometry. Our study provides biochemical and genetic evidence for a spatial regulation of BR signaling that begins with the formation of different BR-receptor complexes. Several lines of evidence indicate that using IP linked to mass spectroscopy is a powerful tool to identify true interactors of BRI1 and BRL3 receptor complexes. First, we purified BRI1 and BRL3 receptor complexes in Arabidopsis that identified a number of interactors for BRI1 that have been previously characterized as BR signaling

components (Schumacher et al., 1999; Li et al., 2002, Nam et al., 2002; Deng et al., 2007). Second, our validation analysis demonstrates that BRL3/ BAK1 interact in native conditions in the plant. Finally, the genetic analysis of *brl1 brl3 bak1-3* triple mutants addressed the functional relevance of the biochemical interactions while unveils novel and cell-type specific functions for BRL3 complex in the control of primary root growth and development.

It is important to point out that the IP procedure we employ here is optimized to increase the identification of potential interactors rather than reducing the number of false positives. Inevitably, this results in a large number of proteins that shared a common membrane location or were resident in the same subcellular membrane compartment. However, a large number of integral abundant membrane proteins (Borner et al., 2005) were missing, suggesting that the enrichment achieved was sufficient. While our approach identified a good number of interactors, previously described BRI1 interactors such as BKI1 (Wang and Chory, 2006) and BSK1 (Tang et al., 2008) were not detected in our study.

These spatially separated BR receptor complexes share common signalling components, as the high number of common proteins revealed (aprox. 50%) including the coreceptor BAK1, that were present in both BRI1 and BRL3 immunoprecipitates. Future studies on the BRL3 specific interactors lists provided here, would be top priority to unveil specific roles for BRL3 signalosome *in planta.*

Other intracellular proteins commonly detected appeared involved in endocytosis processes (Irani et al., 2012) or as part of the BZR1/BES1 mediated responses (Sun et al., 2010; Yu et al., 2011). Whether BRL3 signaling downstream components activate BES1 and BZR1 transcription factors similarly to BRI1, remains unknown. However, preliminary results show that BES1 transcription factor targets and represses BRL3 transcription in Arabidopsis protoplasts, suggesting that BRL3 partially signals through BES1 transcription factor response (Lehner R., Salazar J. and Caño-Delgado, A., unpublished data). Unpublished results in the laboratory unveiled the presense of a subset of cell-type specific BR-signaling components necessary for root development. (Vilarrasa, J., González-García, M.P. and Caño Delgado A.I, unpublished results).

The functional redundancy of BRL3 receptor has been previously addressed, and *bri1* phenotypes can be recued when BRL1 or BRL3 are expressed under BRI1 promoter (Caño-Delgado et al., 2004). Thus, it is possible that part of the commonly identified components in our study may belong to BRI1 signalosome, but appeared in BRL3 complex as a result of BRL3 overexpression. In agreement, co-IPs in *ProBRL3:BRL3-YFP* native lines failed to immunoprecipitate BRI1, while IP in *35S:BRL3-GFP* plants positively detected BRI1 further supporting the capacity of BRI1 to interact with BRL3 when overexpressed in similar tissues. In contrast, the detection of DET3 in both lines that express BRL3 under their native promoter and *35S:BRL3-GFP* lines, support that at least part of the common signaling components identified might be BRL3 specific.

Despite the numerous examples describing the connection of SERK proteins to the BR signaling (Albrecht et al., 2008; Gou et al., 2012), only SERK1 and BAK1 have been shown to interact with BRI1 *in vivo* (Karlova et al., 2006). Our analysis report the interaction of BAK1 with BRL3 receptor, and most importantly our results show that this interaction is functionally relevant for the role of BRL3 signalosome complex in BR-mediated root growth. The predominant localization of the BRL1 and BRL3 receptor proteins in the root stem cell niche together with the defects found QC activity of *bak1-3* combined with *brl1brl3* mutants indicate that BAK1/BRL1/BRL3 containing signalosome that is required for BR-perception in the stem cell niche. Further support is provided by the number of BRL3 interactors identified in this study, which shared an enriched gene expression in the stem cell niche including BRL1, BAK1, RCN1, clathrin heavy chain (At3g08530), VHA-A3 ATPase and an uncharacterized RLK (At3g02880). Future studies will be aiming to evaluate the role of these proteins in cell-type specific BR signaling patways.

Overall, our results showing the different composition of BRI1 and BRL3 complexes advance that spatial regulation of BR signaling may not only be conferred by downstream signaling regulators operating at the transcriptional level, but also at the level of ligand recognition by different BR receptor complexes at the plasma membrane.

Conclusions and future perspectives

Our preliminary shoot analysis of *bri1-301brl1brl3* triple mutant showed that BRL receptors do not account for the number of VB along the vascular ring. Thus, BRL1 and BRL3 may not be participating in the number of VB along the vascular ring as BRI1 does. Therefore, it is tempting to conclude that BRL1 and BRL3 may have specific role for VB in collateral pattern formation, yet in fact their role is redundant to BRI1 (Caño et al 2004). Furthermore, *bak1brl1brl3* mutant root analysis revealed an independent role for the BRL3 receptor complex within the root stele of Arabidopsis. In conclusion, these results suggest that BRL receptors can interact with BRI1 in some cell-types to carry redundant functions while in other cell-types they signal independently from the BRI1 receptor. Our current model proposes that BRs contribute to vascular development by controlling the divison of procambial cells (collateral VB, procambial cells ring and root stele). Since BRs have been shown to control xylem differentiation (Fukuda and chapter 2 of this thesis) we propose that BRs primary control the cell division while cell differentiation defects are a secondary effects of the unbalanced cell division.

In summary, our work identifies novel roles for BRs in both procambial cell division of the shoot inflorescence stem and in QC cell activity in the root apex. We have pioneered the “turn on the microscope turret” by using advanced microscopic tools, mathematical modeling and MS analysis of BR receptor complexes. By revisiting the pleiotropic effect of BRs at a higher magnification we have unveiled the existence of a spatial regulation of BRs in the plant. Moreover, we uncovered a BRL3 function by identification of new components for the cell-type specific BRL3 receptor complex, disclosing a new BR-branched pathway in plant development. We conceive that these BR-branched pathways would be dynamically changing over space an time. For now, we provide a new view of specific and distinct BR signaling pathways in plants, operating in distinct cell types while revealed several evidences connecting BRs signaling to cell division in plant vascular tissues. Future studies tracing back the control of cell-type specific targets to specific BR receptor complexes will help delineating the different BR signalling pathways that control plant development.

Future perspectives

First, analysis on the BRL3 specific interactors lists provided here. This would be of top priority to unveil specific roles for BRL3 signalosome *in planta.* In addition, the setting up of optimal conditions for successful immunoprecipitation of BRL3 complex in native conditions would reduce false positive interactors list obtained in BRL3 over-expressor lines. Second, to further understand whether role of BRL3 signalosome in the QC is independent from BRI1 (González-García) quantitative analysis on quadruple mutant *bri1bak1brl1brl3* roots compared to *bak1bri1* roots should be done (quadruple mutants have been generated during this thesis). Vascular analysis within *bri1bak1brl1brl3* and *bak1bri1* roots stele and shoot VBs. Third, PIN3 protein was identified between BRL3 candidate interactors, and the PIN3 protein is localized in the CSC where BRL3 localizes (Friml et al., 2002). It has been reported that BRs repress the expression of several auxin transport-related genes including PIN3 while auxin induces the expression of BRL3 (Nemhauser et al.; 2004). Altogether, these results suggest a possible molecular connection in the auxin and BRs crosstalk in specific cell types, although direct interaction and molecular mechanism should be investigated in future experiments. Understanding the integration of all plant hormones involved in the vascular tissue development will be key to further study.

CONCLUSIONS

1. Brassinosteroid signaling and auxin transport co-operate to establish the periodic pattern of vascular bundles in Arabidopsis.

1.1. Plant steroid hormones Brassinosteroids modulate vascular bundle number by promoting early procambial divisions in the vascular ring.

1.2. Localization of auxin maxima by DR5 reporter and analysis of *pin1pin2* and *yucca* mutants indicate that auxin polar transport, and not auxin levels, promote the formation of the vascular bundle.

1.3. Mathematical modeling for vascular bundle spacing in shoot inflorescence stem of Arabidopsis established that periodic auxin maxima controlled by polar transport underlie vascular bundle spacing, while Brassinosteroids contribute by modulating the number of procambial cells.

2. Auxin influx carriers modulate the vascular differentiation and periodicity in Arabidopsis shoots.

2.1. Auxin influx carriers promote xylem differentiation within procambial cells forming the vascular bundle and interfascicular fiber cells at the shoot inflorescence stem of Arabidopsis.

2.2. Auxin influx carriers contribute to pattern periodicity by modulating the space between vascular bundles.

3. Brassinosteroid receptors from the BRI1-like family show complementary spatial localization in vascular and stem cells in the plant.

3.1. In the Arabidopsis primary root, BRI1 is widely localized within the root meristem with the exception of the QC cells, where BRI1 protein localization appeared dramatically reduced.

3.2. In the primary root, BRL3 receptor appears to be specifically localized to the stem cell niche, vascular initials and early descendants at the stele and at the phloem-pole pericycle in the root apex.

3.3. In the primary root, BRL1 co-localized with BRL3 at the stem cell niche and at the provascular cells at the root apex.

4. BRI1 and BRL3 receptors belong to common and distinct complexes at the plasma membrane.

4.1. Comparison analysis between both BRI1 and BRL3 pull downs revealed that 54% of the BRL3 interactors are unique for BRL3 signalosome, whereas 46% of the BRL3 interactors were present in both BRI1 and BRL3 receptor complexes.

4.2. Several experimental evidences presented in this study demonstrate that BRL3 interacts with BAK1 co-receptor *in vivo*. In contrast, our results argue for the presence of native BRI1 receptor in BRL3 signalosome.

4.3. The identification of novel yet uncharacterized proteins in BRI1 and BRL3 signalosomes reported in this study represent a promise to further advance in the mechanistic understanding of BRI1 and BRL3-mediated signaling pathways in plants.

5. The BRL1/BRL3/BAK1 receptor complex is functionally required to control BR-mediated root growth, vascular development and stem cell homeostasis.

5.1. Roots of *brl1brl3bak1-3* triple mutants enhanced the *bak1-3* short root phenotype supporting that BRL3 signalosome is required for root growth.

5.2. Roots of *bri1-301brl1brl3* and *bri1-116brl1brl3* mutants do not enhance the *bri1-301* nor *bri1-116* short-root phenotype supporting distinct roles for BRI1 and BRL receptors in Arabidopsis roots.

5.3. Reduced sensitivity of *brl1brl3bak1-3* triple mutants to BL, reveal a role for BRL3/BRL1/BAK1 in BR-mediated root growth and stem cell homeostasis.

5.4. *brl1brl3bak1-3* mutants show hypersensitivity to BR in the stele indicating a specific function for BRL3 signalosome within the root vascular tissues.

6. Multidisciplinary approaches combining genetics and proteomics are a powerful tool to study uncharacterized signaling pathways in plants.

7. Mathematical modeling support experimental analysis to unravel the mechanisms that contribute to plant vascular development.

MATERIAL AND METHODS

1. Methods in plant biology

1.1. Plant Material and Growth Conditions

Arabidopsis thaliana (Arabidopsis) was the plant model used in this PhD thesis. In particular, Columbia (Col-0) was the wild type ecotype for all mutant lines described used in this study. Besides the transgenic lines and mutants generated in this work, seeds were obtained from diverse laboratories as detailed in Table 1.

Table 1. BR and auxin synthesis and signaling mutants analyzed in this study

Name of mutant	Gene	Description	Mutant	Reference
bri1-116	At4g39400	BRI1 strong mutant allele	single	(Li and Chory, 1997)
bri1-301	At4g39400	BRI1 weak mutant allele	single	(Nam and Li, 2002)
cpd	At5g05690	BR-synthesis mutant	single	(Szekeres et al., 1996)
DWF4-ox	At3g50660	BR-synthesis overexpressor	single	(Choe et al., 2001)
BRI1-GFP	At4g39400	BR1 overexpressor	single	(Friedrichsen et al., 2000)
bzr1-D	At1g75080	BR gain-of-function signaing mutant	single	(Wang et al., 2002)
*bes1-D**	At1g19350	BR gain-of-function signaing mutant	single	(Yin et al., 2002)
bin2-1	At4g18710	Dominant mutant of BIN2	single	(Li et al., 2001)
yucca	At4g32540	Auxin synthesis overexpressor		(Zhao et al., 2001)
pin1pin2	At5g57090 At1g73590	Auxin transport mutant	double	B.Scheres lab
DR5:GUS in pin1pin2			double	B.Scheres lab
DR5:GUS in bri1-116			single	Ana Caño lab
DR5-GFP				Kuhlemeier lab
DR5:GFP in aux1lax1lax2			triple	Kuhlemeier lab
aux1lax1lax2lax3			cuadruple	Kuhlemeier lab
pBRL3:BRL3-YFP		Tanslational fusion	PPT®	This work
35S:BRL3-GFP		Tanslational overexpression fusion	Kan®	This work
pBRL1:BRL1-YFP		Tanslational fusion	PPT®	This work
pBRI1:BRI1-GFP		Tanslational fusion	Kan®	N Geldner
pSERK3:SERK3-HA		Tanslational fusion	Hygro ®	De Vries
brl3-1	At3g13380	BR-signaling mutant	single	Ana Caño lab
brl1-1	At1g55610	BR-signaling mutant	single	Ana Caño lab
brl1brl3		BR-signaling mutant	double	Ana Caño lab
serk3-1 (bak1-4)	At4g33430	BR-signaling mutant	single	S. de Vries lab
bak1-4 brl1brl3		BR-signaling mutant	triple	This work
bri1-116brl1brl3		BR-signaling mutant	triple	Ana Caño lab
bri1-301brl1brl3		BR-signaling mutant	triple	Ana Caño lab

*The bes1-D mutant (En-2 background) was introgressed by 7 genetic back-crossings into the Col-0 ecotype

All seeds were surface-sterilized in 35% sodium hypochlorite solution under agitation for 5 minutes followed by 5 consecutive washes using sterile milliQ water (5min. each

one). To synchronize seed germination, seeds were vernalized at 4°C for 48-72 h, and germinated on plates containing sterile 1x MS media (Murashige and Skoog) salt mixture supplemented with 10 g/L of sucrose and 5mM MES/KOH, pH 5.7 previously to agar addition (8 g/L). Alternatively, 0,5x MS media was used diluting MS components to half. For liquid culture, flasks containing 100 mL of sterile 1x MS without agar were used.

In chapter 2, plants were grown under long-day photoperiodic conditions (16h light / 8h dark; 20-23°C) for 5 weeks. Pharmacological treatments were performed in plants grown in magenta boxes containing 100 mL of sterile 1x MS media supplemented with 10 nM BL (BRASSINOLIDE; $C_{28}H_{48}O_6$; Wako®), 5 µM BRZ_{220} (BRASSINAZOLE; T. Asami (RIKEN, Japan), and 10 µM NPA (NAPHTHALENE ACETIC ACID; Duchefa®) respectively. Basal part of shoot inflorescence stems was sectioned from plants at 12 to 22 days after bolting (approx. 5 weeks) for both hand cut and for embedding procedure.

In chapter 3, 10-day-plants were grown on plates on short day photoperiod chambers (8h light / 16h dark; 20-23°C) and transplanted on soil (different mixtures of autoclaved soil supplemented with perlite and vermiculite for aeration were used) where they were grown for a short day photoperiod chambers (8h light / 16h dark; 20-23°C). Basal part of shoot inflorescence stem was sectioned from plants at 12 to 22 days after bolting (approx. 14 weeks) for both hand cut and for embedding procedure.

In chapter 4, 6-day-old T4 homozygous plants of *ProBRL1:BRL1-YFP* and *ProBRL3:BRL3-YFP* grown on MS agar vertically and used for the confocal microscopy expression analysis. Moreover, 10-day-old T4 homozygous seedlings expressing *ProBRI1:BRI1-GFP*, *ProBRL3:BRL3-YFP* and *35S:BRL3-GFP* clones were grown on liquid MS and used for the IP experiments.

1.2. Quantitative Vascular Analysis: Measurement Settings

Quantification of vascular parameters in shoot inflorescence stem sections (stem diameters, number of cells, and IF length) was performed by using ImageJ software (http://rsb.info.nih.gov/ij/). Two orthogonal diameters were measured along the directions of maximal or minimal length and the mean value was used. Similar conclusions are obtained if the pith diameter is included in the analysis. To ensure measurements were made on stationary conditions for bundle number and stem

diameter, we analysed WT sections at different times after bolting at the base of the inflorescence. A Wilcoxon Mann–Whitney rank sum statistical test was used to evaluate whether each mutant genotype dataset followed the same distribution as the data from WT plants.

1.3. Root length and BL sensitivity assays

The root length of 6-day-old seedlings grown vertically on on 1/2 MS agar plates were measured and the data was analysed with ImageJ software (http://rsb.info.nih.gov/ij/). All experiments were repeated for at least 3 times. Student's *t*-test was used to show statistical differences of root lengths between WT Col-0, *bak1-3 and brl1brl3bak1-3* mutants. For BL dose-response curve assays, the average root length for each genotype was divided by the preceding concentration in order to calculate the ratio of root length reduction. The S.E. associated to each ratio was calculated with the corresponding formula for S.E. divisions. The mean ratios between the three replicates were calculated and plotted as well as their corresponding. S.E. Oneway Annova test was done to calculate the BL curve replicates significance (* pvalue<0.01).

2. Methods in molecular biology

2.1. Molecular Cloning

Transgenic lines expressing *35S:BRL3-GFP* were generated by DNA transformation in WT Col-0 plants of *35S:BRL3-GFP (YY178)* construct reported in (Caño-Delgado et al., 2004). *ProBRL3:BRL3-YFP* and *ProBRL1:BRL1-YFP* constructs were cloned using recombination Gateway Multisite Cloning system. DNA sequences were amplified from respective BAC clones (MIRP15, F20N20). Primers used for BRL1 and BRL3 genes cloning are detailed in Table 2. The purified gene PCR products were placed into the Gateway pDONR221® donor vector by BP reaction mixing 50 fmol of the PCR product with 150 ng of the pDONR221 DNA and 1µL of BP clonase enzyme and diluted up to 5µL in TE buffer pH 8.0. Same procedure was done for 2kb promoter PCR product of both receptors by using primers detailed in Table 2, and placed into Gateway® P4P1R vector by using the same DNA proportions as described above. For the tagged YFP a P2RP3 donor vector was used (http://www.psb.ugent.be). Recombination LR reaction

was performed by mixing the three sequenced pENTRY vectors (10 fmol each one) in a three-component pDEST vector. pB7m34GW (25 fmol) adding 2µL LR clonase enzyme, diluted up to 8µL in TE buffer 8.0. All recombination reactions were incubated overnight at 25ºC.

Sequences for all the primers used for genotyping all mutants presented in this thesis are described in Table 2.

Table S2. Primers used in this study

primer	Sequence (5' - 3')	use
bri2.11	5'-gtgagaaacgaaggtggaacagactgcag-3'	*brl1-1* genotyping
bri2.12	5'-cttcttggcatggatacgggaggtaatgg-3'	*brl1-1* genotyping
JMLB	5' ggcaatcagctgttgcccgtctcactggtg 3'	*brl1-1* genotyping
bri4.2	5'-tttagggtgagcatgagatctcgtgggccg-3'	*brl3-1* genotyping
bri4.3	5'-gaaatccctgtaggaatcggaaagcttgag-3'	*brl3-1* genotyping
JMRB	5' gctcatgatcagattgtcgtttcccgcctt 3'	*brl3-1* genotyping
BRI1 F	5' caatcttaactggatttctctgtc 3'	*bri1-116* genotyping*
BRI1 R	5' catcggaaccattgttatcaaacgtc 3'	*bri1-116* genotyping*
NF-pBRL3 F	ggggacaactttgtatagaaaagttgccgagctctaaaagatatgttgagtccatattcct	Cloning P4P1R
NF-pBRL3 R	ggggactgctttttgtacaaacttgccccggggttattagcccacaaagtgttcgat	Cloning P4P1R
NF-pBRL1 F	ggggacaactttgtatagaaaagttgcccctaatattattaaattgatt	Cloning P4P1R
NF-pBRL1 R	ggggactgctttttgtacaaacttgcttggcacagcaagagttcgct	Cloning P4P1R
NF-BRL3 F	ggggacaagtttgtacaaaaaagcaggctccatgaaacaacaatggcagttcttgatc	Cloning P221
NF-BRL3 R	ggggaccactttgtacaagaaagctgggtcaggctccttatctcgtgattcttc	Cloning P221
NF-BRL1 F	ggggacaagtttgtacaaaaaagcaggctccatgaagcagagatggctgttagtgttg	Cloning P221
NF-BRL1 R	ggggaccactttgtacaagaaagctgggtcaggctccttatctcgcgattcttcgac	Cloning P221
YFP F	5' atggtgagcaagggcgag 3'	YFP genotyping
YFP R	5' ttacttgtacagctcgtccatgc 3'	YFP genotyping
serk3-1 F	5' gcactgaaaaacagtttagc 3'	*serk3-1* genotyping
serk3-1 R	5' gatgcaggaaggggagtcaacttggtg 3'	*serk3-1* genotyping
serk3TDNARev	5' gcgtggaccgcttgctgcaact 3'	*serk3-1* genotyping
BRI1-301 F	5' ggaaaccattgggaagatca '3	*bri1-301* genotyping**
BRI1-301 R	5' gctgtttcacccatccaa 3'	*bri1-301* genotyping**

* PCR product was digested by MseI enzyme
** PCR product was digested by DpnII enzyme

2.2 Generation of transgenic lines

Arabidopsis Col-0 ecotype plants expressing BRI1 fused to GFP were described previously (*ProBRI1:BRI1-GFP*, (Geldner et al., 2007)). Wild-type Col-0 seedlings were used as a control.

All LR recombination described above were transformed into competent DH5alpha E.Coli cells by heat shock to amplify DNA plasmid containing the constructs and then transformed intro Agrobacterium strain GV2260 by electroporation. Agrobacterium was selected by antibiotic resistance (Rifampicin Kanamycin and PPT) and transferred to Col-0 WT plants as described in (Clough and Bent, 1998).

3. Methods in biochemistry

3.1. Protein extraction and Western blot

Total proteins were extracted by homogenizing seedlings in two volumes of extraction buffer (50mM Tris-HCl pH 7.5; 150mM NaCl; 1% Triron X-100; 1mM PMSF; 0.1mM Leupeptin; 0.1mM Aproptinin; 0.1.mM Pepstatin A; 0.1mM E-64) on ice. Extracts were incubates 10min on ice, homogenized by 2'' vortex and centrifuged 30min at 13000 rpm at 4ºC. Supernatant was transferred to a new eppendorf tube and they were quantified by the Bradford assay (Bradford, 1976). Aliquots (20-50ug) of total protein were denatured in loading buffer (80 mM Tris-HCl pH 6.8; SDS 1.6%; DTT 0.1M; Glycerol 5%; Bromophenol Blue) at 95ºC for 10 min and stored at -20ºC.

Protein electrophoresis SDS-PAGE gel was prepared at 10% acrylamide (Amresco®) and 5% acrylamide for the stacking gel. Protein samples were run in gels at 100mV for 30min and 120mV for 1hour to 1.5hour depending on the molecular weight of the protein of interest. Protein samples were transferred on nitrocellulose membrane (Hybond-ECL, GE Healthcare®) by blotting at 100mV for 1 hour under agitation on ice. Membrane was blocked during 1 hour with 3% milk in PBS-T (PBS + 0.1% Tween) and rinsed with PBS-T. Primary conjugated antibody antiGFP-HRP was incubated for 2 hours in 3% milk in PBS-T at RT. Alternatively, primary antibodies used in this study were incubated overnight in 3% milk in PBS-T at 4ºC. Membrane was washed with PBS-T for 10 minutes two times. All secondary antibodies were incubated 3% milk in PBS-T during 1 hour at RT. Finally membranes were washed with PBS buffer (without tween) and protein was detected by revealing solution (Western Blot Detection Kit, Pierce®) in LAS-4000 luminescence detector (Fuji).

Primary antibodies dilutions: anti-BRI1 (J. Chory lab; rabbit; 1/1000), anti-HA (Covance®; mouse; 1/1000); antiGFP-HRP conjugated (Miltenyi Biotec ; Macs®; 1/5000). Secondary antibodies dilutions: anti-rabbit (GE Healthcare; dil1/5000) anti-mouse (Sigma ®; 1/5000).

3.2. Immunoprecipitation

Approximately 10g of seedlings were ground in liquid nitrogen using a pestle and mortar. The frozen, powdered material was transferred to a 10-ml Potter homogenizer and 10 ml of extraction buffer (50 mM Tris/HCl, pH 7.5, 150 mM NaCl, 2% Triton X-100, and the Complete Protease Inhibitor Cocktail) was added. After thawing, the powdered material was homogenized by 10 strokes of the plunger. The resulting extract was left on ice for 30 min, followed by centrifugation at 20,000g 3 times for 10 min at 4°C. The supernatant was incubated, under rotation at 4°C, with 200 µl of anti-GFP beads (Miltenyi Biotec) for 1 hour. Magnetic beads with attached proteins were immobilized on a magnetic separator (MACS, Miltenyi Biotec) and washed 4 times with 200 µl extraction buffer containing 0.1 % Triton X-100. Bound proteins were eluted from the immobilized beads with 50µl hot (95°C) SDS-PAGE loading buffer. Three independent biological replicates were prepared.

Co-immunoprecipitation experiments were done in the same conditions as the IPs described above but instead of 10g of starting material, 5g were used for homozygous lines co-expressing *ProBRL3:BRL3-YFP* and *ProBAK1:BAK1-HA* constructs.

3.3. Protein tryptic digestion and sample preparation for LC-MS/MS analysis

Eluted proteins were separated in a 10% SDS-PAGE, which was run until the bromophenol blue tracking dye moved 5 cm. After rinsing with MiliQ water, the gel was fixed in 5% acetic acid / 45% water / 50% methanol and stained with Colloidal Blue (Invitrogen) overnight followed by a 5-time wash with MiliQ water. Each lane was cut into 8 slices, and proteins in each slice were reduced with 10 mM dithiothreitol at 60°C for 1 hour and alkylated with 20mM iodoacetate in the dark for 1 hour. After two freeze-thaw cycles, proteins in the slices were digested overnight with a minimal volume of sequencing-grade trypsin (10ng/µl) in 50mM ammonium bicarbonate at room temperature. Peptides were extracted from the slices by sonication, 10% (v/v) trifluoroacetic acid was added to the extracts to decrease the pH below 4. Peptide

samples were measured by nLCMS as described in (Lu et al., 2011) and analysed with Bioworks as described (van Esse et al., 2008).

3.4. Maxquant analysis

For a quantitative analysis of the data, peak intensities were determined and normalized by the MaxQuant software (Cox and Mann, 2008; Cox et al., 2011). MaxQuant algorithms were used to calculate the intensity levels of peptides found in the triplicates IPs for BRI1, BRL3 or WT. The output data resolved Intensity Based Absolute Quantification values (iBAQ) for all the proteins present in BRI1 complex and the WT control. Perseus software was further used for filtering and statistical analysis of the MaxQuant output (Hubner et al., 2010; Peng et al., 2012; Smaczniak et al., 2012). Previously published Detergent Membrane Resistant Domains protein content data (Borner et al., 2005) was crossed to the high confidence list of putative interactors where few were detected and removed from the list.

3.5. MS data statistics

For identifying differently expressed proteins we evaluated the log ratio between two conditions (the average of ratios within the three replicates) and consider all proteins than differ by more than an arbitrary cut off value to be in sample and not in the control.

Col-0 WT control data was loaded as one group separately from the BRI1 or BRL3 data set and T-student test was applied. The “Vulcano Plot” graph summarized both fold-change and t-test criteria. It is a scatter-plot of the negative log 10 (transformed p-values) against the Log 10 protein ratios. The ratio between Sample and Control is named “t-test difference” and represented in Log_{10} scale (Protein abundance ratio (Sample / Control)). X-axis represents protein abundance ratio (Sample/Control) in Log_{10} scale. Y-axis represents total peak intensity in Log_{10} scale. FDR: False Discovery Rate. Perseus uses both the p-values and the ratio to determine whether the ratio observed significantly differs from the control one. S0: artificial groups variance. It controls the relative importance of t-test p-value and difference between means. At S0=0 only the p-value matters, while at nonzero S0 also the difference of means plays a role. At S0=1 both the p-value and the ratio (difference of means) are equally

important to decide whether there is a significant difference between sample and control for a given protein.

4. Methods in cell biology

4.1. Paraffin embedding

In chapter 2, Arabidopsis stems were fixed overnight in 3.7% (vol/vol) formaldehyde. Samples were dehydrated with a graded series of ethanol/histoclear (3:1, 1:1, 1:3, histoclear) and embedded in paraplast (Sigma). Transverse stem sections (6 µm) were made by using a Microtome (Jung-Autocut, Leica®). Sections were stained with 0.1% Toluidine blue or Phloroglucinol solution (saturated with HCl), and visualized by using an Axiophot microscope (Zeiss®).

4.2. GUS activity staining

Shoot-inflorescence stem hand-cut sectioned and fixed on ice-cold 90% acetone for 20min on ice, rinsed with water and incubated 100nM sodium phosphate buffer (pH 7.2), 10mM sodium EDTA, 0.1% Triton X-100, 1mg/mL 5-bromo-4-chloro-3indolyl-b-D-glucuronide (X-Gluc; Duchefa, Haarlem, The Netherlands), 10mM potassium Ferrocyanide ($K_3[Fe(CN)_6]$) and potassium Ferricyanide $K_4[Fe(CN)_6]$), for 20min in vacuum and finally incubated at 37ºC overnight. Samples were rinsed three times in water, stained with Ruthenium Red (Sigma) for 1 min and mounted in water.

4.3. Historesin embedding

In chapter 3, inflorescence stem sections from both WT and mutant Arabidopsis plants were fixed at 4ºC overnight in 1.25% Glutaraldehyde in 0.1M sodium cacodylate buffer (pH 7.4; Electron Microscopy Science). Fixer solution was removed by water rinse (x2). Samples were dehydrated through increasing graded series of ethanol: 30%, 50%, 70%, 90% and 100% ethanol dilutions for 30min each one. Next, 50% Historesin-I (Technkovit®) in ethanol solution was added and incubated for 30min, followed by Historesin-I 100% solution wash (1h). New Historesin-I 100% solution was added and samples were kept at 4ºC overnight. Blocks were done by placing samples into plastic molds, which were filled with 100% Historesin-II solution (Technkovit®). Each mold was covered with parafilm and kept overnight at 4ºC to accelerate their solidification.

Historesin-I (for 100mL): 100mL Historesin + 1g Hardener-I

Historesin-II (for 15mL): 15mL Historesin-I + 1mL Hardener-II

Transverse stem sections (3-5 µm) were done using a Leica Microtome (Microtome RM2265, Leica®). Sections were stained with 0.1% Toluidine blue in 0.1M NaPO4 buffer pH7.0, rinsed and mounted in water for microscopical visualization in Axiophot Microscope (Zeiss®) microscope. GFP-fluorescence was observed in hand-made sections from the same part of the stem in a Stereomicroscope (SZX16, Olympus®)

5. Imaging

5.1. Confocal microscopy

To analyse the YFP and GFP localization in *ProBRL1:BRL1-YFP, ProBRL3:BRL3-YFP, 35S:BRL3-GFP* and *ProBRI1:BRI1-GFP* lines, 6-day-old roots were stained in 10mg/ml propidium iodide (PI, Sigma) and visualized after excitation by a Kr/Ar 488 nm laser line. PI and GFP were detected with a band-pass 570-670 nm filter and 500-545 nm filter, respectively. For the yellow fluorescent protein (YFP), the excitation wavelength was 488 nm and fluorescence was collected in the range of 493-536 nm (rendered in green). A FV 1000 confocal microscope (Olympus®, Tokyo, Japan) was used. Different Z stacks and transversal optical sections were processed using Olympus FV software and assembled with Photoshop CS (Adobe Systems, San Jose, CA, USA). Starch granules in columella cells were visualized by a modified Pseudo Schiff propidium iodide (mPS)-PI staining method (Truernit et al., 2008):

6-day-old seedlings were fixed in 50% Methanol 10% Acetic Acid fixation solution overnight at 4ºC. Samples were rinsed with water two times and transferred to 1% periodic acid solution for 30min. Next, samples were incubated during 1-2 hours with 15mL Schiff reagent + 1mL PI (1mg/mL) solution. Finally, samples were mounted on a glass slide with Hoyer's solution and covered with a cover slide. Samples were stored in darkness drying for a few days and analysed in confocal microscopy.

Schiff reagent: 100 mM sodium metabisulphite and 0.15 N HCl; PI to a final concentration of 100 mg/mL was freshly added.

Hoyer's solution: 30 g gum arabic, 200 g chloral hydrate, 20 g glycerol, and 50 mL water.

5.2. Arabidopsis protoplast FRET-FLIM analysis

For determining heterodimerization among receptors, PMON999YFP/CFP vectors containing *35s:BRL3-YFP/CFP*, *35s:BRL1-YFP*, *35s:BRI1-YFP* and *35:BAK1-YFP* were generated by J. Russinova and F. Breukelen. Maxiprep DNA extraction was done to obtain 1ug/mL plasmid DNA for all the protoplast experiments. Protoplast isolation from rosette leaves of 4-week-old Col-0 WT plants was done as described in (Wu et al., 2009). Protoplast transfection by adding PEG/ Ca^{2+} was performed as described in (Russinova et al., 2004). For FLIM measurements, Hamamatsu R3809U MCP PMT (Hamamatsu City, Japan) was used, which has a time resolution of 50 ps. FRET between CFP and YFP was detected by monitoring donor emission using a 470–500 nm band-pass filter. Donor FLIM lifetimes (CFP) were analysed with SPCImage 3.10 software (Becker & Hickl) using a two-component decay model. Several cells (n > 20) were analysed. Statistical significance of differences between samples was determined using a two-tailed Student's T-test (* pvalue<0.01).

6. Theoretical methods

6.1. Mathematical modeling (chapter 2)

We set a model of auxin dynamics across a ring of vascular cells and the surrounding apoplast in which stochastic cell division is incorporated. The model can evaluate the effect of changes in efflux carriers, cell number, and dynamics on auxin distribution. Both active polar transport and diffusion is taken into account (Jonsson et al., 2006). The model reads

$$\frac{dA_i}{dt} = \varepsilon \sum_{j \in n(i)} I_{ij} a_j - \varepsilon \sum_{j \in n(i)} E_{ij} A_i$$

$$\frac{da_i}{dt} = \sum_{j \in N(i)} E_{ji} A_j - \sum_{j \in N(i)} I_{ji} a_i + D \nabla_i^2 a_i$$

where A_i and a_i stand for auxin concentrations in cell i and in the apoplast i, respectively, and space has been discretized (Figure 3). E_{ij} and I_{ij} are the efflux and influx transport coefficients or permeability between cell i and apoplast j, which depend on the level of efflux and influx carriers, respectively. Influx and efflux permeability are detailed in SI Text. D represents the effective diffusion rate along the apoplast. ε is the ratio between the linear size of the apoplast and the linear size of cells. n(i) runs over the apoplast neighbouring cell i, while N(i) runs over cells surrounding apoplast i. We included cell proliferation dynamics and considered that tissue cell proliferation occurs at a slower time scale than auxin dynamics. Cells divided at random and, as a first approximation, we assumed they reached their final growth very rapidly (Ibañes et al., 2006), expanding the provascular ring and preserving its circular shape.

6.2. Mathematical modeling (chapter 3)

We used a mathematical model of polar auxin transport proposed by Sahlin et al. (Sahlin et al., 2009) with the inclusion of apoplastic auxin transport as in the article by Ibañes et al. (Ibañes et al., 2009). In this model, auxin is pumped into the cell through the influx carriers, which are homogeneously distributed in the cell. Moreover, auxin is pumped from inside the cell to the apoplast through the efflux carriers, which can be polarly distributed in the cells. As in Sahlin et al., efflux carrier's localization depends on the level of auxin from neighbouring cells. It is also taken into account that a fraction of the auxin due to pH conditions is protonated, and this auxin fraction is passively transported throughout the tissue. Auxin production and degradation occurs inside cells. Apart from the assumption of the polarization mechanism for the efflux carriers, this model is a very realistic approach to the chemiosmotic model of auxin transport. The dimensional model equations for cytosolic auxin concentration in cell *i* and apoplastic auxin concentration in the apoplastic compartment *i* read

$$\frac{dA_i}{d\tau} = -\sum_{j\epsilon n(i)} W_{ij} J_{ij} - \nu_c A_i + \sigma_c$$
$$\frac{da_i}{d\tau} = \sum_{j\epsilon N(i)} W_{ji} \frac{V_{cell}}{V_{ap}} J_{ji} + D\, \nabla_i^2 a_i \qquad (1)$$

with τ being time, D the apoplastic diffusion, σ_c and ν_c the auxin production and degradation rates, V_{cell} the cell volume, V_{ap} the apoplast volume , W_{ij} the area of the cell wall of cell *i* facing the apoplast *j*. ∇_i^2 is the discrete Laplacian J_{ij} stands for the auxin flux from the cell *i* to the apoplast *j* and contains the protonated auxin transport, and both active transports due to the influx and efflux carriers.

For convenience, we adimensionalized the model in time yet we did not adimensionalize the auxin concentration. The resulting model parameters can be related to physico-chemical magnitudes that have been measured or can be estimated. In our study, we chose to mainly vary the following effective dimensional parameters: the influx parameter *I*, the efflux parameter E, the apoplastic diffusion *D* and the protonated auxin diffusion rate D_{ca}. We applied our model to one line of cells with periodic boundary conditions. We neglected cell division for focusing on the pattern emergency.

We performed linear stability analysis over the homogeneous state to study the pattern formation capabilities of the model in relation to the parameters of interest, and to predict how the characteristic wavelength of the resulting pattern will depend on such parameters.

6.3. Simulation details (chapter 3)

We integrated our dynamical model for auxin transport (nondimensional version in time of Eqs. 1) through a Runge-Kutta method of 4th order with time step dt=0.001 being *t* the nondimensional time. Most of the parameter values were set according to already published work, some of it based on experimental data. Unless otherwise stated, we set homogeneous initial conditions with small noise, and we stopped the simulations when the steady state was reached.

CATALAN SUMMARY

RESUM EN CATALÀ

Ruta de senyalització dels Brassinosteroides

Aquesta tesis doctoral té com a objectiu principal investigar noves funcions de les hormones vegetals esteroides, Brassinoesteroides (BRs), en el desenvolupament del teixit vascular de la planta. Per tal d'assolir aquest objectiu hem utilitzat una aproximació multidisciplinària, combinant models matemàtics i computacionals amb anàlisis exhaustius dels fenotips vasculars de plantes mutants en BRs, així com tècniques de proteòmica amb microscòpia confocal, amb l'objectiu d'identificar nous components de senyalització de BR amb una resolució cel·lular. Els nostres resultats indiquen l'inici d'una ruta alternativa a la visió clàssica de la ruta de senyalització dels BRs descrita fins al moment.

El nom de Brassinosteroides se'ls va adjudicar quan varen ser descoberts al pol·len de la planta *Brassica napus*, on són molt abundants. Els BRs tenen una estructura química molt hidrofòbica, i provenen dels esterols, que formen part de les membranes de les cèl·lules vegetals. Els BRs han estat molt estudiats tant a nivell fisiològic com molecular, principalment a les plantes model *Arabidopsis thaliana* (Arabidopsis) i *Oryza sativa* (arròs). De fet, la ruta de la transducció de la senyal dels BRs és una de les rutes de senyalització més ben caracteritzades en plantes (capítol 1). Els esteroides juguen un paper clau en el creixement i el desenvolupament d'eucariotes multicel·lulars. Tot i que l'estructura de la hormona és molt similar als esteroides d'animals, tenen diferents mecanismes de percepció, ja que en les cèl·lules vegetals la hormona s'uneix al receptor BRI1 (BRASSINOSTEROID INSENSITIVE 1), localitzat a la membrana, mentre que en les cèl·lules animals el receptor principal es troba localitzat al nucli. BRI és una proteïna receptora del tipus LRR-RLK (LEUCINE-RICH REPEAT - RECEPTOR-LIKE KINASE) amb un domini extracel·lular molt ric en leucines on es troba el lloc d'unió a la hormona i un domini quinasa intracel·lular que transmet la senyal a través d'una cascada de proteïnes quinases i fosfatases citoplasmàtiques, fins al nucli, on s'activa la resposta de gens essencials pel desenvolupament i creixement de la planta.

Estudis bioquímics i estructurals han demostrat que la Brassinòlida (BL, la hormona més activa) s'uneix al receptor en el seu domini LRR extracel·lular, anomenat domini illa, que es troba entre les repeticions 21 i 22 LRR. Quan el receptor BRI1 percep aquesta unió, la proteïna repressora de la senyal BKI1 (BRI1 KINASE INHIBITOR 1) deixa BRI1 lliure, i aquest s'activa/heterodimeritza amb una altra LRR-RLK anomenada BAK1 (BRI1 ASSOCIATED KINASE 1), que es el co-receptor de BRI1 que permetrà iniciar la transmissió de la senyal cap a dins de la cèl·lula. La unió de BRI1 amb BAK1 provoca l'activació de múltiples fosforilacions entre els dominis intracel·lulars de les dues proteïnes que causa finalment la fosforilació i activació de la quinasa citoplasmàtica BSK1 (BR SIGNALING KINASE 1). A la vegada, aquesta BSK1 fosforila la fosfatasa BSU1 (BRI1 SUPPRESSOR 1) activant-la, i provocant així la desfosforilació i inactivació de la quinasa BIN2 (BR INSENSITIVE 2). Quan els nivells de BR fora la cèl·lula són baixos, la quinasa BIN2 manté la via de senyalització de BRs reprimida, fosforilant els factors de transcripció BZR1 i BES1 (BRASSINAZOLE RESISTANT 1 i BRI1 EMS SUPPRESSOR 1) que queden retinguts de manera inactiva al citoplasma (Figura 1A). Llavors, les fosfoproteines 14-3-3 s'uneixen a BES1 i BZR1 promovent així la seva degradació pel proteosoma. En canvi, quan els nivells de BRs augmenten, s'activa el receptor BRI1, BAK1 i les proteïnes BSK1 i BSU1, que conclouen desfosforilant i inactivant BIN2, de manera que la ruta de senyalització de BRs s'activa (Figura 1B). Els factors de transcripció BES1 i BZR1 són llavors desfosforilats per la fosfatasa PP2A i poden entrar al nucli, on activaran la transcripció d'aproximadament 2000 gens de resposta a la hormona.

A més de la senyalització, les rutes de biosíntesi i homeòstasis dels BRs també han estat caracteritzades, i són essencials perquè la planta tingui un creixement i desenvolupament adequats. A més, s'ha descrit que el receptor BRI1 pot endocitar-se a diferents compartiments cel·lulars on s'inactiva, proveint així un altre mecanisme d'atenuació de la senyal de BRs.

En general, mutacions del gens que codifiquen per la majoria dels components de senyalització descrits anteriorment resulten en defectes dramàtics en el creixement i desenvolupament de la planta, les fulles, els hipocòtils, la flor, i en la germinació de les llavors, entre d'altres. Fins ara, les proteïnes BRI1, BES1 i BZR1 s'havien descrit com a proteïnes localitzades de manera ubiqua a la planta, però estudis més recents, entre ells els resultats presentats en aquesta tesis (capítol 4), revelen que en realitat aquestes proteïnes tenen patrons de localització específics per algunes cèl·lules, mentre es troben absents a unes altres.

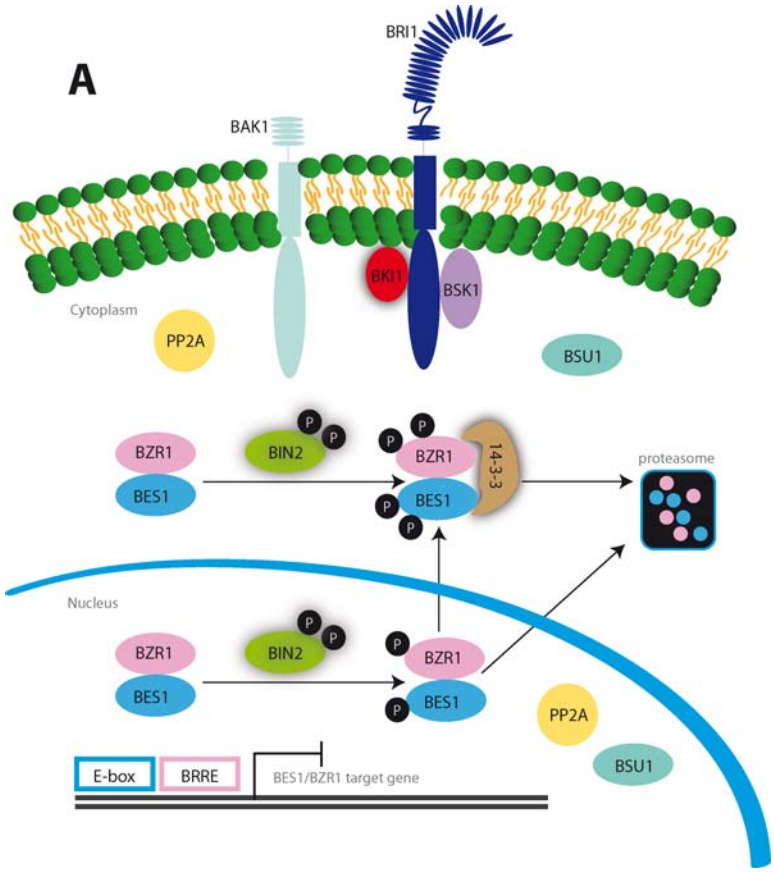

Figure 1. Ruta de senyalització dels BRs d'Arabidopsis
(A) Representació esquemàtica de la ruta de senyalització dels BRs inactiva.
En absència de lligand BL, BKI1 està reprimint les activitats quinasa de BRI1 i BSK1 a la membrana. Tant al citoplasma com al nucli, la quinasa BIN2 es troba reprimint la senyalització dels BRs fosforilant els factors de transcripció BZR1 i BES1 (BRASSINAZOLE RESISTANT 1 and BRI1 EMS SUPPRESSOR 1), la qual cosa els reté inactius al citoplasma. Les formes fosforilades de BES1 i BZR1 interaccionen amb les fosfoproteïnes 14-3-3 que promouen la seva degradació al proteosoma.

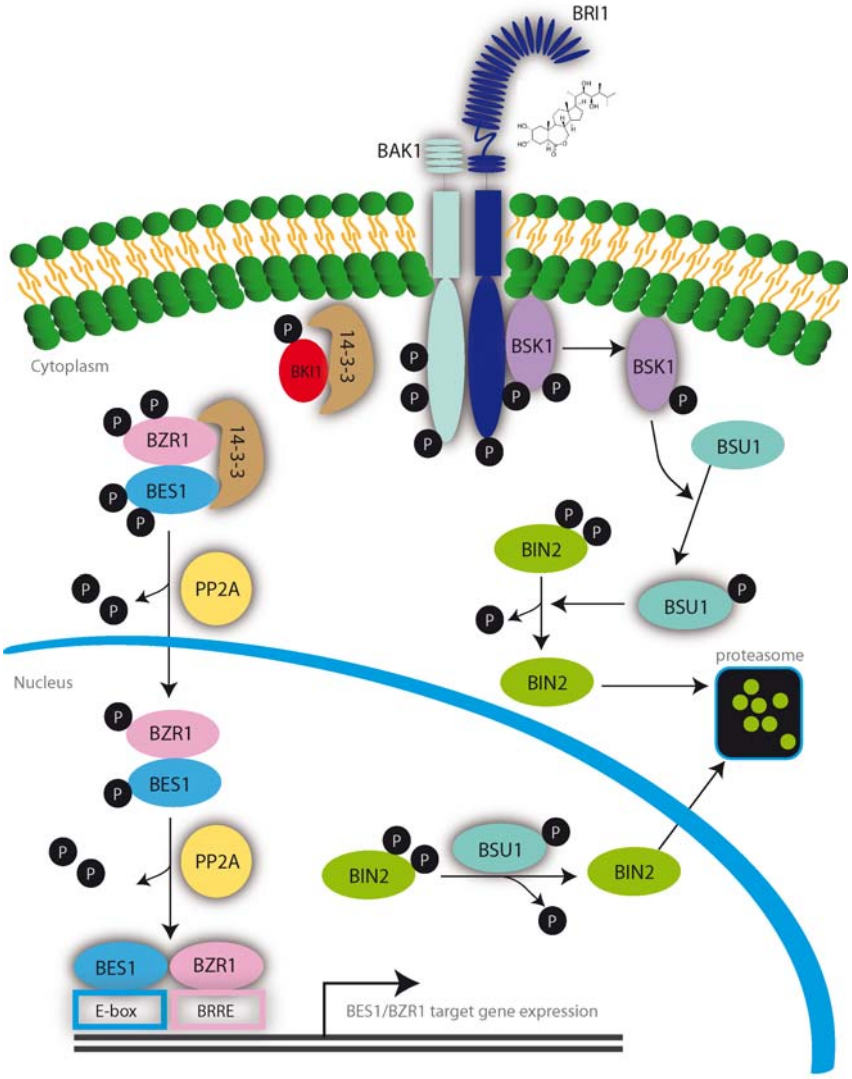

Figure 1. Ruta de senyalització dels BRs d'Arabidopsis
(B) Representació esquemàtica de la ruta de senyalització dels BRs activa.
En presència del lligand BL, aquest s'uneix al domini extracel·lular del receptor BRI1. EL domini quinasa del receptor BRI1 fosforila BKI1 i s'allibera, la qual cosa permet la heterodimerització de BRI1 amb el seu coreceptor BAK1. Esdeveniments de transfosforilació entre BRI1 i BAK1 activen i fosforilen BSK1. BSK1 fosforila la fosfatasa BSU1 activant-la. BSU1 inactiva la quinasa BIN2 enviant-la a degradació pel proteosoma. Llavors, BZR1 i BES1 són desfosforilats per la fosfatasa PP2A, permetent així que les formes actives de BZR1 i BES1 entrin al nucli i activin la transcripció d'aproximadament 2000 gens de resposta a BRs.

La senyalització dels Brassinoesteroides està estretament relacionada amb el desenvolupament vascular

El sistema vascular de la planta transporta aigua i nutrients, que són essencials per al desenvolupament i creixement adequats de les plantes. Els teixits vasculars s'organitzen d'una manera complexa i es troben formats per diferents tipus cel·lulars especialitzats, que són l'objecte de múltiples esdeveniments de senyalització i regulació gènica. Atès que la major part de la biomassa vegetal a la terra prové dels teixits del xilema, l'estudi dels mecanismes subjacents en el desenvolupament vascular esdevé essencial. Mentre que els efectes dels BRs en el control del creixement cel·lular han estat àmpliament estudiats, noves evidències vinculen la senyalització dels BRs al desenvolupament vascular, suggerint un paper més específic pels BRs en tipus de cèl·lules específiques dins del teixit vascular.

Estudis inicials utilitzant Zinnia elegans (Zinnia) com a sistema model per a l'anàlisi in vitro dels elements traqueals (ET), van demostrar que els BRs es requereixen per iniciar el procés de diferenciació de les cèl·lules del mesòfil. Els teixits conductors de les plantes vasculars es componen de TEs alineats que han entrat en la mort cel·lular programada. Els BRs són un factor clau en la iniciació de la formació de la paret secundària per mort cel·lular programada en plantes. El potent inhibidor de la síntesi BR Brassinazol provoca una reducció de la diferenciació del xilema en Arabidopsis. A més, els mutants biosintètics de BRs DWARF4 i DIM1 presenten alteracions en la formació de la paret cel·lular secundària. Aquests resultats suggereixen que els BRs promouen la diferenciació del xilema, mentre que els nivells BRs són essencials per al desenvolupament adequat del floema. Els BRs regulen components de la paret cel·lular a nivell transcripcional mitjançant el control de l'expressió dels gens CESA (cel·lulosa sintasa A), que són regulats directament per BES1. Els mutants en CESA-3 també mostren defectes de cel·lulosa i una major lignificació de les parets cel·lulars secundàries, mentre que la senyalització dels BRs regula pectinases paret cel·lular, confirmant així la relació directa entre la senyalització de BRs i la diferenciació de xilema.

El teixit vascular d'Arabidopsis s'organitza en una disposició radial dels feixos vasculars i la seva alternança periòdica amb fibres interfasciculars, que junts formen l'anell vascular. Aquest patró sorgeix d'un anell de cèl·lules procambial que divideixen i es diferencien en el xilema i el floema, donant lloc a feixos vasculars col·laterals al voltant de la procàmbium. Mutants deficients en BRs presenten una reducció de la diferenciació del xilema i un menor nombre de paquets vasculars en la tija d'Arabidopsis. A banda de BRI1, dos receptors de BRs addicionals BRL1 i BRL3 (BRI1-LIKE 1 i BRI1-LIKE 3) es van identificar gràcies a l'alt percentatge d'homologia amb el receptor BRI1 en Arabidopsis i arròs. Mentre BRL1 i BRL3 mostren una capacitat similar d'unió a la hormona a la de BRI1, el patró d'expressió d'aquests receptors difereix de la de BRI1 doncs es troba enriquit en els teixits vasculars. Anàlisis genètics revelen que els receptors BRL funcionen de forma redundant amb BRI1 en el patró col·lateral del feix vascular. Aquesta especialització funcional dels homòlegs de BRI1 pot haver ocorregut durant l'evolució abans de la separació de les monocotiledònies / dicotiledònies ja que els homòlegs d'arròs OsBRI1 i OsBRL3 també funcionen en cèl·lules específiques del teixit vascular. A més de BRL1 i BRL3, BRL2 (BRI1-LIKE 2) un receptor BR no actiu de la família BRI1, presenta una funció en la formació del patró de venació de les fulles d'Arabidopsis. Una caracterització quantitativa de diversos de pèrdua de la funció i el guany de la funció de senyalització de BR i els mutants de síntesi es va dur a terme per entendre millor la contribució BR amb el desenvolupament vascular. Els diferents paràmetres es van establir per primera vegada a la tija principal de plantes salvatges (Col-0; WT) adultes i seguidament es van mesurar els mateixos paràmetres en els mutants de BRs. Les dades quantitatives juntament amb modelatge computacional que integrava les dades experimentals amb les prediccions teòriques indiquen un paper per BRs en la promoció de les cèl·lules procambial d'Arabidopsis. D'altra banda, els canvis induïts per BRs en el nombre de cèl·lules procambials és crucial per a la determinació del nombre de feixos vasculars, que es formen prèviament segons els nivells de concentració d'auxina (màxims). En resum, el transport d'auxina i la senyalització dels BRs són necessaris per a un correcte establiment del patró vascular periòdic en la tija d'Arabidopsis.

Un gran nombre d'estudis suggereixen esdeveniments on concorren accions dels BRs i d'auxines. No s'ha proporcionat cap prova per al transport dels BRS a llarga distància mentre que l'auxina és transportada activament a través dels teixits de les plantes. Així, podria ser que els BRs es beneficiïn de la mobilitat de la senyal d'auxines per transferir la seva funció a diferents teixits de la planta.

Estudis addicionals en aquesta línia contribuiran a delimitar les funcions específiques i coordinades dels BRs i l'auxina en els teixits vasculars. Per tant, per tal d'investigar funcions específiques dels BRs en el desenvolupament vascular es podrien dur a terme les següents aproximacions: (i) la purificació de complexos de receptors dels BRL específics dels teixits vasculars, (ii) la caracterització dels perfils transcriptòmic i metabolòmic de les cèl·lules vasculars en resposta a BRs i (iii) l'anàlisi quantitativa dels mutants de BRs utilitzant microscòpia de super-resolució per visualitzar els teixits vasculars en detall.

El poder dels estudis en arrels per a la comprensió de l'acció dels BRs en el desenvolupament de la planta

L'arrel primària d'Arabidopsis ofereix un sistema òptim per l'estudi de la senyalització de BRs en el desenvolupament de la planta. Les arrels primàries mostren un patró simple i estereotipat de les capes de cèl·lules amb una separació espacial de les activitats cel·lulars al llarg de l'eix longitudinal, que s'ha utilitzat àmpliament per a l'estudi del desenvolupament de la planta.

Estudis previs de les respostes dels BRs utilitzant l'hipocòtil i l'elongació del pecíol i les fulles han demostrat que els BRs són moduladors importants en l'elongació de les cèl·lules de la planta. A més, s'han observat defectes severs en el creixement en els mutants deficients de BRs, els quals són indicatius de la importància del paper dels BRs en el creixement cel·lular, mentre que la funció dels BRs en les divisions cel·lulars ha tingut molta controvèrsia fins el moment. L'anàlisi quantitativa dels defectes del patró vascular (aquesta tesi), juntament amb la caracterització dels mutants de BRs a les arrels, han establert que el control dels BRs en el creixement de les plantes és també degut al seu paper en la divisió cel·lular.

A través de l'anàlisi d'arrels dels mutants de BR s'ha establert un nou paper dels BRs en la progressió del cicle cel·lular. Els mutants de pèrdua de funció de BRs i les mutacions amb guany de funció de BRs resulten en arrels més curtes a causa d'una reducció de la longitud del meristema de l'arrel. Aquesta reducció és causada per alteracions en la progressió del cicle cel·lular. A més, la percepció de BRs a través de les cèl·lules epidèrmiques de és suficient per controlar el creixement de les arrels i la planta, suggerint noves funcions dels BRs en tipus cel·lulars específics.
El nínxol de cèl·lules mare està format pel centre quiescent (QC), envoltada per les cèl·lules mare que donen lloc als diferents tipus de cèl·lules de l'arrel. Al costat distal del QC es troben les cèl·lules mare de la columel·la (CSC), les cèl·lules filles de les quals es diferencien en cèl·lules que contenen midó i que poden detectar la gravetat. A les plantes WT, les cèl·lules del QC es divideixen poques vegades i les CSC mostren majoritàriament una sola capa de cèl·lules indiferenciades. L'aplicació exògena de BRs i l'anàlisi genètica del mutant *bri1* van revelar un paper primordial dels BRs en la diferenciació de les CSC, que indica un nou paper dels BRs en el control de la dinàmica de les cèl·lules mare de l'arrel. Recentment, també s'ha mostrat una funció específica dels BRs en l'activitat de les cèl·lules del QC . Tot i que BRI1 es localitza gairebé en totes les cèl·lules del meristema de l'arrel, les proteïnes BRL1 i BRL3 s'expressen principalment en les cèl·lules mare del nínxol, on es veu disminuïda la densitat de BRI1. Aquests resultats, juntament amb la immunoprecipitació en viu i les dades d'espectrometria de masses per als complexos receptors de BRI1 i BRL3, suggereixen l'existència de diferents complexos receptors de BRs en diferents tipus cel·lulars. Nosaltres proposem un model que mostra funcions específiques i no redundants per al receptor BRL3 en el control de l'activitat del QC en l'àpex de l'arrel d'Arabidopsis (Fàbregas et al. 2013 i presentat a la Figura 2 i al capítol 4 d'aquesta tesi). Aquest paper dels BRs en la divisió cel·lular que va ser descobert principalment en les arrels es veu recolzat pel reduït nombre de cèl·lules dels mutants de síntesi de BRs en la fulla, que és causada per una progressió més lenta del cicle cel·lular. L'anàlisi del cicle cel·lular amb gens marcadors com la Ciclina B1, 1, KNOLLE i CDK va demostrar que no només la síntesi, sinó també mutants de la senyalització de BRs presenten alterat el seu cicle cel·lular. A més de promoure l'expansió cel·lular i la diferenciació vascular, els BRs

regulen el desenvolupament d'estomes en fulles d'Arabidopsis. Els estomes són petits porus presents en les fulles i en la superfície de l'epidermis de la tija que tenen una funció d'intercanvi de gasos. En les dicotiledònies, la majoria d'ells estan en l'epidermis inferior de les fulles. Tant mutacions amb guany de funció de BRs com l'aplicació exògena de BL redueixen el nombre d'estomes per unitat de superfície foliar. Per contra, les fulles de mutants de pèrdua de funció de BRs mostren agrupament d'estomes i un major nombre d'estomes per unitat de superfície foliar. Assaigs de fosforilació, doble híbrid en llevat, i co-immunoprecipitació *in vivo* van demostrar que BIN2 interactua la MAPK quinasa YODA (YDA) per inhibir l'activitat de YDA. En resum, els BRs controlen el desenvolupament i formació d'estomes mitjançant la inhibició tant de l'activitat YDA a les fulles d'Arabidopsis. A més, els factors de transcripció que participen en el desenvolupament dels estomes SPCH, MUTE i FAMA, estan regulats per una via de senyalització repressiva que consisteix en els factors EPF, la família de LRR-RLKs ERECTA i la LRR-RLK TOO MANY MOUTH (TMM). Aigües avall d'aquests receptors hi ha les quinases de senyalització de MAPK, YODA, MKK4/MKK5 i MPK3/MPK6, l'activació de les quals inactiva SPCH per fosforilació. Un estudi recent va revelar que els mutants de pèrdua de funció de BRs *cpd* i *bri1* mostren menys estomes en hipocòtils mentre que els mutants de guany de la funció de BRs DWARF4 i BRI1-GFP mostren més estomes a l'hipocòtil. Així, es descriu un paper positiu dels BRs en els estomes de l'hipocòtil a la vegada que un paper d'inhibició dels BRs en la formació d'estomes en cotilèdons. Una hipòtesis es que els cotilèdons i els hipocòtils poden respondre de manera diferent als BRs degut a una regulació espacial diferent de les proteïnes BIN2. Així, l'alta abundància dels components del mòdul de senyalització MAPK en les cèl·lules de cotilèdons, permetria que la quinasa BIN2 per reprimís YDA i MKK4, promovent la formació dels estomes en els cotilèdons. En canvi, els nivells baixos de MAPK en hipocòtil permetrien que BIN2 regulés de SPCH, reprimint la formació d'estomes en l' hipocòtil.

Els BRs controlen la fertilitat masculina mitjançant la regulació de gens clau per al desenvolupament de les anteres i el pol·len d'Arabidopsis. Fins ara, els defectes en l'elongació del tub pol·línic s'han entès com la principal causa de l'esterilitat masculina en els mutants de BRs. Una anàlisi més detallada dels mutants de BRs ha posat de manifest que els defectes en la fertilitat masculina són causats per defectes en el desenvolupament dels grans de pol·len, en lloc de per un allargament fallat del tub pol·línic. Els mutants *cpd* i *bri1* mostren unes micròspores mares més petites i aquestes presenten un nombre menor de grans de pol·len, confirmant així que el paper dels BRs en el control de la divisió cel·lular és una tendència general en el desenvolupament de la planta.

Posteriorment, es van descriure dos nous receptors de BRs, BRL1 i BRL3 (BRASSINOSTEROID RECEPTOR LIKE 1 i 3) del tipus LRR-RLK, que varen ser descoberts gràcies a l'elevada homologia que comparteixen amb el receptor principal BRI1. Ambdós receptors BRL1 i BRL3 es troben localitzats de manera específica en el teixit vascular d'Arabidopsis. Tot i que els principals components del senyal ja han estat identificats pel seu homòleg més pròxim, el receptor BRI1, els complexes de BRL1 i BRL3 juntament amb els candidats co-receptors així com els components de la ruta de senyalització encara no s'han descrit. Per tal d'entendre millor la funció d'aquests receptors de BRs, tant similars en seqüència però amb diferent localització, com també per tal d'investigar funcions de BRs específiques pels diferents tipus cel·lulars, vam plantejar diferents aproximacions:

1. Estudi de la contribució dels Brassinoesteroides en la formació del patró vascular de la tija d'Arabidopsis
2. Identificació de nous components de senyalització del receptor BRL3, involucrats en la regulació del desenvolupament vascular.
3. Caracterització funcional del signalosoma de BRL3 en el creixement i en el desenvolupament de la planta.

Els Brassinosteroids juntament amb les auxines, juguen un paper essencial en la formació del patró de feixos vasculars periòdics de la tija d'Arabidopsis

El sistema vascular té la funció de transportar d'aigua, sals i nutrients, els quals són essencials pel correcte creixement i desenvolupament de les plantes. Els teixits vasculars de les plantes estan formats per diferents tipus cel·lulars que s'organitzen formant diferents patrons. A la tija de la planta model Arabidopsis, el teixit vascular mostra un patró radial format per feixos vasculars separats entre ells per distàncies equidistants. Tot i així, el mecanisme pel qual el teixit vascular forma aquest patró radial organitzat, és desconegut.

En aquesta tesi hem fet servir la combinació de la biologia experimental juntament amb fórmules matemàtiques i prediccions computacionals ("Systems Biology") per tal d'estudiar la funció dels BRs en el patró vascular de la planta model Arabidopsis. Disposant d'una amplia bateria de mutants de les ruta de síntesi i senyalització de BRs inclòs el receptor BRI1, vam analitzar quantitativament el seu patró vascular a la tija d'Arabidopsis. Primer, vam establir els paràmetres vasculars en les plantes silvestres [Col-0 wild type, (WT)] per identificar un patró estàndard. D'aquesta manera vam observar que les plantes silvestres presenten aproximadament 5 feixos vasculars en la seva tija principal, distribuïts de manera equidistant en un anell de cèl·lules procambials, que també van ser comptabilitzades. Vam revelar que tots els mutants de pèrdua de funció de BRs presentaven menys feixos vasculars mentre que els mutants de guany de funció de BRs, mostraven un augment en el número de feixos vasculars.

A continuació, vam analitzar tots i cadascun dels mutants mesurant els mateixos paràmetres establerts per al WT i comptabilitzant les cèl·lules procambials que formen l'anell vascular. A la vegada, vam iniciar una col·laboració amb la Dra. Marta Ibañes, física de la Universitat de Barcelona, que va construir un model matemàtic per simular la formació del patró vascular. Gràcies a la construcció d'aquest model vam descobrir que els màxims d'auxina, creats pel transport polar de l'auxina, són els responsables de posicionar els feixos vasculars, i de la formació de cadascun d'ells dins l'anell vascular. A més, el model preveu que els nivells d'auxina totals de la planta no afecten

el patró radial del teixit vascular a la tija. L'auxina és una hormona vegetal molt important, ja que té múltiples funciones en la morfogènesis i el desenvolupament de les plantes. Anteriorment ja s'havien descrit funcions essencials del transport polar de l'auxina en diferents òrgans com l'arrel, les fulles i el meristema apical.

Així, com es mostra en el capítol 2 d'aquesta tesi, vam demostrar que el transport polar de l'auxina és essencial per la correcta disposició periòdica dels feixos vasculars al voltant de l'anell de cèl·lules procambials. El transport polar de l'auxina es fa a través de proteïnes transportadores que exporten l'auxina fora la cèl·lula, anomenades PIN (PINFORMED; exportadors d'auxina) Experimentalment, vam confirmar la importància del correcte posicionament asimètric de les proteïnes PIN en la cèl·lula. Vam analitzar el fenotip vascular dels mutants *pin1pin2* i de plantes tractades amb inhibidors químics dels transportadors d'auxina (NPA) observant així que el patró radial es dissipava, de manera que en aquestes plantes els pics de feixos vasculars ja no estaven definits. A més, vam demostrar que és el transport el que afecta el patró, i no els nivells totals d'auxina, analitzant els mutants *yucca* que tot i tenir un 50% més d'auxina que les plantes WT, presenten un patró vascular normal.

El model també proposava una funció nova pels BRs, en el qual els BRs modulen el nombre de feixos vasculars a través de canvis en el nombre de cèl·lules procambials en l'anell vascular. A continuació, vam validar experimentalment el model, quantificant els fenotips de tos els mutants de BRs presentats en el capítol 2 d'aquesta tesis, i comprovant així que els BRs promouen les divisions de les cèl·lules procambials.

En resum, aquest estudi demostra que el transport polar de l'auxina i la senyalització de BRs determinen el patró radial dels feixos vasculars de la tija principal de les plantes d'Arabidopsis. Així doncs, les nostes dades experimentals juntament amb l'elaboració d'un nou model matemàtic ens va permetre entendre com s'elabora el patró radial de la tija d'Arabidopsis, i els resultats es van publicar a la revista PNAS (Ibañes et al., 2009) (veure també addendum; (Fàbregas et al., 2010); capítol 2 i addendum al capítol 2).

Els transportadors d'importació d'auxina controlen el desenvolupament del teixit vascular d'Arabidopsis

L'auxina és una hormona vegetal molt important, ja que té múltiples funcions en la morfogènesi i el desenvolupament de les plantes. Com ja hem mostrat anteriorment, els transportadors d'exportació d'auxina (PIN) juguen un paper molt important en el patró vascular de la tija, posicionant i promovent la formació dels feixos vasculars en l'anell de cèl·lules procambials de la tija (capítol 2). En canvi, el paper dels transportadors d'importació d'auxina en el teixit vascular de la tija encara no estava definit. Novament vam combinar un model matemàtic amb les nostres eines experimentals per tal de desxifrar el paper dels importadors d'auxina dins la cèl·lula durant la formació del patró vascular, en col·laboració amb la Dra. Marta Ibañes i el Dr. Pau Formosa.

En la planta model Arabidopsis es coneixen quatre importadors d'auxina: AUX1, LAX1, LAX2 i LAX3. D'aquests, AUX1 és el més estudiat, i té un paper molt important en el gravitropisme de les arrels (Marchant et al., 1999; Marchant et al., 2002). Recentment, s'ha descobert que els quatre gens tenen un paper redundant en el patró de fil·lotaxi espiral que presenta el meristema apical d'Arabidopsis (Bainbridge et al., 2008). LAX2 també va ser descobert com a regulador del desenvolupament vascular de la venació dels cotiledons (Peret et al., 2012).

Així doncs, vam formular un model matemàtic que proposava un nou paper pels importadors d'auxina, en el qual mostràvem que faciliten la formació del patró i modulen tant la periodicitat com la intensitat dels pics o màxims d'auxina. Per tal de validar-lo, vam analitzar els fenotips vascular de les tiges de quàdruples mutants a*ux1lax1lax2lax3* i vam observar que els mutants mostraven un número significativament reduït de feixos vasculars comparat amb les plantes silvestres WT. Quan vam comptabilitzar el nombre de cèl·lules procambials de l'anell vascular, vam identificar que no era la causa d'aquesta disminució de feixos vascular, com havíem observat prèviament amb els BRs. Aquests resultats demostren que la importació

d'auxina dins les cèl·lules promou la periodicitat dels feixos vasculars modulant la distància que els separa, i avancen que no ho fan per divisions procambials.
A més, les nostres dades experimentals també mostren que els mutants d'importadors d'auxina tenen una forta mancança en la diferenciació del xilema, tant en la zona interfascicular, on les cèl·lules del xilema no presenten les característiques de cèl·lula diferenciada (les parets no es tenyeixen de la mateixa coloració que les cèl·lules xilemàtiques), com en els feixos vasculars. Anàlisis més detallades dels feixos vasculars dels mutants a*ux1lax1lax2lax3* revelen que els mutants d'importació d'auxina tenen un augment molt significatiu en el número de capes de cèl·lules procambials (desdiferenciades) entre el floema i el xilema (**capítol 3**). Els nostres resultats mostren 3, 4, 5 i fins a 6 capes de cèl·lules no diferenciades en els mutants a*ux1lax1lax2lax3 versus* les dues capes de cèl·lules procambials de les plantes silvestres WT. Aquest resultats doncs, vam confirmar una funció nova i essencial dels importadors d'auxina en la diferenciació de les cèl·lules del xilema en el teixit vascular de la tija d'Arabidopsis.

Funcions noves i específiques per a la senyalització de BRs a través dels receptor BRL3 (específics de cèl·lules vasculars)

Les proteïnes BRL1 i BRL3 (BRASSINOSTEROID RECEPTOR LIKE 1 i 3) són dos receptors altament homòlegs al receptor BRI1 que ja s'han descrit anteriorment, i s'ha demostrat que els dos uneixen la hormona, per tant són veritables receptors de BRs. (Caño Delgado 2004). El receptor principal BRI1 és molt més abundant a la planta que no pas BRL1 i BRL3, els promotors dels quals tenen una expressió específica del teixit vascular. BRL1 i BRL3 tenen un paper redundant amb BRI1 en el desenvolupament dels feixos vasculars, concretament en la formació del colateral patró xilema/floema. Tot i així, BRI1 té moltes altres funcions definides i clares en el creixement i desenvolupament de molts òrgans de la planta, mentre que l'estudi dels receptors BRL1 i BRL3 ha estat més compromès degut a que la seva expressió és molt baixa, quasi indetectable, i a la manca de fenotips evidents dels mutants *brl1* i *brl3*.

Nosaltres vam observar que, a diferència de BRI1, els mutants *knock-out* (KO) d'aquests dos receptors BRL1 y BRL3, no mostraven cap fenotip en el nombre de cèl·lules procambials de l'anell vascular de la tija de la planta adulta. Per entendre quina necessitat té la planta de disposar de tres receptors tant altament homòlegs que poden percebre la mateixa hormona, vam utilitzar una aproximació bioquímica en col·laboració amb el Prof. Sacco de Vries de la Universitat de Wageningen (Holanda) per tal de purificar els complexes dels receptors de BRs BRI1 i BRL3 in vivo i els seus interactors. Això ens ha permès entendre millor el paper funcional d'aquests receptors en la planta. Els resultats d'aquests experiments estan resumits a un article que actualment es troba en revisió en la revista Plant Cell (capítol 4).

En primer lloc, vam purificar els receptors BRI1 i BRL3 en col·laboració amb el laboratori del Prof. de Vries. Per a dur a terme aquest experiment, primer vam generar plantes transgèniques on els receptors s'expressaven sota el seu propi promotor i fusionats a la proteïna fluorescent GFP o YFP. El receptor BRI1 presenta alts nivells d'expressió al meristema de l'arrel principal mentre que els receptors BRL1 i BRL3 mostren una localització més reduïda i específica, en el nínxol de cèl·lules mare de l'arrel. Un cop vam tenir línies homozigotes per ambdós receptors, vam dur a terme la purificació dels complexes proteics per immunoprecipitació amb anticossos GFP, en condicions natives. Un cop vam tenir els complexes proteics purificats, vam utilitzar mètodes avançats d'espectrometria de masses per tal d'identificar totes les proteïnes que interaccionen amb ambdós receptors. Així, vam poder identificar components dels complexes receptors de BRI1 i BRL3 en planta, a la vegada que vam poder determinar elements de senyalització tant comuns com específics per cadascun dels receptors.
D'entre tots els candidats a interactors de BRL3, es va identificar el coreceptor BAK1 i altres proteïnes presents al complex receptor de BRI1, però en canvi BRL3 no va ser identificat en les llistes d'interactors de BRI1. Aquests resultats suggereixen l'existència de diferents complexes receptors en diferents dominis cel·lulars. Per tal de validar aquests resultats, ens vam centrar en els interactors de BRL3 , en concret el coreceptor BAK1. BAK1 està descrit com a coreceptor de BRI1, tal i com hem exposat anteriorment (Figura 1, capítol 1).

La interacció de BRL3 i BAK1 es va validar en primer lloc clonant els dos receptors amb dues proteïnes fluorescents diferents (CFP i YFP) i expressant-los en protoplastos d'Arabidopsis, on mitjançant la tècnica de FRET-FLIM es va poder confirmar la seva interacció directa. A continuació, es van realitzar assajos de co-immunoprecipitació en planta que expressaven a la vegada el receptor BRL3 fusionat a la YFP i el coreceptor BAK1 fusionat a la proteïna HA. Immunoprecipitant la proteïna fluorescent YFP amb anticossos específics, i per tant el receptor BRL3 fusionat a ella, vam poder detectar la proteïna BAK1 dins la fracció immunoprecipitada, mostrant així una tercera evidència experimental *in vivo* de la seva interacció amb BRL3. De la mateixa manera, la proteïna BRL1 va ser detectada entre els candidats de BRL3, i també es va demostrar que interacciona directament amb el co-receptor BAK1 mitjançant assajos FRET-FLIM i co-immunoprecipitacions.

Finalment, vam generar triples mutants *brl1brl3bak1-3*, per investigar si el complex proteic BRL3/BRL1/BAK1 específic d'aquestes cèl·lules tenia alguna rellevància funcional en la planta.

Primer vam mesurar arrels de plàntules de sis dies de WT, *brl1brl3*, *bak1-3* i *brl1brl3bak1-3*. Els mutants de BRs es caracteritzen per presentar una arrel més curta que les plantes WT, com hem referenciat en el capítol 1 d'aquesta tesi. Els nostres resultats confirmen que les arrels dels mutants de BRs *bri1-301, bri1-116* i *bak1-3* presenten arrels més curtes que el WT de manera significativa. En canvi, el dobles mutants *brl1brl3* tenen una arrel WT.

Tot i així, les anàlisi de les plantes *brl1brl3bak1-3* revelen que tenen una arrel significativament més curta que les plantes *bak1-3*, indicant que els signalosoma de BRL3 contribueix al creixement de l'arrel juntament amb BRL1 i BAK1.

Tant l'aplicació exògena del BL com els mutants de guany de funció de BR provoquen una reducció de la longitud total de l'arrel a la vegada augmenten les divisions de les cèl·lules mare del nínxol. D'acord amb aquests efectes descrits anteriorment, les plantes *brl1brl3bak1-3* presenten més insensibilitat a la hormona BL que la resta de mutants analitzats, tant a nivell d'elongació de l'arrel com a nivell del nínxol de cèl·lules mare. A més, el teixit provascular de l'arrel dels mutants *brl1brl3bak1-3* presenta hipersensibilitat a la BL comparat amb la resta de mutants i el WT.

En conclusió, tots aquestes anàlisi genètiques de triples mutants *brl1brl3bak1-3* revelen una funció no redundant per al signalosoma de BRL3 en el creixement i desenvolupament de l'arrel i en les activitats cel·lulars del teixit provascular i del nínxol de cèl·lules mare, on es troba localitzat. D'aquesta manera, vam adjudicar una rellevància funcional a les interaccions proteïna-proteïna observades anteriorment. En resum, el nostre estudi demostra la formació de complexes receptors de BRs específics de tipus cel·lular, els quals participen en diferents activitats cel·lulars durant el creixement i desenvolupament de l'arrel, a la vegada que revela la immunoprecipitació dels receptors LRR quinasa com una eïna potent i vàlida per tal d'estudiar mecanismes de senyalització amb resolució cel·lular en el desenvolupament de les plantes.

BIBLIOGRAPHY

Abas, L., Benjamins, R., Malenica, N., Paciorek, T., Wisniewska, J., Moulinier-Anzola, J.C., Sieberer, T., Friml, J., and Luschnig, C. (2006). Intracellular trafficking and proteolysis of the Arabidopsis auxin-efflux facilitator PIN2 are involved in root gravitropism. Nature cell biology **8,** 249-256.

Albrecht, C., Russinova, E., Kemmerling, B., Kwaaitaal, M., and de Vries, S.C. (2008). Arabidopsis SOMATIC EMBRYOGENESIS RECEPTOR KINASE proteins serve brassinosteroid-dependent and -independent signaling pathways. Plant physiology **148,** 611-619.

Altamura, M.M., Possenti, M., Matteucci, A., Baima, S., Ruberti, I., and Morelli, G. (2001). Development of the Vascular System in the Inflorescence Stem of Arabidopsis. New Phytologist **151,** 381-389.

Asami, T., Min, Y.K., Nagata, N., Yamagishi, K., Takatsuto, S., Fujioka, S., Murofushi, N., Yamaguchi, I., and Yoshida, S. (2000). Characterization of brassinazole, a triazole-type brassinosteroid biosynthesis inhibitor. Plant physiology **123,** 93-100.

Bainbridge, K., Guyomarc'h, S., Bayer, E., Swarup, R., Bennett, M., Mandel, T., and Kuhlemeier, C. (2008). Auxin influx carriers stabilize phyllotactic patterning. Genes & development **22,** 810-823.

Bao, F., Shen, J., Brady, S.R., Muday, G.K., Asami, T., and Yang, Z. (2004). Brassinosteroids interact with auxin to promote lateral root development in Arabidopsis. Plant physiology **134,** 1624-1631.

Bayer, E.M., Smith, R.S., Mandel, T., Nakayama, N., Sauer, M., Prusinkiewicz, P., and Kuhlemeier, C. (2009). Integration of transport-based models for phyllotaxis and midvein formation. Genes & development **23,** 373-384.

Bell, E.M., Lin, W.C., Husbands, A.Y., Yu, L., Jaganatha, V., Jablonska, B., Mangeon, A., Neff, M.M., Girke, T., and Springer, P.S. (2012). Arabidopsis LATERAL ORGAN BOUNDARIES negatively regulates brassinosteroid accumulation to limit growth in organ boundaries. Proceedings of the National Academy of Sciences of the United States of America **109,** 21146-21151.

Benkova, E., Michniewicz, M., Sauer, M., Teichmann, T., Seifertova, D., Jurgens, G., and Friml, J. (2003). Local, efflux-dependent auxin gradients as a common module for plant organ formation. Cell **115,** 591-602.

Bergmann, D.C., and Sack, F.D. (2007). Stomatal development. Annual review of plant biology **58,** 163-181.

Berleth, T., and Mattsson, J. (2000). Vascular development: tracing signals along veins. Current opinion in plant biology **3,** 406-411.

Berleth, T., and Sachs, T. (2001). Plant morphogenesis: long-distance coordination and local patterning. Current opinion in plant biology **4,** 57-62.

Blilou, I., Xu, J., Wildwater, M., Willemsen, V., Paponov, I., Friml, J., Heidstra, R., Aida, M., Palme, K., and Scheres, B. (2005). The PIN auxin efflux facilitator network controls growth and patterning in Arabidopsis roots. Nature **433,** 39-44.

Borner, G.H., Sherrier, D.J., Weimar, T., Michaelson, L.V., Hawkins, N.D., Macaskill, A., Napier, J.A., Beale, M.H., Lilley, K.S., and Dupree, P. (2005). Analysis of detergent-resistant membranes in Arabidopsis. Evidence for plasma membrane lipid rafts. Plant physiology **137,** 104-116.

Caño-Delgado, A., Penfield, S., Smith, C., Catley, M., and Bevan, M. (2003). Reduced cellulose synthesis invokes lignification and defense responses in Arabidopsis thaliana. The Plant journal : for cell and molecular biology **34,** 351-362.

Caño-Delgado, A., Lee, J.Y., and Demura, T. (2010). Regulatory mechanisms for specification and patterning of plant vascular tissues. Annual review of cell and developmental biology **26,** 605-637.

Caño-Delgado, A., Yin, Y., Yu, C., Vafeados, D., Mora-García, S., Cheng, J.C., Nam, K.H., Li, J., and Chory, J. (2004). BRL1 and BRL3 are novel brassinosteroid receptors that function in vascular differentiation in Arabidopsis. Development **131,** 5341-5351.

Caño-Delgado, A.I., and Blazquez, M.A. (2013). Spatial control of plant steroid signaling. Trends Plant Sci **18,** 235-236.

Carland, F.M., Berg, B.L., FitzGerald, J.N., Jinamornphongs, S., Nelson, T., and Keith, B. (1999). Genetic regulation of vascular tissue patterning in Arabidopsis. The Plant cell **11,** 2123-2137.

Ceserani, T., Trofka, A., Gandotra, N., and Nelson, T. (2009). VH1/BRL2 receptor-like kinase interacts with vascular-specific adaptor proteins VIT and VIK to influence leaf venation. The Plant journal : for cell and molecular biology **57,** 1000-1014.

Choe, S., Dilkes, B.P., Fujioka, S., Takatsuto, S., Sakurai, A., and Feldmann, K.A. (1998). The DWF4 gene of Arabidopsis encodes a cytochrome P450 that mediates multiple 22alpha-hydroxylation steps in brassinosteroid biosynthesis. The Plant cell **10,** 231-243.

Choe, S., Fujioka, S., Noguchi, T., Takatsuto, S., Yoshida, S., and Feldmann, K.A. (2001). Overexpression of DWARF4 in the brassinosteroid biosynthetic pathway results in increased vegetative growth and seed yield in Arabidopsis. The Plant journal : for cell and molecular biology **26,** 573-582.

Choe, S., Noguchi, T., Fujioka, S., Takatsuto, S., Tissier, C.P., Gregory, B.D., Ross, A.S., Tanaka, A., Yoshida, S., Tax, F.E., and Feldmann, K.A. (1999a). The Arabidopsis dwf7/ste1 mutant is defective in the delta7 sterol C-5 desaturation step leading to brassinosteroid biosynthesis. The Plant cell **11,** 207-221.

Choe, S., Dilkes, B.P., Gregory, B.D., Ross, A.S., Yuan, H., Noguchi, T., Fujioka, S., Takatsuto, S., Tanaka, A., Yoshida, S., Tax, F.E., and Feldmann, K.A. (1999b). The Arabidopsis dwarf1 mutant is defective in the conversion of 24-methylenecholesterol to campesterol in brassinosteroid biosynthesis. Plant physiology **119,** 897-907.

Clay, N.K., and Nelson, T. (2002). VH1, a provascular cell-specific receptor kinase that influences leaf cell patterns in Arabidopsis. The Plant cell **14,** 2707-2722.

Clough, S.J., and Bent, A.F. (1998). Floral dip: a simplified method for Agrobacterium-mediated transformation of Arabidopsis thaliana. The Plant journal : for cell and molecular biology **16,** 735-743.

Clouse, S.D. (2011). Brassinosteroid signal transduction: from receptor kinase activation to transcriptional networks regulating plant development. The Plant cell **23,** 1219-1230.

Clouse, S.D., and Sasse, J.M. (1998). BRASSINOSTEROIDS: Essential Regulators of Plant Growth and Development. Annual review of plant physiology and plant molecular biology **49,** 427-451.

Clouse, S.D., Langford, M., and McMorris, T.C. (1996). A brassinosteroid-insensitive mutant in Arabidopsis thaliana exhibits multiple defects in growth and development. Plant physiology **111,** 671-678.

Cox, J., and Mann, M. (2008). MaxQuant enables high peptide identification rates, individualized p.p.b.-range mass accuracies and proteome-wide protein quantification. Nature biotechnology **26,** 1367-1372.

Cox, J., Neuhauser, N., Michalski, A., Scheltema, R.A., Olsen, J.V., and Mann, M. (2011). Andromeda: a peptide search engine integrated into the MaxQuant environment. Journal of proteome research **10,** 1794-1805.

de Reuille, P.B., Bohn-Courseau, I., Ljung, K., Morin, H., Carraro, N., Godin, C., and Traas, J. (2006). Computer simulations reveal properties of the cell-cell signaling network at the shoot apex in Arabidopsis. Proceedings of the National Academy of Sciences of the United States of America **103,** 1627-1632.

DeLuna, A., Vetsigian, K., Shoresh, N., Hegreness, M., Colon-González, M., Chao, S., and Kishony, R. (2008). Exposing the fitness contribution of duplicated genes. Nature genetics **40,** 676-681.

Deng, Z., Zhang, X., Tang, W., Oses-Prieto, J.A., Suzuki, N., Gendron, J.M., Chen, H., Guan, S., Chalkley, R.J., Peterman, T.K., Burlingame, A.L., and Wang, Z.Y. (2007). A proteomics study of brassinosteroid response in Arabidopsis. Molecular & cellular proteomics : MCP **6,** 2058-2071.

Dettmer, J., Elo, A., and Helariutta, Y. (2009). Hormone interactions during vascular development. Plant molecular biology **69,** 347-360.

Dettmer, J., Hong-Hermesdorf, A., Stierhof, Y.D., and Schumacher, K. (2006). Vacuolar H+-ATPase activity is required for endocytic and secretory trafficking in Arabidopsis. The Plant cell **18,** 715-730.

Dhonukshe, P., Tanaka, H., Goh, T., Ebine, K., Mahonen, A.P., Prasad, K., Blilou, I., Geldner, N., Xu, J., Uemura, T., Chory, J., Ueda, T., Nakano, A., Scheres, B.,

and Friml, J. (2008). Generation of cell polarity in plants links endocytosis, auxin distribution and cell fate decisions. Nature **456,** 962-966.

Dolan, L., Janmaat, K., Willemsen, V., Linstead, P., Poethig, S., Roberts, K., and Scheres, B. (1993). Cellular organisation of the Arabidopsis thaliana root. Development **119,** 71-84.

Esau, K. (1965). Fixation Images of Sieve Element Plastids in Beta. Proceedings of the National Academy of Sciences of the United States of America **54,** 429-437.

Esau, K. (1977). Virus-like particles in nuclei of phloem cells in spinach leaves infected with the curly top virus. Journal of ultrastructure research **61,** 78-88.

Essau, K. (1965). Plant Anatomy, Edition 2. John Wiley & Sons, New York.

Fàbregas, N., Ibañes, M., and Caño-Delgado, A.I. (2010). A systems biology approach to dissect the contribution of brassinosteroid and auxin hormones to vascular patterning in the shoot of Arabidopsis thaliana. Plant signaling & behavior **5,** 903-906.

Fisher, K., and Turner, S. (2007). PXY, a receptor-like kinase essential for maintaining polarity during plant vascular-tissue development. Curr Biol **17,** 1061-1066.

Fletcher, J.C. (2002). Shoot and floral meristem maintenance in arabidopsis. Annual review of plant biology **53,** 45-66.

Fosket, D.E., and Torrey, J.G. (1969). Hormonal control of cell proliferation and xylem differentiation in cultured tissues of Glycine max var. Biloxi. Plant physiology **44,** 871-880.

Friedrichsen, D.M., Joazeiro, C.A., Li, J., Hunter, T., and Chory, J. (2000). Brassinosteroid-insensitive-1 is a ubiquitously expressed leucine-rich repeat receptor serine/threonine kinase. Plant physiology **123,** 1247-1256.

Friml, J. (2003). Auxin transport - shaping the plant. Current opinion in plant biology **6,** 7-12.

Friml, J., Wisniewska, J., Benkova, E., Mendgen, K., and Palme, K. (2002). Lateral relocation of auxin efflux regulator PIN3 mediates tropism in Arabidopsis. Nature **415,** 806-809.

Friml, J., Vieten, A., Sauer, M., Weijers, D., Schwarz, H., Hamann, T., Offringa, R., and Jurgens, G. (2003). Efflux-dependent auxin gradients establish the apical-basal axis of Arabidopsis. Nature **426,** 147-153.

Fuentes, S., Canamero, R.C., and Serna, L. (2012). Relationship between brassinosteroids and genes controlling stomatal production in the Arabidopsis hypocotyl. The International journal of developmental biology **56,** 675-680.

Fukuda, H. (1997). Tracheary Element Differentiation. The Plant cell **9,** 1147-1156.

Fukuda, H. (2000). Programmed cell death of tracheary elements as a paradigm in plants. Plant molecular biology **44,** 245-253.

Fukuda, H. (2004). Signals that control plant vascular cell differentiation. Nature reviews. Molecular cell biology **5,** 379-391.

Fukuda, H., and Komamine, A. (1980). Establishment of an Experimental System for the Study of Tracheary Element Differentiation from Single Cells Isolated from the Mesophyll of Zinnia elegans. Plant physiology **65,** 57-60.

Fukuda, H., Ito, M., Sugiyama, M., and Komamine, A. (1994). Mechanisms of the proliferation and differentiation of plant cells in cell culture systems. The International journal of developmental biology **38,** 287-299.

Galweiler, L., Guan, C., Muller, A., Wisman, E., Mendgen, K., Yephremov, A., and Palme, K. (1998). Regulation of polar auxin transport by AtPIN1 in Arabidopsis vascular tissue. Science **282,** 2226-2230.

Geldner, N., Hyman, D.L., Wang, X., Schumacher, K., and Chory, J. (2007). Endosomal signaling of plant steroid receptor kinase BRI1. Genes & development **21,** 1598-1602.

Gendron, J.M., Liu, J.S., Fan, M., Bai, M.Y., Wenkel, S., Springer, P.S., Barton, M.K., and Wang, Z.Y. (2012). Brassinosteroids regulate organ boundary formation in the shoot apical meristem of Arabidopsis. Proceedings of the National Academy of Sciences of the United States of America **109,** 21152-21157.

Goda, H., Shimada, Y., Asami, T., Fujioka, S., and Yoshida, S. (2002). Microarray analysis of brassinosteroid-regulated genes in Arabidopsis. Plant physiology **130,** 1319-1334.

González-García, M.P., Vilarrasa-Blasi, J., Zhiponova, M., Divol, F., Mora-García, S., Russinova, E., and Caño-Delgado, A.I. (2011). Brassinosteroids control meristem size by promoting cell cycle progression in Arabidopsis roots. Development **138,** 849-859.

Gou, X., Yin, H., He, K., Du, J., Yi, J., Xu, S., Lin, H., Clouse, S.D., and Li, J. (2012). Genetic evidence for an indispensable role of somatic embryogenesis receptor kinases in brassinosteroid signaling. PLoS genetics **8,** e1002452.

Grieneisen, V.A., Xu, J., Maree, A.F., Hogeweg, P., and Scheres, B. (2007). Auxin transport is sufficient to generate a maximum and gradient guiding root growth. Nature **449,** 1008-1013.

Gudesblat, G.E., and Russinova, E. (2011). Plants grow on brassinosteroids. Current opinion in plant biology **14,** 530-537.

Gudesblat, G.E., Schneider-Pizon, J., Betti, C., Mayerhofer, J., Vanhoutte, I., van Dongen, W., Boeren, S., Zhiponova, M., de Vries, S., Jonak, C., and Russinova, E. (2012). SPEECHLESS integrates brassinosteroid and stomata signalling pathways. Nature cell biology **14,** 548-554.

Guo, H., Li, L., Ye, H., Yu, X., Algreen, A., and Yin, Y. (2009a). Three related receptor-like kinases are required for optimal cell elongation in Arabidopsis thaliana. Proceedings of the National Academy of Sciences of the United States of America **106,** 7648-7653.

Guo, Y., Qin, G., Gu, H., and Qu, L.J. (2009b). Dof5.6/HCA2, a Dof transcription factor gene, regulates interfascicular cambium formation and vascular tissue development in Arabidopsis. The Plant cell **21,** 3518-3534.

Guo, Z., Fujioka, S., Blancaflor, E.B., Miao, S., Gou, X., and Li, J. (2010). TCP1 modulates brassinosteroid biosynthesis by regulating the expression of the key biosynthetic gene DWARF4 in Arabidopsis thaliana. The Plant cell **22,** 1161-1173.

Hacham, Y., Sela, A., Friedlander, L., and Savaldi-Goldstein, S. (2012). BRI1 activity in the root meristem involves post-transcriptional regulation of PIN auxin efflux carriers. Plant signaling & behavior **7,** 68-70.

Hacham, Y., Holland, N., Butterfield, C., Ubeda-Tomas, S., Bennett, M.J., Chory, J., and Savaldi-Goldstein, S. (2011). Brassinosteroid perception in the epidermis controls root meristem size. Development **138,** 839-848.

He, J.X., Gendron, J.M., Yang, Y., Li, J., and Wang, Z.Y. (2002). The GSK3-like kinase BIN2 phosphorylates and destabilizes BZR1, a positive regulator of the brassinosteroid signaling pathway in Arabidopsis. Proceedings of the National Academy of Sciences of the United States of America **99,** 10185-10190.

He, J.X., Gendron, J.M., Sun, Y., Gampala, S.S., Gendron, N., Sun, C.Q., and Wang, Z.Y. (2005). BZR1 is a transcriptional repressor with dual roles in brassinosteroid homeostasis and growth responses. Science **307,** 1634-1638.

Hossain, Z., McGarvey, B., Amyot, L., Gruber, M., Jung, J., and Hannoufa, A. (2012). DIMINUTO 1 affects the lignin profile and secondary cell wall formation in Arabidopsis. Planta **235,** 485-498.

Hothorn, M., Belkhadir, Y., Dreux, M., Dabi, T., Noel, J.P., Wilson, I.A., and Chory, J. (2011). Structural basis of steroid hormone perception by the receptor kinase BRI1. Nature **474,** 467-471.

Hu, Y., Bao, F., and Li, J. (2000). Promotive effect of brassinosteroids on cell division involves a distinct CycD3-induction pathway in Arabidopsis. The Plant journal : for cell and molecular biology **24,** 693-701.

Hubner, N.C., Bird, A.W., Cox, J., Splettstoesser, B., Bandilla, P., Poser, I., Hyman, A., and Mann, M. (2010). Quantitative proteomics combined with BAC TransgeneOmics reveals in vivo protein interactions. The Journal of cell biology **189,** 739-754.

Ibañes, M., Kawakami, Y., Rasskin-Gutman, D., and Belmonte, J.C. (2006). Cell lineage transport: a mechanism for molecular gradient formation. Mol Syst Biol **2,** 57.

Ibañes, M., Fàbregas, N., Chory, J., and Caño-Delgado, A.I. (2009). Brassinosteroid signaling and auxin transport are required to establish the periodic pattern of Arabidopsis shoot vascular bundles. Proceedings of the National Academy of Sciences of the United States of America **106,** 13630-13635.

Irani, N.G., Di Rubbo, S., Mylle, E., Van den Begin, J., Schneider-Pizon, J., Hnilikova, J., Sisa, M., Buyst, D., Vilarrasa-Blasi, J., Szatmari, A.M., Van Damme, D., Mishev,

K., Codreanu, M.C., Kohout, L., Strnad, M., Caño-Delgado, A.I., Friml, J., Madder, A., and Russinova, E. (2012). Fluorescent castasterone reveals BRI1 signaling from the plasma membrane. Nature chemical biology **8,** 583-589.

Jaillais, Y., Hothorn, M., Belkhadir, Y., Dabi, T., Nimchuk, Z.L., Meyerowitz, E.M., and Chory, J. (2011). Tyrosine phosphorylation controls brassinosteroid receptor activation by triggering membrane release of its kinase inhibitor. Genes & development **25,** 232-237.

Jonsson, H., Heisler, M.G., Shapiro, B.E., Meyerowitz, E.M., and Mjolsness, E. (2006). An auxin-driven polarized transport model for phyllotaxis. Proceedings of the National Academy of Sciences of the United States of America **103,** 1633-1638.

Jurgens, G. (2001). Apical-basal pattern formation in Arabidopsis embryogenesis. Embo J **20,** 3609-3616.

Kafri, R., Levy, M., and Pilpel, Y. (2006). The regulatory utilization of genetic redundancy through responsive backup circuits. Proceedings of the National Academy of Sciences of the United States of America **103,** 11653-11658.

Kafri, R., Springer, M., and Pilpel, Y. (2009). Genetic redundancy: new tricks for old genes. Cell **136,** 389-392.

Kang, J., Tang, J., Donnelly, P., and Dengler, N. (2003). Primary Vascular Pattern and Expression of ATHB-8 in Shoots of Arabidopsis. New Phytologist **158,** 443-454.

Karlova, R., Boeren, S., Russinova, E., Aker, J., Vervoort, J., and de Vries, S. (2006). The Arabidopsis SOMATIC EMBRYOGENESIS RECEPTOR-LIKE KINASE1 protein complex includes BRASSINOSTEROID-INSENSITIVE1. The Plant cell **18,** 626-638.

Kim, H.B., Kwon, M., Ryu, H., Fujioka, S., Takatsuto, S., Yoshida, S., An, C.S., Lee, I., Hwang, I., and Choe, S. (2006). The regulation of DWARF4 expression is likely a critical mechanism in maintaining the homeostasis of bioactive brassinosteroids in Arabidopsis. Plant physiology **140,** 548-557.

Kim, T.W., and Wang, Z.Y. (2010). Brassinosteroid signal transduction from receptor kinases to transcription factors. Annual review of plant biology **61,** 681-704.

Kim, T.W., Guan, S., Burlingame, A.L., and Wang, Z.Y. (2011). The CDG1 kinase mediates brassinosteroid signal transduction from BRI1 receptor kinase to BSU1 phosphatase and GSK3-like kinase BIN2. Molecular cell **43,** 561-571.

Kim, T.W., Michniewicz, M., Bergmann, D.C., and Wang, Z.Y. (2012). Brassinosteroid regulates stomatal development by GSK3-mediated inhibition of a MAPK pathway. Nature **482,** 419-422.

Kinoshita, T.- Caño-Delgado, A., Seto, H., Hiranuma, S., Fujioka, S., Yoshida, S., and Chory, J. (2005). Binding of brassinosteroids to the extracellular domain of plant receptor kinase BRI1. Nature **433,** 167-171.

Klahre, U., Noguchi, T., Fujioka, S., Takatsuto, S., Yokota, T., Nomura, T., Yoshida, S., and Chua, N.H. (1998). The Arabidopsis DIMINUTO/DWARF1 gene encodes a protein involved in steroid synthesis. The Plant cell **10,** 1677-1690.

Kuppusamy, K.T., Chen, A.Y., and Nemhauser, J.L. (2009). Steroids are required for epidermal cell fate establishment in Arabidopsis roots. Proceedings of the National Academy of Sciences of the United States of America **106,** 8073-8076.

Lampugnani, E.R., Kilinc, A., and Smyth, D.R. (2013). Auxin controls petal initiation in Arabidopsis. Development **140,** 185-194.

Lee, D.K., Geisler, M., and Springer, P.S. (2009). LATERAL ORGAN FUSION1 and LATERAL ORGAN FUSION2 function in lateral organ separation and axillary meristem formation in Arabidopsis. Development **136,** 2423-2432.

Lee, K., Avondo, J., Morrison, H., Blot, L., Stark, M., Sharpe, J., Bangham, A., and Coen, E. (2006). Visualizing Plant Development and Gene Expression in Three Dimensions Using Optical Projection Tomography. The Plant cell**,** tpc.106.043042.

Li, J., and Chory, J. (1997). A putative leucine-rich repeat receptor kinase involved in brassinosteroid signal transduction. Cell **90,** 929-938.

Li, J., Nam, K.H., Vafeados, D., and Chory, J. (2001). BIN2, a new brassinosteroid-insensitive locus in Arabidopsis. Plant physiology **127,** 14-22.

Li, J., Nagpal, P., Vitart, V., McMorris, T.C., and Chory, J. (1996). A role for brassinosteroids in light-dependent development of Arabidopsis. Science **272,** 398-401.

Li, J., Wen, J., Lease, K.A., Doke, J.T., Tax, F.E., and Walker, J.C. (2002). BAK1, an Arabidopsis LRR receptor-like protein kinase, interacts with BRI1 and modulates brassinosteroid signaling. Cell **110,** 213-222.

Li, L., Xu, J., Xu, Z.H., and Xue, H.W. (2005). Brassinosteroids stimulate plant tropisms through modulation of polar auxin transport in Brassica and Arabidopsis. The Plant cell **17,** 2738-2753.

Ljung, K., Bhalerao, R.P., and Sandberg, G. (2001). Sites and homeostatic control of auxin biosynthesis in Arabidopsis during vegetative growth. The Plant journal : for cell and molecular biology **28,** 465-474.

Lu, J., Boeren, S., de Vries, S.C., van Valenberg, H.J., Vervoort, J., and Hettinga, K. (2011). Filter-aided sample preparation with dimethyl labeling to identify and quantify milk fat globule membrane proteins. Journal of proteomics **75,** 34-43.

Lucas, W.J., Groover, A., Lichtenberger, R., Furuta, K., Yadav, S.R., Helariutta, Y., He, X.Q., Fukuda, H., Kang, J., Brady, S.M., Patrick, J.W., Sperry, J., Yoshida, A., Lopez-Millan, A.F., Grusak, M.A., and Kachroo, P. (2013). The Plant Vascular System: Evolution, Development and Functions. Journal of integrative plant biology **55,** 294-388.

Mahonen, A.P., Bonke, M., Kauppinen, L., Riikonen, M., Benfey, P.N., and Helariutta, Y. (2000). A novel two-component hybrid molecule regulates vascular morphogenesis of the Arabidopsis root. Genes & development **14,** 2938-2943.

Mahonen, A.P., Bishopp, A., Higuchi, M., Nieminen, K.M., Kinoshita, K., Tormakangas, K., Ikeda, Y., Oka, A., Kakimoto, T., and Helariutta, Y. (2006). Cytokinin signaling and its inhibitor AHP6 regulate cell fate during vascular development. Science **311,** 94-98.

Marchant, A., Kargul, J., May, S.T., Muller, P., Delbarre, A., Perrot-Rechenmann, C., and Bennett, M.J. (1999). AUX1 regulates root gravitropism in Arabidopsis by facilitating auxin uptake within root apical tissues. Embo J **18,** 2066-2073.

Marchant, A., Bhalerao, R., Casimiro, I., Eklof, J., Casero, P.J., Bennett, M., and Sandberg, G. (2002). AUX1 promotes lateral root formation by facilitating indole-3-acetic acid distribution between sink and source tissues in the Arabidopsis seedling. The Plant cell **14,** 589-597.

Mattsson, J., Sung, Z.R., and Berleth, T. (1999). Responses of plant vascular systems to auxin transport inhibition. Development **126,** 2979-2991.

Mattsson, J., Ckurshumova, W., and Berleth, T. (2003). Auxin signaling in Arabidopsis leaf vascular development. Plant physiology **131,** 1327-1339.

Miyazawa, Y., Nakajima, N., Abe, T., Sakai, A., Fujioka, S., Kawano, S., Kuroiwa, T., and Yoshida, S. (2003). Activation of cell proliferation by brassinolide application in tobacco BY-2 cells: effects of brassinolide on cell multiplication, cell-cycle-related gene expression, and organellar DNA contents. Journal of experimental botany **54,** 2669-2678.

Mora-García, S., Vert, G., Yin, Y., Caño-Delgado, A., Cheong, H., and Chory, J. (2004). Nuclear protein phosphatases with Kelch-repeat domains modulate the response to brassinosteroids in Arabidopsis. Genes & development **18,** 448-460.

Mouchel, C.F., Osmont, K.S., and Hardtke, C.S. (2006). BRX mediates feedback between brassinosteroid levels and auxin signalling in root growth. Nature **443,** 458-461.

Moussaieff, A., Rogachev, I., Brodsky, L., Malitsky, S., Toal, T.W., Belcher, H., Yativ, M., Brady, S.M., Benfey, P.N., and Aharoni, A. (2013). High-resolution metabolic mapping of cell types in plant roots. Proceedings of the National Academy of Sciences of the United States of America **110,** E1232-1241.

Muller, A., Guan, C., Galweiler, L., Tanzler, P., Huijser, P., Marchant, A., Parry, G., Bennett, M., Wisman, E., and Palme, K. (1998). AtPIN2 defines a locus of Arabidopsis for root gravitropism control. Embo J **17,** 6903-6911.

Mussig, C., Fischer, S., and Altmann, T. (2002). Brassinosteroid-regulated gene expression. Plant physiology **129,** 1241-1251.

Mussig, C., Shin, G.H., and Altmann, T. (2003). Brassinosteroids promote root growth in Arabidopsis. Plant physiology **133,** 1261-1271.

Nagata, N., Asami, T., and Yoshida, S. (2001). Brassinazole, an inhibitor of brassinosteroid biosynthesis, inhibits development of secondary xylem in cress plants (Lepidium sativum). Plant & cell physiology **42,** 1006-1011.

Nakamura, A., Goda, H., Shimada, Y., and Yoshida, S. (2004). Brassinosteroid selectively regulates PIN gene expression in Arabidopsis. Bioscience, biotechnology, and biochemistry **68,** 952-954.

Nakamura, A., Fujioka, S., Sunohara, H., Kamiya, N., Hong, Z., Inukai, Y., Miura, K., Takatsuto, S., Yoshida, S., Ueguchi-Tanaka, M., Hasegawa, Y., Kitano, H., and Matsuoka, M. (2006). The role of OsBRI1 and its homologous genes, OsBRL1 and OsBRL3, in rice. Plant physiology **140,** 580-590.

Nam, K.H., and Li, J. (2002). BRI1/BAK1, a receptor kinase pair mediating brassinosteroid signaling. Cell **110,** 203-212.

Neff, M.M., Nguyen, S.M., Malancharuvil, E.J., Fujioka, S., Noguchi, T., Seto, H., Tsubuki, M., Honda, T., Takatsuto, S., Yoshida, S., and Chory, J. (1999). BAS1: A gene regulating brassinosteroid levels and light responsiveness in Arabidopsis. Proceedings of the National Academy of Sciences of the United States of America **96,** 15316-15323.

Nemhauser, J.L., Mockler, T.C., and Chory, J. (2004). Interdependency of brassinosteroid and auxin signaling in Arabidopsis. PLoS biology **2,** E258.

Ohashi-Ito, K., Kubo, M., Demura, T., and Fukuda, H. (2005). Class III homeodomain leucine-zipper proteins regulate xylem cell differentiation. Plant & cell physiology **46,** 1646-1656.

Peng, K., van Lent, J.W., Boeren, S., Fang, M., Theilmann, D.A., Erlandson, M.A., Vlak, J.M., and van Oers, M.M. (2012). Characterization of novel components of the baculovirus per os infectivity factor complex. Journal of virology **86,** 4981-4988.

Peng, P., Yan, Z., Zhu, Y., and Li, J. (2008). Regulation of the Arabidopsis GSK3-like kinase BRASSINOSTEROID-INSENSITIVE 2 through proteasome-mediated protein degradation. Molecular plant **1,** 338-346.

Peret, B., Swarup, K., Ferguson, A., Seth, M., Yang, Y., Dhondt, S., James, N., Casimiro, I., Perry, P., Syed, A., Yang, H., Reemmer, J., Venison, E., Howells, C., Perez-Amador, M.A., Yun, J., Alonso, J., Beemster, G.T., Laplaze, L., Murphy, A., Bennett, M.J., Nielsen, E., and Swarup, R. (2012). AUX/LAX genes encode a family of auxin influx transporters that perform distinct functions during Arabidopsis development. The Plant cell **24,** 2874-2885.

Perrot-Rechenmann, C. (2010). Cellular responses to auxin: division versus expansion. Cold Spring Harbor perspectives in biology **2,** a001446.

Przemeck, G.K., Mattsson, J., Hardtke, C.S., Sung, Z.R., and Berleth, T. (1996). Studies on the role of the Arabidopsis gene MONOPTEROS in vascular development and plant cell axialization. Planta **200,** 229-237.

Reinhardt, D. (2003). Vascular patterning: more than just auxin? Curr Biol **13,** R485-487.

Reinhardt, D., Mandel, T., and Kuhlemeier, C. (2000). Auxin regulates the initiation and radial position of plant lateral organs. The Plant cell **12,** 507-518.

Reinhardt, D., Pesce, E.R., Stieger, P., Mandel, T., Baltensperger, K., Bennett, M., Traas, J., Friml, J., and Kuhlemeier, C. (2003). Regulation of phyllotaxis by polar auxin transport. Nature **426,** 255-260.

Rienties, I.M., Vink, J., Borst, J.W., Russinova, E., and de Vries, S.C. (2005). The Arabidopsis SERK1 protein interacts with the AAA-ATPase AtCDC48, the 14-3-3 protein GF14lambda and the PP2C phosphatase KAPP. Planta **221,** 394-405.

Roh, H., Jeong, C.W., Fujioka, S., Kim, Y.K., Lee, S., Ahn, J.H., Choi, Y.D., and Lee, J.S. (2012). Genetic evidence for the reduction of brassinosteroid levels by a BAHD acyltransferase-like protein in Arabidopsis. Plant physiology **159,** 696-709.

Rolland-Lagan, A.G., and Prusinkiewicz, P. (2005). Reviewing models of auxin canalization in the context of leaf vein pattern formation in Arabidopsis. The Plant journal : for cell and molecular biology **44,** 854-865.

Rubery, P.H., and Sheldrake, A.R. (1973). Effect of pH and surface charge on cell uptake of auxin. Nature: New biology **244,** 285-288.

Russinova, E., Borst, J.W., Kwaaitaal, M., Caño-Delgado, A., Yin, Y., Chory, J., and de Vries, S.C. (2004). Heterodimerization and endocytosis of Arabidopsis brassinosteroid receptors BRI1 and AtSERK3 (BAK1). The Plant cell **16,** 3216-3229.

Ryu, H., Kim, K., Cho, H., Park, J., Choe, S., and Hwang, I. (2007). Nucleocytoplasmic shuttling of BZR1 mediated by phosphorylation is essential in Arabidopsis brassinosteroid signaling. The Plant cell **19,** 2749-2762.

Sachs, T. (1981). The control of the patterned differentiation of vascular tissues. Adv. Bot. Res. **9,** 151-262.

Sahlin, P., Soderberg, B., and Jonsson, H. (2009). Regulated transport as a mechanism for pattern generation: capabilities for phyllotaxis and beyond. J Theor Biol **258,** 60-70.

Sanchez-Fernandez, R., Davies, T.G., Coleman, J.O., and Rea, P.A. (2001). The Arabidopsis thaliana ABC protein superfamily, a complete inventory. The Journal of biological chemistry **276,** 30231-30244.

Santner, A., and Estelle, M. (2009). Recent advances and emerging trends in plant hormone signalling. Nature **459,** 1071-1078.

Savaldi-Goldstein, S., Peto, C., and Chory, J. (2007). The epidermis both drives and restricts plant shoot growth. Nature **446,** 199-202.

Scacchi, E., Salinas, P., Gujas, B., Santuari, L., Krogan, N., Ragni, L., Berleth, T., and Hardtke, C.S. (2010). Spatio-temporal sequence of cross-regulatory events in root meristem growth. Proceedings of the National Academy of Sciences of the United States of America **107,** 22734-22739.

Scarpella, E., Marcos, D., Friml, J., and Berleth, T. (2006). Control of leaf vascular patterning by polar auxin transport. Genes & development **20,** 1015-1027.

Scheres, B. (2013). Rooting plant development. Development **140,** 939-941.

Scheres, B., and Xu, J. (2006). Polar auxin transport and patterning: grow with the flow. Genes & development **20,** 922-926.

Schumacher, K., Vafeados, D., McCarthy, M., Sze, H., Wilkins, T., and Chory, J. (1999). The Arabidopsis det3 mutant reveals a central role for the vacuolar H(+)-ATPase in plant growth and development. Genes & development **13,** 3259-3270.

Serna, L. (2013). What Causes Opposing Actions of Brassinosteroids on Stomatal Development? Plant physiology.

She, J., Han, Z., Kim, T.W., Wang, J., Cheng, W., Chang, J., Shi, S., Wang, J., Yang, M., Wang, Z.Y., and Chai, J. (2011). Structural insight into brassinosteroid perception by BRI1. Nature **474,** 472-476.

Shiu, S.H., and Bleecker, A.B. (2001). Receptor-like kinases from Arabidopsis form a monophyletic gene family related to animal receptor kinases. Proceedings of

the National Academy of Sciences of the United States of America **98,** 10763-10768.

Shuai, B., Reynaga-Pena, C.G., and Springer, P.S. (2002). The lateral organ boundaries gene defines a novel, plant-specific gene family. Plant physiology **129,** 747-761.

Sieburth, L.E., and Deyholos, M.K. (2006). Vascular development: the long and winding road. Current opinion in plant biology **9,** 48-54.

Smaczniak, C., Li, N., Boeren, S., America, T., van Dongen, W., Goerdayal, S.S., de Vries, S., Angenent, G.C., and Kaufmann, K. (2012). Proteomics-based identification of low-abundance signaling and regulatory protein complexes in native plant tissues. Nat Protoc **7,** 2144-2158.

Smith, R.S., Guyomarc'h, S., Mandel, T., Reinhardt, D., Kuhlemeier, C., and Prusinkiewicz, P. (2006). A plausible model of phyllotaxis. Proceedings of the National Academy of Sciences of the United States of America **103,** 1301-1306.

Sun, Y., Fan, X.Y., Cao, D.M., Tang, W., He, K., Zhu, J.Y., He, J.X., Bai, M.Y., Zhu, S., Oh, E., Patil, S., Kim, T.W., Ji, H., Wong, W.H., Rhee, S.Y., and Wang, Z.Y. (2010). Integration of brassinosteroid signal transduction with the transcription network for plant growth regulation in Arabidopsis. Developmental cell **19,** 765-777.

Swarup, K., Benkova, E., Swarup, R., Casimiro, I., Peret, B., Yang, Y., Parry, G., Nielsen, E., De Smet, I., Vanneste, S., Levesque, M.P., Carrier, D., James, N., Calvo, V., Ljung, K., Kramer, E., Roberts, R., Graham, N., Marillonnet, S., Patel, K., Jones, J.D., Taylor, C.G., Schachtman, D.P., May, S., Sandberg, G., Benfey, P., Friml, J., Kerr, I., Beeckman, T., Laplaze, L., and Bennett, M.J. (2008). The auxin influx carrier LAX3 promotes lateral root emergence. Nature cell biology **10,** 946-954.

Symons, G.M., and Reid, J.B. (2004). Brassinosteroids do not undergo long-distance transport in pea. Implications for the regulation of endogenous brassinosteroid levels. Plant physiology **135,** 2196-2206.

Symons, G.M., Ross, J.J., Jager, C.E., and Reid, J.B. (2008). Brassinosteroid transport. Journal of experimental botany **59,** 17-24.

Szekeres, M., Nemeth, K., Koncz-Kalman, Z., Mathur, J., Kauschmann, A., Altmann, T., Redei, G.P., Nagy, F., Schell, J., and Koncz, C. (1996). Brassinosteroids rescue the deficiency of CYP90, a cytochrome P450, controlling cell elongation and de-etiolation in Arabidopsis. Cell **85,** 171-182.

Takahashi, T., Gasch, A., Nishizawa, N., and Chua, N.H. (1995). The DIMINUTO gene of Arabidopsis is involved in regulating cell elongation. Genes & development **9,** 97-107.

Tang, W., Deng, Z., and Wang, Z.Y. (2010). Proteomics shed light on the brassinosteroid signaling mechanisms. Current opinion in plant biology **13,** 27-33.

Tang, W., Kim, T.W., Oses-Prieto, J.A., Sun, Y., Deng, Z., Zhu, S., Wang, R., Burlingame, A.L., and Wang, Z.Y. (2008). BSKs mediate signal transduction from the receptor kinase BRI1 in Arabidopsis. Science **321,** 557-560.

Tang, W., Yuan, M., Wang, R., Yang, Y., Wang, C., Oses-Prieto, J.A., Kim, T.W., Zhou, H.W., Deng, Z., Gampala, S.S., Gendron, J.M., Jonassen, E.M., Lillo, C., DeLong, A., Burlingame, A.L., Sun, Y., and Wang, Z.Y. (2011). PP2A activates brassinosteroid-responsive gene expression and plant growth by dephosphorylating BZR1. Nature cell biology **13,** 124-131.

Thummel, C.S., and Chory, J. (2002). Steroid signaling in plants and insects--common themes, different pathways. Genes & development **16,** 3113-3129.

Truernit, E., Bauby, H., Dubreucq, B., Grandjean, O., Runions, J., Barthelemy, J., and Palauqui, J.-C. (2008). High-Resolution Whole-Mount Imaging of Three-Dimensional Tissue Organization and Gene Expression Enables the Study of Phloem Development and Structure in Arabidopsis. The Plant cell **20,** 1494-1503.

Uggla, C., Moritz, T., Sandberg, G., and Sundberg, B. (1996). Auxin as a positional signal in pattern formation in plants. Proceedings of the National Academy of Sciences of the United States of America **93,** 9282-9286.

Ulmasov, T., Murfett, J., Hagen, G., and Guilfoyle, T.J. (1997). Aux/IAA proteins repress expression of reporter genes containing natural and highly active synthetic auxin response elements. The Plant cell **9,** 1963-1971.

van Esse, G.W., van Mourik, S., Stigter, H., ten Hove, C.A., Molenaar, J., and de Vries, S.C. (2012). A mathematical model for BRASSINOSTEROID INSENSITIVE1-mediated signaling in root growth and hypocotyl elongation. Plant physiology **160,** 523-532.

van Esse, G.W., Westphal, A.H., Surendran, R.P., Albrecht, C., van Veen, B., Borst, J.W., and de Vries, S.C. (2011). Quantification of the brassinosteroid insensitive1 receptor in planta. Plant physiology **156,** 1691-1700.

van Esse, H.P., Van't Klooster, J.W., Bolton, M.D., Yadeta, K.A., van Baarlen, P., Boeren, S., Vervoort, J., de Wit, P.J., and Thomma, B.P. (2008). The Cladosporium fulvum virulence protein Avr2 inhibits host proteases required for basal defense. The Plant cell **20,** 1948-1963.

Vandenbussche, F., Petrasek, J., Zadnikova, P., Hoyerova, K., Pesek, B., Raz, V., Swarup, R., Bennett, M., Zazimalova, E., Benkova, E., and Van Der Straeten, D. (2010). The auxin influx carriers AUX1 and LAX3 are involved in auxin-ethylene interactions during apical hook development in Arabidopsis thaliana seedlings. Development **137,** 597-606.

Vert, G., Walcher, C.L., Chory, J., and Nemhauser, J.L. (2008). Integration of auxin and brassinosteroid pathways by Auxin Response Factor 2. Proceedings of the National Academy of Sciences of the United States of America **105,** 9829-9834.

Vert, G., Nemhauser, J.L., Geldner, N., Hong, F., and Chory, J. (2005). Molecular mechanisms of steroid hormone signaling in plants. Annual review of cell and developmental biology **21,** 177-201.

Vilarrasa-Blasi, J., González-García, M.P., and A.I., C.-D. (2012). Brassinosteroid signaling in root development. The Arabidopsis Book.

Walcher, C.L., and Nemhauser, J.L. (2012). Bipartite promoter element required for auxin response. Plant physiology **158,** 273-282.

Wang, M., Liu, X., Wang, R., Li, W., Rodermel, S., and Yu, F. (2012a). Overexpression of a putative Arabidopsis BAHD acyltransferase causes dwarfism that can be rescued by brassinosteroid. Journal of experimental botany **63,** 5787-5801.

Wang, X., and Chory, J. (2006). Brassinosteroids regulate dissociation of BKI1, a negative regulator of BRI1 signaling, from the plasma membrane. Science **313,** 1118-1122.

Wang, X., Kota, U., He, K., Blackburn, K., Li, J., Goshe, M.B., Huber, S.C., and Clouse, S.D. (2008). Sequential transphosphorylation of the BRI1/BAK1 receptor kinase complex impacts early events in brassinosteroid signaling. Developmental cell **15,** 220-235.

Wang, X., Goshe, M.B., Soderblom, E.J., Phinney, B.S., Kuchar, J.A., Li, J., Asami, T., Yoshida, S., Huber, S.C., and Clouse, S.D. (2005). Identification and functional analysis of in vivo phosphorylation sites of the Arabidopsis BRASSINOSTEROID-INSENSITIVE1 receptor kinase. The Plant cell **17,** 1685-1703.

Wang, Z.Y., Bai, M.Y., Oh, E., and Zhu, J.Y. (2012b). Brassinosteroid signaling network and regulation of photomorphogenesis. Annual review of genetics **46,** 701-724.

Wang, Z.Y., Seto, H., Fujioka, S., Yoshida, S., and Chory, J. (2001). BRI1 is a critical component of a plasma-membrane receptor for plant steroids. Nature **410,** 380-383.

Wang, Z.Y., Nakano, T., Gendron, J., He, J., Chen, M., Vafeados, D., Yang, Y., Fujioka, S., Yoshida, S., Asami, T., and Chory, J. (2002). Nuclear-localized BZR1 mediates brassinosteroid-induced growth and feedback suppression of brassinosteroid biosynthesis. Developmental cell **2,** 505-513.

Wenzel, C.L., Schuetz, M., Yu, Q., and Mattsson, J. (2007). Dynamics of MONOPTEROS and PIN-FORMED1 expression during leaf vein pattern formation in Arabidopsis thaliana. The Plant journal : for cell and molecular biology **49,** 387-398.

Witthoft, J., Caesar, K., Elgass, K., Huppenberger, P., Kilian, J., Schleifenbaum, F., Oecking, C., and Harter, K. (2011). The activation of the Arabidopsis P-ATPase 1 by the brassinosteroid receptor BRI1 is independent of threonine 948 phosphorylation. Plant signaling & behavior **6,** 1063-1066.

Wolf, S., Mravec, J., Greiner, S., Mouille, G., and Hofte, H. (2012). Plant cell wall homeostasis is mediated by brassinosteroid feedback signaling. Current biology : CB **22,** 1732-1737.

Wu, F.H., Shen, S.C., Lee, L.Y., Lee, S.H., Chan, M.T., and Lin, C.S. (2009). Tape-Arabidopsis Sandwich - a simpler Arabidopsis protoplast isolation method. Plant methods **5,** 16.

Wu, G., Wang, X., Li, X., Kamiya, Y., Otegui, M.S., and Chory, J. (2011). Methylation of a phosphatase specifies dephosphorylation and degradation of activated brassinosteroid receptors. Science signaling **4,** ra29.

Xie, L., Yang, C., and Wang, X. (2011). Brassinosteroids can regulate cellulose biosynthesis by controlling the expression of CESA genes in Arabidopsis. Journal of experimental botany **62,** 4495-4506.

Xu, W., Huang, J., Li, B., Li, J., and Wang, Y. (2008). Is kinase activity essential for biological functions of BRI1? Cell research **18,** 472-478.

Yamamoto, R., Demura, T., and Fukuda, H. (1997). Brassinosteroids induce entry into the final stage of tracheary element differentiation in cultured Zinnia cells. Plant & cell physiology **38,** 980-983.

Yamamoto, R., Fujioka, S., Demura, T., Takatsuto, S., Yoshida, S., and Fukuda, H. (2001). Brassinosteroid levels increase drastically prior to morphogenesis of tracheary elements. Plant physiology **125,** 556-563.

Yamamoto, R., Fujioka, S., Iwamoto, K., Demura, T., Takatsuto, S., Yoshida, S., and Fukuda, H. (2007). Co-regulation of brassinosteroid biosynthesis-related genes during xylem cell differentiation. Plant & cell physiology **48,** 74-83.

Ye, Q., Zhu, W., Li, L., Zhang, S., Yin, Y., Ma, H., and Wang, X. (2010). Brassinosteroids control male fertility by regulating the expression of key genes involved in Arabidopsis anther and pollen development. Proceedings of the National Academy of Sciences of the United States of America **107,** 6100-6105.

Yin, Y., Wang, Z.Y., Mora-García, S., Li, J., Yoshida, S., Asami, T., and Chory, J. (2002). BES1 accumulates in the nucleus in response to brassinosteroids to regulate gene expression and promote stem elongation. Cell **109,** 181-191.

Yu, X., Li, L., Zola, J., Aluru, M., Ye, H., Foudree, A., Guo, H., Anderson, S., Aluru, S., Liu, P., Rodermel, S., and Yin, Y. (2011). A brassinosteroid transcriptional network revealed by genome-wide identification of BESI target genes in

Arabidopsis thaliana. The Plant journal : for cell and molecular biology **65,** 634-646.

Zhao, Y., Christensen, S.K., Fankhauser, C., Cashman, J.R., Cohen, J.D., Weigel, D., and Chory, J. (2001). A role for flavin monooxygenase-like enzymes in auxin biosynthesis. Science **291,** 306-309.

Zhiponova, M.K., Vanhoutte, I., Boudolf, V., Betti, C., Dhondt, S., Coppens, F., Mylle, E., Maes, S., González-García, M.P., Caño-Delgado, A.I., Inze, D., Beemster, G.T., De Veylder, L., and Russinova, E. (2013). Brassinosteroid production and signaling differentially control cell division and expansion in the leaf. The New phytologist **197,** 490-502.

Zhong, R., Taylor, J.J., and Ye, Z.H. (1997). Disruption of interfascicular fiber differentiation in an Arabidopsis mutant. The Plant cell **9,** 2159-2170.

Zhou, A., Wang, H., Walker, J.C., and Li, J. (2004). BRL1, a leucine-rich repeat receptor-like protein kinase, is functionally redundant with BRI1 in regulating Arabidopsis brassinosteroid signaling. The Plant journal : for cell and molecular biology **40,** 399-409.

APENDIX 1:

ANNEXED SUPPLEMENTARY TABLES

FROM CHAPTER 4

APENDIX

1

APENDIX

1

APENDIX

1

APENDIX 2: CV AND PUBLICATIONS

APENDIX 2

CURRICULUM VITAE

Norma Fàbregas Vallvé

Juny 2013

Personal Information

Name: Norma Fàbregas Vallvé

Nationality: Spanish

Address: C/Tamarit 122, SAtic-3ª 08015, Barcelona, Spain

Contact: norma.fàbregas@cragenomica.es // +34 639 79 28 36

Education

2009 - Master degree (MSc) in Developmental Biology and Genetics.

University of Barcelona (UB)

Dissertation: "Brassinosteroids modulate vascular pattern in the shoot of Arabidopsis thaliana"

MSc Supervisor: Dr. Ana I. Caño-Delgado

2008 – Summer school course

Computational and Mathematical Modeling for Plant Systems Biology

Date and place: Ghent, Belgium, 1-5th September

2007 - Degree in Biochemistry

University of Barcelona (UB)

Work experience

2008-2013 – PhD Research

The experimental work was carried out at the molecular biology department of the Centre for Research in Agrigenomics (CRAG) CSIC-IRTA-UAB-UB (Barcelona, Spain) under the supervision of Dr. Ana I. Caño-Delgado.

2010 – Wageningen

4 months - Short stay at the University of Wageningen to perform *in vivo* protein immunoprecipitation coupled to mass spectrometry and FRET-FLIM assays.

2008 – Initiation to Scientific Research Training fellowship by CRAG.

Fellowships and awards

Short-term stance scholarship BE-AGAUR 2009-2010, at the laboratory of Prof. Sacco de Vries in the University of Wageningen, Holland.

PhD fellowship FI (AGAUR) from Generalitat de Catalunya (2008-2011)

Publications

Specific roles for BRL3 signalosome complex in Arabidopsis root development
Fàbregas N, Li N, Boeren S, de Vries S and Caño-Delgado AI.
The Plant Cell (submitted; June 2013)

Turning on the microscopy turret: a new view for the study of Brassinosteroid signaling in plant development.
Fàbregas N, Ibañes M, Caño-Delgado AI.
Physiologia Plantarum (Review invitation; July 2013)

A systems biology approach to dissect the contribution of Brassinosteroid and auxin hormones to vascular patterning in the shoot of Arabidopsis thaliana.
Fàbregas N, Ibañes M, Caño-Delgado AI.
Plant Signal Behav. 2010 Jul;5(7):903-6. Epub 2010 Jul 1.

Brassinosteroid signaling and auxin transport are required to establish the periodic pattern of Arabidopsis shoot vascular bundles.

Ibañes M, **Fàbregas N**, Chory J, Caño-Delgado AI.
PNAS (Proc Natl Acad Sci U S A). 2009 Aug 11;106(32):13630-5. doi: 10.1073/pnas.0906416106. Epub 2009 Jul 28.

Oral Communications

Norma Fàbregas, Na Li, Sacco de Vries and Ana Caño-Delgado
Cellular specificity of the Brassinosteroid perception complexes in plants
1st International Brassinosteroid Hormone Conference. Barcelona, España
Oral Communication. June 2012

Norma Fàbregas, Marta Ibañes and Ana Caño-Delgado
Brassinosteroids modulate shoot vascular patterning in Arabidopsis
Exchange PhD student retreat Wageningen-Barcelona
Oral Communication. April 2009

Posters presentation

Norma Fàbregas, Na Li, Sacco de Vries and Ana Caño-Delgado
Revealing Brassinosteroid signaling through BRL3 vascular receptor in Arabidopsis
Plant Growth Biology and Modeling. Elche, España.
Abstract Book and Poster Presentation. June 2011

Norma Fàbregas, Na Li, Sacco de Vries and Ana Caño-Delgado
Revealing Brassinosteroid signaling through BRL3 vascular receptor in Arabidopsis
XXXIV Congreso de la Sociedad Española de Bioquímica y Biologia Molecular (SEBBM). Barcelona, España.
Abstract Book and Poster Presentation. June 2011

Norma Fàbregas, Marta Ibañes and Ana Caño-Delgado
Brassinosteroids modulate shoot vascular patterning in Arabidopsis

2nd Languedoc Roussillon – Catalogne meeting on plant integrative biology. Roses, España

Abstract Book and Poster Presentation. March 2009

Norma Fàbregas, Marta Ibañes and Ana Caño-Delgado

Brassinosteroids modulate shoot vascular patterning in Arabidopsis

IX Reunión de Biologia Molecular de Plantas. Santiago de Compostela, España.

Abstract Book and Poster Presentation. July 2008

Membership and services

Spanish Society for Biochemistry and Molecular Biology (SEBBM) member since June 2011.

Languages

Catalan and Spanish as mother languages.

Excellent English skills.

Particular Skills

Familiarized with PowerPoint, Adobe Photoshop & Illustrator, Microsoft Excel, Image J and confocal microscopy use and software. Good skills in proteomics and mass spectrometry data analysis. Well trained in the use of multidisciplinary techniques by combining molecular genetics with mathematical modeling and proteomics high throughput data with accurate genetic and microscopy analysis.

Organizer of an exchange retreat between Wageningen University PhD students (Holland) and CSIC PhD students (Barcelona). Oral presentations and discussions.

Flexible, responsible, open-minded and enthusiastic.

APENDIX 2

APENDIX 2